Transport Processes and Separation Process Principles

(INCLUDES UNIT OPERATIONS)

FOURTH EDITION

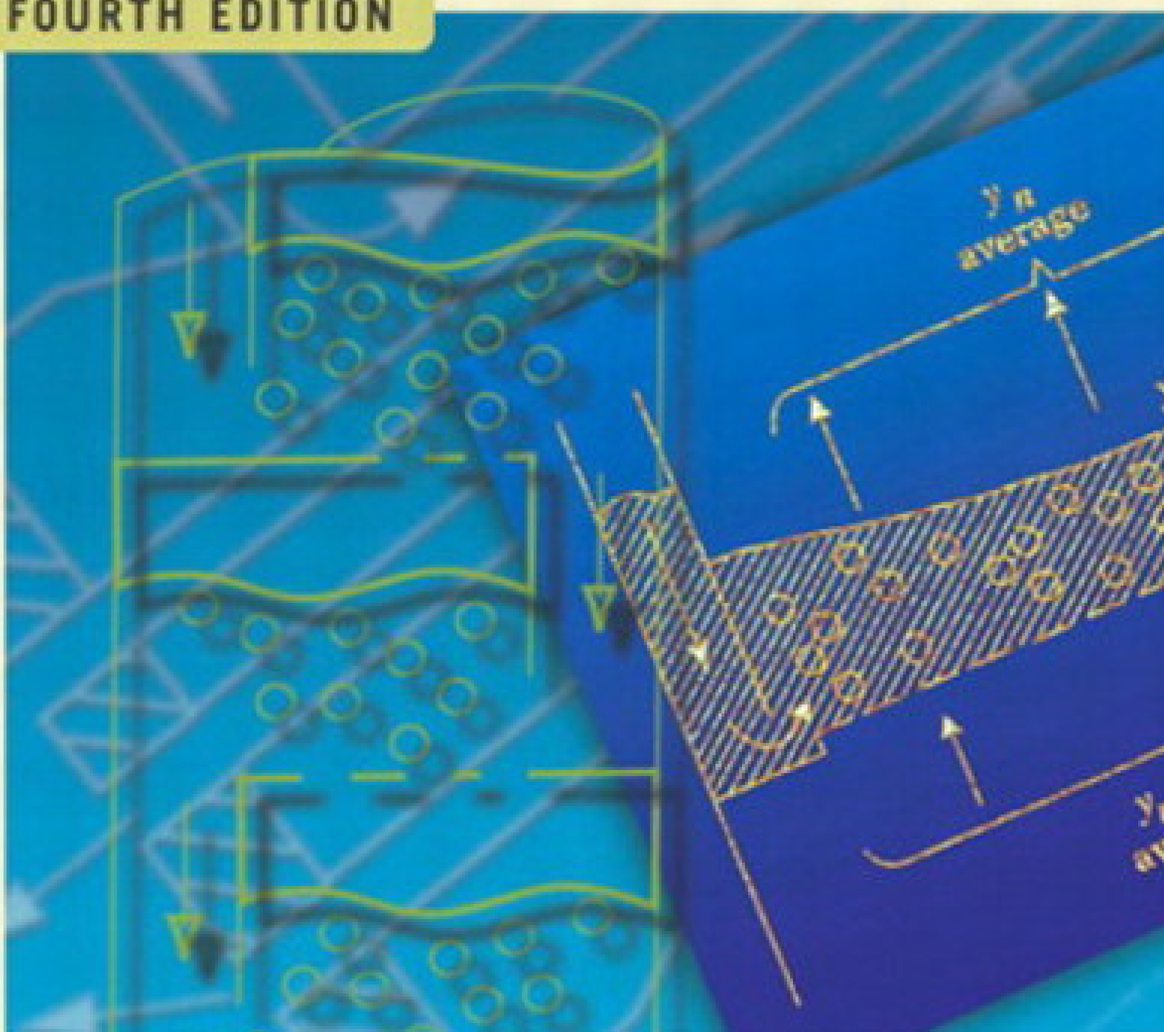

CHRISTIE JOHN GEANKOPLIS

Table of Contents

Chapter 3. Principles of Momentum Transfer and Applications

FLOW PAST IMMERSED OBJECTS AND PACKED AND FLUIDIZED BEDS

Definition of Drag Coefficient for Flow Past Immersed Objects

Introduction and types of drag

In Chapter 2 we were concerned primarily with the momentum transfer and frictional losses for flow of fluids inside conduits or pipes. In this section we consider in some detail the flow of fluids around solid, immersed objects.

The flow of fluids outside immersed bodies appears in many chemical engineering applications and other processing applications. These occur, for example, in flow past spheres in settling, flow through packed beds in drying and filtration, flow past tubes in heat exchangers, and so on. It is useful to be able to predict the frictional losses and/or the force on the submerged objects in these various applications.

In the examples of fluid friction inside conduits that we considered in Chapter 2, the transfer of momentum perpendicular to the surface resulted in a tangential shear stress or drag on the smooth surface parallel to the direction of flow. This force exerted by the fluid on the solid in the direction of flow is called *skin* or *wall drag.* For any surface in contact with a flowing fluid, skin friction will exist. In addition to skin friction, if the fluid is not flowing parallel to the surface but must change direction to pass around a solid body such as a sphere, significant additional frictional losses will occur; this is called *form drag.*

In Fig. 3.1-1a the flow of fluid is parallel to the smooth surface of the flat, solid plate, and the force F in newtons on an element of area dA m^2 of the plate is the wall shear stress τ_w times the area dA, or $\tau_w\, dA$. The total force is the sum of the integrals of these quantities evaluated over the entire area of the plate. Here the transfer of momentum to the surface results in a tangential stress or skin drag on the surface.

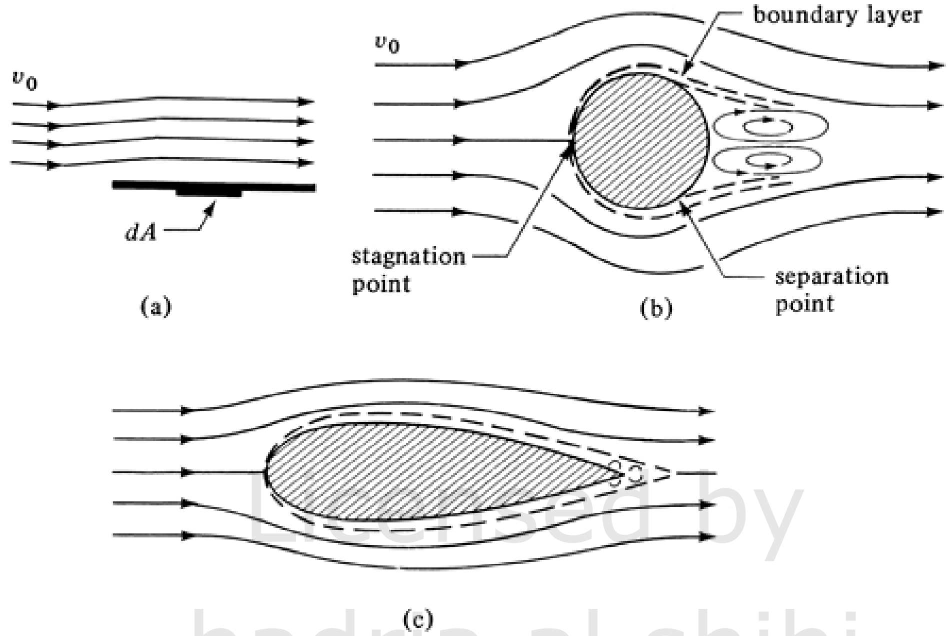

Figure 3.1-1. Flow past immersed objects: (a) flat plate, (b) sphere, (c) streamlined object.

In many cases, however, the immersed body is a blunt-shaped solid which presents various angles to the direction of the fluid flow. As shown in Fig. 3.1-1b, the free-stream velocity is v_0 and is uniform on approaching the blunt-shaped body suspended in a very large duct. Lines called *streamlines* represent the path of fluid elements around the suspended body. The thin boundary layer adjacent to the solid surface is shown as a dashed line; at the edge of this layer the velocity is essentially the same as the bulk fluid velocity adjacent to it. At the front center of the body, called the *stagnation point,* the fluid velocity will be zero; boundary-layer growth begins at this point and continues over the surface until the layer separates. The tangential stress on the body because of the velocity gradient in the boundary layer is the skin friction. Outside the boundary layer the fluid changes direction to pass around the solid and also accelerates near the front and then decelerates. Because of these effects, an additional force is exerted by the fluid on the body. This phenomenon, called *form drag,* is in addition to the skin drag in the boundary layer.

In Fig. 3.1-1b, as shown, separation of the boundary layer occurs and a wake, covering the entire rear of the object, occurs where large eddies are present and contribute to the form drag. The point of separation depends on the shape of the particle, Reynolds number, and so on, and is discussed in detail elsewhere (S3).

Form drag for bluff bodies can be minimized by streamlining the body (Fig. 3.1-1c), which forces the separation point toward the rear of the body, greatly reducing the size of the wake. Additional discussion of turbulence and boundary layers is given in Section 3.10.

Drag coefficient

From the preceding discussion it is evident that the geometry of the immersed solid is a major factor in determining the amount of total drag force exerted on the body. Correlations of the geometry and flow characteristics for solid objects suspended or held in a free stream (immersed objects) are similar in concept and form to the friction factor-Reynolds number correlation given for flow inside conduits. In flow through conduits, the friction factor was defined as the ratio of the drag force per unit area (shear stress) to the product of density times velocity head, as given in Eq. (2.10-4).

In a similar manner, for flow past immersed objects the drag coefficient C_D is defined as the ratio of the total drag force per unit area to $\rho v_0^2/2$:

Equation 3.1-1.

$$C_D = \frac{F_D/A_p}{\rho v_0^2/2} \qquad \text{(SI)}$$

$$C_D = \frac{F_D/A_p}{\rho v_0^2/2g_c} \qquad \text{(English)}$$

where F_D is the total drag force in N, A_p is an area in m^2, C_D is dimensionless, v_0 is free-stream velocity in m/s, and ρ is density of fluid in kg/m^3. In English units, F_D is in 1b$_f$, v_0 is in ft/s, ρ is in 1b$_m$/ft^3, and A_p is in ft^2. The area A_p used is the area obtained by projecting the body on a plane perpendicular to the line of flow. For a sphere, $A_p = \pi D_p^2/4$, where D_p is sphere diameter; for a cylinder whose axis is perpendicular to the flow direction, $A_p = LD_P$, where L = cylinder length. Solving Eq. (3.1-1) for the total drag force,

Equation 3.1-2.

$$F_D = C_D \frac{v_0^2}{2} \rho A_p$$

The Reynolds number for a given solid immersed in a flowing liquid is

Equation 3.1-3.

$$N_{\text{Re}} = \frac{D_p v_0 \rho}{\mu} = \frac{D_p G_0}{\mu}$$

where $G_0 = v_0\rho$.

Flow Past Sphere, Long Cylinder, and Disk

For each particular shape of object and orientation of the object with respect to the direction of flow, a different relation of C_D versus N_{Re} exists. Correlations of drag coefficient versus Reynolds number are shown in Fig. 3.1-2 for spheres, long cylinders, and disks. The face of the disk and the axis of the cylinder are perpendicular to the direction of flow. These curves have been determined experimentally. However, in the laminar region for low Reynolds numbers, less than about 1.0, the experimental drag force for a sphere is the same as the theoretical Stokes' law equation as follows:

Equation 3.1-4.

$$F_D = 3\pi\mu D_p v_0$$

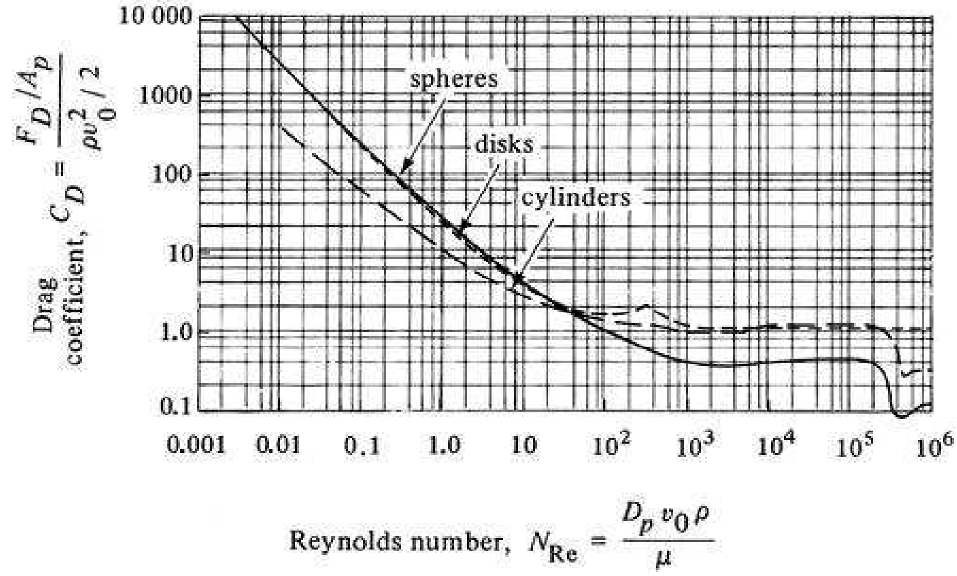

*Figure 3.1-2. Drag coefficients for flow past immersed spheres, long cylinders, and disks. (Reprinted with permission from C. E. Lapple and C. B. Shepherd, Ind. Eng. Chem., **32**, 606 (1940). Copyright by the American Chemical Society.)*

Combining Eqs. (3.1-2) and (3.1-4) and solving for C_D, the drag coefficient predicted by Stokes' law is

Equation 3.1-5.

$$C_D = \frac{24}{D_p v_0 \rho/\mu} = \frac{24}{N_{Re}}$$

The variation of C_D with N_{Re} (Fig. 3.1-2) is quite complicated because of the interaction of the factors that control skin drag and form drag. For a sphere, as the Reynolds number is increased beyond the Stokes' law range, separation occurs and a wake is formed. Further increases in N_{Re} cause shifts in the separation point. At about $N_{Re} = 3 \times 10^5$ the sudden drop in C_D is the result of the boundary layer becoming completely turbulent and the point of separation moving downstream. In the region of N_{Re} about 1×10^3 to 2×10^5, the drag coefficient is approximately constant for each shape and $C_D = 0.44$ for a sphere. Above N_{Re} about 5×10^5, the drag coefficients are again approximately constant, with C_D being 0.13 for a sphere, 0.33 for a cylinder, and 1.12 for a disk. Additional discussions and theory concerning flow past spheres are given in Section 3.9E.

For derivations of theory and detailed discussions of the drag force for flow parallel to a flat plate, Section 3.10 on boundary-layer flow and turbulence should be consulted. The flow of fluids normal to banks of cylinders or tubes occurs in heat exchangers and other processing applications. The banks of tubes can be arranged in a number of different geometries. Because of the many possible geometric tube configurations and spacings, it is not possible to have one correlation for the data on pressure drop and friction factors. Details of the many correlations available are given elsewhere (P1).

EXAMPLE 3.1-1. Force on a Submerged Sphere

Air at 37.8°C and 101.3 kPa absolute pressure flows at a velocity of 23 m/s past a sphere having a diameter of 42 mm. What are the drag coefficient C_D and the force on the sphere?

Solution: From Appendix A.3, for air at 37.8°C, $\rho = 1.137$ kg/m^3 and $\mu = 1.90 \times 10^{-5}$ Pa · s. Also, $D_p = 0.042$ m and $v_0 = 23.0$ m/s. Using Eq. (3.1-3),

$$N_{Re} = \frac{D_p v_0 \rho}{\mu} = \frac{0.042(23.0)(1.137)}{1.90 \times 10^{-5}} = 5.781 \times 10^4$$

From Fig. 3.1-2 for a sphere, C_D = 0.47. Substituting into Eq. (3.1-2), where $A_p = \pi D_p^2/4$ for a sphere,

$$F_D = C_D \frac{v_0^2}{2} \rho A_p = (0.47)\frac{(23.0)^2}{2}(1.137)(\pi)\frac{(0.042)^2}{4} = 0.1958 \text{ N}$$

EXAMPLE 3.1-2. Force on a Cylinder in a Tunnel

Water at 24°C is flowing past a long cylinder at a velocity of 1.0 m/s in a large tunnel. The axis of the cylinder is perpendicular to the direction of flow. The diameter of the cylinder is 0.090 m. What is the force per meter length on the cylinder?

Solution: From Appendix A.2, for water at 24°C, ρ = 997.2 kg/m^3 and $\mu = 0.9142 \times 10^{-3}$ Pa · s. Also, D_p = 0.090 m, L = 1.0 m, and v_0 = 1.0 m/s. Using Eq. (3.1-3),

$$N_{Re} = \frac{D_p v_0 \rho}{\mu} = \frac{0.090(1.0)(997.2)}{0.9142 \times 10^{-3}} = 9.817 \times 10^4$$

From Fig. 3.1-2 for a long cylinder, C_D = 1.4. Substituting into Eq. (3.1-2), where $A_p = LD_p$ = 1.0(0.090) = 0.090 m^2,

$$F_D = C_D \frac{v_0^2}{2} \rho A_p = (1.4)\frac{(1.0)^2}{2}(997.2)(0.09) = 62.82 \text{ N}$$

Flow in Packed Beds

Introduction

A system of considerable importance in chemical and other process engineering fields is the packed bed or packed column, which is used for a fixed-bed catalytic reactor, adsorption of a solute, absorption, filter bed, and so on. The packing material in the bed may be spheres, irregular particles, cylinders, or various kinds of commercial packings. In the discussion to follow it is assumed that the packing is everywhere uniform and that little or no channeling occurs. The ratio of diameter of the tower to packing diameter should be a minimum of 8:1 to 10:1 for wall effects to be small. In the theoretical approach used, the packed column is regarded as a bundle of crooked tubes of varying cross-sectional area. The theory developed in Chapter 2 for single straight tubes is used to develop the results for the bundle of crooked tubes.

Laminar flow in packed beds

Certain geometric relations for particles in packed beds are used in the derivations for flow. The void fraction ε in a packed bed is defined as

Equation 3.1-6.

$$\varepsilon = \frac{\text{volume of voids in bed}}{\text{total volume of bed (voids plus solids)}}$$

The specific surface of a particle a_v in m^{-1} is defined as

Equation 3.1-7.

$$a_v = \frac{S_p}{v_p}$$

where S_p is the surface area of a particle in m^2 and v_p the volume of a particle in m^3. For a spherical particle,

Equation 3.1-8.

$$a_v = \frac{6}{D_p}$$

where D_p is diameter in m. For a packed bed of nonspherical particles, the effective particle diameter D_p is defined as

Equation 3.1-9.

$$D_P = \frac{6}{a_v}$$

Since (1 - ε) is the volume fraction of particles in the bed,

Equation 3.1-10.

$$a = a_v(1 - \varepsilon) = \frac{6}{D_p}(1 - \varepsilon)$$

where a is the ratio of total surface area in the bed to total volume of bed (void volume plus particle volume) in m^{-1}.

EXAMPLE 3.1-3. Surface Area in Packed Bed of Cylinders

A packed bed is composed of cylinders having a diameter D = 0.02 m and a length $h = D$. The bulk density of the overall packed bed is 962 kg/m^3 and the density of the solid cylinders is 1600 kg/m^3.

a. Calculate the void fraction ε.
b. Calculate the effective diameter D_p of the particles.
c. Calculate the value of a in Eq. (3.1-10).

Solution: For part (a), taking 1.00 m^3 of packed bed as a basis, the total mass of the bed is (962 kg/m^3)(1.00 m^3) = 962 kg. This mass of 962 kg is also the mass of the solid cylinders. Hence, volume of cylinders = 962 kg/(1600 kg/m^3) = 0.601 m^3. Using Eq. (3.1-6),

$$\varepsilon = \frac{\text{volume of voids in bed}}{\text{total volume of bed}} = \frac{1.000 - 0.601}{1.000} = 0.399$$

For the effective particle diameter D_p in part (b), for a cylinder where $h = D$, the surface area of a particle is

$$S_p = (2)\frac{\pi D^2}{4}\text{ (ends)} + \pi D(D)\text{ (sides)} = \tfrac{3}{2}\pi D^2$$

The volume v_p of a particle is

$$v_p = \frac{\pi}{4}D^2(D) = \frac{\pi D^3}{4}$$

Substituting into Eq. (3.1-7),

$$a_v = \frac{S_p}{v_p} = \frac{\frac{3}{2}\pi D^2}{\frac{1}{4}\pi D^3} = \frac{6}{D}$$

Finally, substituting into Eq. (3.1-9),

$$D_p = \frac{6}{a_v} = \frac{6}{6/D} = D = 0.02 \text{ m}$$

Hence, the effective diameter to use is $D_p = D = 0.02$ m. For part (c), using Eq. (3.1-10),

$$a = \frac{6}{D_p}(1 - \varepsilon) = \frac{6}{0.02}(1 - 0.399) = 180.3 \text{ m}^{-1}$$

The average interstitial velocity in the bed is v m/s and is related to the superficial velocity v' based on the cross section of the empty container by

Equation 3.1-11.

$$v' = \varepsilon v$$

The hydraulic radius r_H for flow defined in Eq. (2.10-21) is modified as follows (B2):

Equation 3.1-12.

$$r_H = \frac{\begin{pmatrix}\text{cross-sectional area} \\ \text{available for flow}\end{pmatrix}}{(\text{wetted perimeter})}$$

$$= \frac{\text{void volume available for flow}}{\text{total wetted surface of solids}}$$

$$= \frac{\text{volume of voids/volume of bed}}{\text{wetted surface/volume of bed}} = \frac{\varepsilon}{a}$$

Combining Eqs. (3.1-10) and (3.1-12),

Equation 3.1-13.

$$r_H = \frac{\varepsilon}{6(1 - \varepsilon)} D_p$$

Since the equivalent diameter D for a channel is $D = 4r_H$, the Reynolds number for a packed bed is as follows, using Eq. (3.1-13) and $v' = \varepsilon v$:

Equation 3.1-14.

$$N_{\text{Re}} = \frac{(4r_H)v\rho}{\mu} = \frac{4\varepsilon}{6(1 - \varepsilon)} D_p \frac{v'}{\varepsilon} \frac{\rho}{\mu} = \frac{4}{6(1 - \varepsilon)} \frac{D_p v' \rho}{\mu}$$

For packed beds Ergun (E1) defined the Reynolds number as above but without the 4/6 term:

Equation 3.1-15.

$$N_{\mathrm{Re},p} = \frac{D_p v' \rho}{(1-\varepsilon)\mu} = \frac{D_p G'}{(1-\varepsilon)\mu}$$

where $G' = v'\rho$.

For laminar flow, the Hagen-Poiseuille equation (2.10-2) can be combined with Eq. (3.1-13) for r_H and Eq. (3.1-11) to give

Equation 3.1-16.

$$\Delta p = \frac{32\mu v\,\Delta L}{D^2} = \frac{32\mu(v'/\varepsilon)\,\Delta L}{(4r_H)^2} = \frac{(72)\mu v'\,\Delta L(1-\varepsilon)^2}{\varepsilon^3 D_p^2}$$

The true ΔL is larger because of the tortuous path, and use of the hydraulic radius predicts too large a v'. Experimental data show that the constant should be 150, which gives the Blake-Kozeny equation for laminar flow, void fractions less than 0.5, effective particle diameter D_p, and $N_{\mathrm{Re},p} < 10$:

Equation 3.1-17.

$$\Delta p = \frac{150\mu v'\,\Delta L}{D_p^2}\frac{(1-\varepsilon)^2}{\varepsilon^3}$$

Turbulent flow in packed beds

For turbulent flow we use the same procedure by starting with Eq. (2.10-5) and substituting Eqs. (3.1-11) and (3.1-13) into this equation to obtain

Equation 3.1-18.

$$\Delta p = \frac{3f\rho(v')^2\,\Delta L}{D_p}\frac{1-\varepsilon}{\varepsilon^3}$$

For highly turbulent flow the friction factor should approach a constant value. Also, it is assumed that all packed beds should have the same relative roughness. Experimental data indicate that $3f = 1.75$. Hence, the final equation for turbulent flow for $N_{\mathrm{Re},p} > 1000$, which is called the Burke-Plummer equation, becomes

Equation 3.1-19.

$$\Delta p = \frac{1.75\rho(v')^2\,\Delta L}{D_p}\frac{1-\varepsilon}{\varepsilon^3}$$

Adding Eq. (3.1-17) for laminar flow and Eq. (3.1-19) for turbulent flow, Ergun (E1) proposed the following general equation for low, intermediate, and high Reynolds numbers, which has been tested experimentally:

Equation 3.1-20.

$$\Delta p = \frac{150\mu v'\Delta L}{D_p^2}\frac{(1-\varepsilon)^2}{\varepsilon^3} + \frac{1.75\rho(v')^2\,\Delta L}{D_p}\frac{1-\varepsilon}{\varepsilon^3}$$

Rewriting Eq. (3.1-20) in terms of dimensionless groups,

Equation 3.1-21.

$$\frac{\Delta p \rho}{(G')^2} \frac{D_p}{\Delta L} \frac{\varepsilon^3}{1-\varepsilon} = \frac{150}{N_{\mathrm{Re},p}} + 1.75$$

See also Eq. (3.1-33) for another form of Eq. (3.1-21). The Ergun equation (3.1-21) can be used for gases by taking the density ρ of the gas as the arithmetic average of the inlet and outlet pressures. The velocity v' changes throughout the bed for a compressible fluid, but G' is a constant. At high values of $N_{\mathrm{Re},p}$, Eqs. (3.1-20) and (3.1-21) reduce to Eq. (3.1-19), and to Eq. (3.1-17) for low values. For large pressure drops with gases, Eq. (3.1-20) can be written in differential form (P1).

EXAMPLE 3.1-4. Pressure Drop and Flow of Gases in Packed Bed

Air at 311 K is flowing through a packed bed of spheres having a diameter of 12.7 mm. The void fraction ε of the bed is 0.38 and the bed has a diameter of 0.61 m and a height of 2.44 m. The air enters the bed at 1.10 atm abs at the rate of 0.358 kg/s. Calculate the pressure drop of the air in the packed bed. The average molecular weight of air is 28.97.

Solution: From Appendix A.3, for air at 311 K, $\mu = 1.90 \times 10^{-5}$ Pa · s. The cross-sectional area of the bed is $A = (\pi/4)D^2 = (\pi/4)(0.61)^2 = 0.2922$ m². Hence, $G' = 0.358/0.2922 = 1.225$ kg/m² · s (based on empty cross section of container or bed). $D_p = 0.0127$ m, $\Delta L = 2.44$ m, and inlet pressure $p_1 = 1.1(1.01325 \times 10^5) = 1.115 \times 10^5$ Pa.

From Eq. (3.1-15),

$$N_{\mathrm{Re},p} = \frac{D_p G'}{(1-\varepsilon)\mu} = \frac{0.0127(1.225)}{(1-0.38)(1.90 \times 10^{-5})} = 1321$$

To use Eq. (3.1-21) for gases, the density ρ to use is the average at the inlet p_1 and outlet p_2 pressures, or at $(p_1 + p_2)/2$. This is trial and error since p_2 is unknown. Assuming that $\Delta p = 0.05 \times 10^5$ Pa, $p_2 = 1.115 \times 10^5 - 0.05 \times 10^5 = 1.065 \times 10^5$ Pa. The average pressure is $p_{\mathrm{av}} = (1.115 \times 10^5 + 1.065 \times 10^5)/2 = 1.090 \times 10^5$ Pa. The average density to use is

Equation 3.1-22.

$$\rho_{\mathrm{av}} = \frac{M}{RT} p_{\mathrm{av}}$$

$$= \frac{28.97(1.090 \times 10^5)}{8314.34(311)} = 1.221 \text{ kg/m}^3$$

Substituting into Eq. (3.1-21) and solving for Δp,

$$\frac{\Delta p(1.221)}{(1.225)^2} \frac{0.0127}{2.44} \frac{(0.38)^3}{1-0.38} = \frac{150}{1321} + 1.75$$

Solving, $\Delta p = 0.0497 \times 10^5$ Pa. This is close enough to the assumed value, so a second trial is not needed.

Shape factors

Many particles in packed beds are often irregular in shape. The equivalent diameter of a particle is defined as the diameter of a sphere having the same volume as this particle. The sphericity shape factor φ_S of a particle is the ratio of the surface area of this sphere having the same volume as the particle to the actual surface area of the particle. For a sphere, the surface area $S_p = \pi D_p^2$ and the volume $v_p = \pi D_p^3/6.$ Hence, for any particle, $\phi_S = \pi D_p^2/S_p$, where S_p is the actual surface area of the particle and D_p is the diameter (equivalent diameter) of the sphere having the same volume as the particle. Then

Equation 3.1-23.

$$\frac{S_p}{v_p} = \frac{\pi D_p^2/\phi_S}{\pi D_p^3/6} = \frac{6}{\phi_S D_p}$$

From Eq. (3.1-7),

Equation 3.1-24.

$$a_v = \frac{S_p}{v_p} = \frac{6}{\phi_S D_p}$$

Then Eq. (3.1-10) becomes

Equation 3.1-25.

$$a = \frac{6}{\phi_S D_p}(1 - \varepsilon)$$

For a sphere, φ_S = 1.0. For a cylinder where diameter = length, φ_S is calculated to be 0.874, and for a cube, φ_S is calculated to be 0.806. For granular materials it is difficult to measure the actual volume and surface area to obtain the equivalent diameter. Hence, D_p is usually taken to be the nominal size from a screen analysis or visual length measurements. The surface area is determined by adsorption measurements or measurement of the pressure drop in a bed of particles. Then Eq. (3.1-23) is used to calculate φ_S (Table 3.1-1). Typical values for many crushed materials are between 0.6 and 0.7. For convenience, for the cylinder and the cube, the nominal diameter is sometimes used (instead of the equivalent diameter), which then gives a shape factor of 1.0.

Table 3.1-1. Shape Factors (Sphericity) of Some Materials

Material	*Shape Factor, φ_S*	*Reference*
Spheres	1.0	
Cubes	0.81	
Cylinders, $D_p = h$ (length)	0.87	
Berl saddles	0.3	(B4)
Raschig rings	0.3	(C2)
Coal dust, pulverized	0.73	(C2)
Sand, average	0.75	(C2)
Crushed glass	0.65	(C2)

Mixtures of particles

For mixtures of particles of various sizes we can define a mean specific surface a_{vm} as

Equation 3.1-26.

$$a_{vm} = \sum x_i a_{vi}$$

where x_i is volume fraction. Combining Eqs. (3.1-24) and (3.1-26),

Equation 3.1-27.

$$D_{pm} = \frac{6}{a_{vm}} = \frac{6}{\sum x_i (6/\phi_S D_{pi})} = \frac{1}{\sum x_i/(\phi_S D_{pi})}$$

where D_{pm} is the effective mean diameter for the mixture.

EXAMPLE 3.1-5. Mean Diameter for a Particle Mixture

A mixture contains three sizes of particles: 25% by volume of 25 mm size, 40% of 50 mm, and 35% of 75 mm. The sphericity is 0.68. Calculate the effective mean diameter.

Solution: The following data are given: $x_1 = 0.25$, $D_{p1} = 25$ mm; $x_2 = 0.40$, $D_{p2} = 50$; $x_3 = 0.35$, $D_{p3} = 75$; $\varphi_S = 0.68$. Substituting into Eq. (3.1-27),

$$D_{\text{pm}} = \frac{1}{0.25/(0.68 \times 25) + 0.40/(0.68 \times 50) + 0.35/(0.68 \times 75)}$$

$$= 30.0 \text{ mm}$$

Darcy's empirical law for laminar flow

Equation (3.1-17) for laminar flow in packed beds shows that the flow rate is proportional to Δp and inversely proportional to the viscosity μ and length ΔL. This is the basis for Darcy's law, as follows, for purely viscous flow in consolidated porous media:

Equation 3.1-28.

$$v' = \frac{q'}{A} = -\frac{k}{\mu}\frac{\Delta p}{\Delta L}$$

where v' is superficial velocity based on the empty cross section in cm/s, q' is flow rate in cm^3/s, A is empty cross section in cm^2, μ is viscosity in cp, Δp is pressure drop in atm, ΔL is length in cm, and k is permeability in (cm^3 flow/s) · (cp) · (cm length)/(cm^2 area) · (atm pressure drop). The units used for k of cm^2 · cp/s · atm are often given in darcy or in millidarcy (1/1000 darcy). Hence, if a porous medium has a permeability of 1 darcy, a fluid of 1 cp viscosity will flow at 1 cm^3/s per 1 cm^2 cross section with a Δp of 1 atm per cm length. This equation is often used in measuring permeabilities of underground oil reservoirs.

Flow in Fluidized Beds

Types of fluidization in beds

In a packed bed of small particles, when a fluid enters at sufficient velocity from the bottom and passes up through the particles, the particles are pushed upward and the bed expands and becomes fluidized. Two general types of fluidization, *particulate fluidization* and *bubbling fluidization,* can occur.

In *particulate fluidization,* as the fluid velocity is increased the bed continues to expand and remains homogeneous for a time. The particles move farther apart and their motion becomes more rapid. The average bed density at a given velocity is the same in all regions of the bed. An example is catalytic cracking catalysts fluidized by gases. This type of fluidization is very desirable in promoting intimate contact between the gas and solids. Liquids often give particulate fluidization.

In *bubbling fluidization,* the gas passes through the bed as voids or bubbles which contain few particles, and only a small percentage of the gas passes in the spaces between individual particles. The expansion of the bed is small as gas velocity is increased. Sand and glass beads provide examples of this behavior. Since most of the gas is in bubbles, little contact occurs between the individual particles and the bubbles.

Particles which behave as above have been classified by Geldart (G2) into classes. Those called Type A, which exhibit particulate fluidization in gases, fall into the following approximate ranges: For $\Delta\rho = (\rho_p - \rho) = 2000$ kg/m^3, $D_p = 20–125$ μm; $\Delta\rho = 1000$, $D_p = 25−250$; $\Delta\rho = 500$, $D_p = 40–450$; $\Delta\rho = 200$, $D_p = 100–1000$. For those called Type B, which exhibit bubbling fluidization, approximate ranges are as follows: $\Delta\rho = 2000$, $D_p = 125−700$ μm; $\Delta\rho = 1000$, $D_p = 250−1000$; $\Delta\rho = 500$, $D_p = 450−1500$; $\Delta\rho = 200$, $D_p = 1000−2000$.

Another type of behavior, called *slugging,* can occur in bubbling since the bubbles tend to coalesce and grow as they rise in the bed. If the column is small in diameter with a deep bed, bubbles can become large and fill the entire cross section and travel up the tower separated by slugs of solids.

Minimum velocity and porosity for particulate fluidization

When a fluid flows upward through a packed bed of particles at low velocities, the particles remain stationary. As the fluid velocity is increased, the pressure drop increases according to the Ergun equation (3.1-20). Upon further increases in velocity, conditions finally occur where the force of the pressure drop times the cross-sectional area equals the gravitational force on the mass of particles. Then the particles begin to move, and this is the onset of fluidization or minimum fluidization. The fluid velocity at which fluidization begins is the minimum fluidization velocity v'_{mf} in m/s based on the empty cross section of the tower (superficial velocity).

The porosity of the bed when true fluidization occurs is the minimum porosity for fluidization, ε_{mf}. Some typical values of ε_{mf} for various materials are given in Table 3.1-2. The bed expands to this voidage or porosity before particle motion appears. This minimum voidage can be determined experimentally by subjecting the bed to a rising gas stream and measuring the height of the bed L_{mf} in m. Generally, it appears best to use gas as the fluid rather than a liquid, since liquids give somewhat higher values of ε_{mf}.

Table 3.1-2. Void Fraction, ε_{mf}, at Minimum Fluidization Conditions (L2)

	Particle Size, D_P (mm)			
Type of Particles	**0.06**	**0.10**	**0.20**	**0.40**
		Void fraction, ε_{mf}		
Sharp sand ($\varphi_S = 0.67$)	0.60	0.58	0.53	0.49
Round sand ($\varphi_S = 0.86$)	0.53	0.48	0.43	(0.42)
Anthracite coal ($\varphi_S = 0.63$)	0.61	0.60	0.56	0.52
Absorption carbon	0.71	0.69		
Fischer Tropsch catalyst ($\varphi_S = 0.58$)		0.58	0.56	(0.54)

As stated earlier, the pressure drop increases as the gas velocity is increased until the onset of minimum fluidization. Then, as the velocity is further increased, the pressure drop decreases very slightly, and then it remains practically unchanged as the bed continues to expand or increase in porosity with increases in velocity. The bed resembles a boiling liquid. As the bed expands with increase in velocity, it continues to retain its top horizontal surface. Eventually, as the velocity is increased much further, entrainment of particles from the actual fluidized bed becomes appreciable.

The relation between bed height L and porosity ε is as follows for a bed having a uniform cross-sectional area A. Since the volume $LA(1-\varepsilon)$ is equal to the total volume of solids if they existed as one piece,

Equation 3.1-29.

$$L_1 A(1-\varepsilon_1) = L_2 A(1-\varepsilon_2)$$

Equation 3.1-30.

$$\frac{L_1}{L_2} = \frac{1-\varepsilon_2}{1-\varepsilon_1}$$

where L_1 is height of bed with porosity ε_1 and L_2 is height with porosity ε_2.

Pressure drop and minimum fluidizing velocity

As a first approximation, the pressure drop at the start of fluidization can be determined as follows. The force obtained from the pressure drop times the cross-sectional area must equal the gravitational force exerted by the mass of the particles minus the buoyant force of the displaced fluid:

Equation 3.1-31.

$$\Delta p A = L_{mf} A(1-\varepsilon_{mf})(\rho_p - \rho)g$$

Hence,

Equation 3.1-32.

$$\frac{\Delta p}{L_{mf}} = (1-\varepsilon_{mf})(\rho_p - \rho)g \qquad \text{(SI)}$$

$$\frac{\Delta p}{L_{mf}} = (1-\varepsilon_{mf})(\rho_p - \rho)\frac{g}{g_c} \qquad \text{(English)}$$

Often we have irregular-shaped particles in the bed, and it is more convenient to use the particle size and shape factor in the equations. First we substitute for the effective mean diameter D_p the term $\varphi_S D_P$, where D_P now represents the particle size of a sphere having the same volume as the particle and φ_S the shape factor. Often, the value of D_P is approximated by using the nominal size from a sieve analysis. Then Eq. (3.1-20) for pressure drop in a packed bed becomes

Equation 3.1-33.

$$\frac{\Delta p}{L} = \frac{150\mu v'}{\phi_S^2 D_P^2}\frac{(1-\varepsilon)^2}{\varepsilon^3} + \frac{1.75\rho(v')^2}{\phi_S D_P}\frac{1-\varepsilon}{\varepsilon^3}$$

where $\Delta L = L$, bed length in m.

Equation (3.1-33) can now be used by a small extrapolation for packed beds to calculate the minimum fluid velocity v'_{mf} at which fluidization begins by substituting v'_{mf} for v', ε_{mf} for ε, and L_{mf} for L, and combining the result with Eq. (3.1-32) to give

Equation 3.1-34.

$$\frac{1.75 D_P^2 (v'_{mf})^2 \rho^2}{\phi_S \varepsilon_{mf}^3 \mu^2} + \frac{150(1-\varepsilon_{mf}) D_P v'_{mf} \rho}{\phi_S^2 \varepsilon_{mf}^3 \mu} - \frac{D_P^3 \rho(\rho_p - \rho) g}{\mu^2} = 0$$

Defining a Reynolds number as

Equation 3.1-35.

$$N_{\mathrm{Re},mf} = \frac{D_P v'_{mf} \rho}{\mu}$$

Eq. (3.1-34) becomes

Equation 3.1-36.

$$\frac{1.75 (N_{\mathrm{Re},mf})^2}{\phi_S \varepsilon_{mf}^3} + \frac{150(1-\varepsilon_{mf})(N_{\mathrm{Re},mf})}{\phi_S^2 \varepsilon_{mf}^3} - \frac{D_P^3 \rho(\rho_p - \rho) g}{\mu^2} = 0$$

When $N_{\mathrm{Re},mf} < 20$ (small particles), the first term of Eq. (3.1-36) can be dropped, and when $N_{\mathrm{Re},mf} > 1000$ (large particles), the second term drops out.

If the terms ε_{mf} and/or φ_S are not known, Wen and Yu (W4) found for a variety of systems that

Equation 3.1-37.

$$\phi_S \varepsilon_{mf}^3 \cong \frac{1}{14}, \qquad \frac{1-\varepsilon_{mf}}{\phi_S^2 \varepsilon_{mf}^3} \cong 11$$

Substituting into Eq. (3.1-36), the following simplified equation is obtained:

Equation 3.1-38.

$$N_{\mathrm{Re},mf} = \left[(33.7)^2 + 0.0408 \frac{D_P^3 \rho(\rho_p - \rho) g}{\mu^2}\right]^{1/2} - 33.7$$

This equation holds for a Reynolds-number range of 0.001 to 4000, with an average deviation of ± 25%. Alternative equations are available in the literature (K1, W4).

EXAMPLE 3.1-6. Minimum Velocity for Fluidization

Solid particles having a size of 0.12 mm, a shape factor φ_S of 0.88, and a density of 1000 kg/m^3 are to be fluidized using air at 2.0 atm abs and 25°C. The voidage at minimum fluidizing conditions is 0.42.

a. If the cross section of the empty bed is 0.30 m^2 and the bed contains 300 kg of solid, calculate the minimum height of the fluidized bed.
b. Calculate the pressure drop at minimum fluidizing conditions.
c. Calculate the minimum velocity for fluidization.
d. Use Eq. (3.1-38) to calculate v'_{mf} assuming that data for φ_S and ε_{mf} are not available.

Solution: For part (a), the volume of solids = 300 kg/(1000 kg/m^3) = 0.300 m^3. The height the solids would occupy in the bed if $\varepsilon_1 = 0$ is L_1 = 0.300 m^3/(0.30 m^2 cross section) = 1.00 m. Using Eq. (3.1-30) and calling $L_{mf} = L_2$ and $\varepsilon_{mf} = \varepsilon_2$,

$$\frac{L_1}{L_{mf}} = \frac{1 - \varepsilon_{mf}}{1 - \varepsilon_1}$$

$$\frac{1.00}{L_{mf}} = \frac{1 - 0.42}{1 - 0}$$

Solving, L_{mf} = 1.724 m.

The physical properties of air at 2.0 atm and 25°C (Appendix A.3) are $\mu = 1.845 \times 10^{-5}$ Pa · s, $\rho = 1.187 \times 2 = 2.374$ kg/m^3, and $p = 2.0265 \times 10^5$ Pa. For the particle, D_P = 0.00012 m, ρ_p = 1000 kg/m^3, φ_S = 0.88, and ε_{mf} = 0.42.

For part (b), using Eq. (3.1-32) to calculate Δp,

$$\Delta p = L_{mf}(1 - \varepsilon_{mf})(\rho_p - \rho)g$$

$$= 1.724(1 - 0.42)(1000 - 2.374)(9.80665) = 0.0978 \times 10^5 \text{ Pa}$$

To calculate v'_{mf} for part (c), Eq. (3.1-36) is used:

$$\frac{1.75(N_{\text{Re},mf})^2}{(0.88)(0.42)^3} + \frac{150(1 - 0.42)(N_{\text{Re},mf})}{(0.88)^2(0.42)^3} - (0.00012)^3\frac{2.374(1000 - 2.374)(9.80665)}{(1.845 \times 10^{-5})^2} = 0$$

Solving,

$$N_{\text{Re},mf} = 0.07764 = \frac{D_p v'_{mf} \rho}{\mu} = \frac{0.00012(v'_{mf})(2.374)}{1.845 \times 10^{-5}}$$

$$v'_{mf} = 0.005029 \text{ m/s}$$

Using the simplified Eq. (3.1-38) for part (d),

$$N_{\text{Re},mf} = \left[(33.7)^2 + \frac{0.0408(0.00012)^3(2.374)(1000 - 2.374)(9.80665)}{(1.845 \times 10^{-5})^2}\right]^{1/2} - 33.7$$

$$= 0.07129$$

Solving, v'_{mf} = 0.004618 m/s.

Solving, v'_{mf} = 0.004618 m/s.

Expansion of fluidized beds

For the case of small particles and where $N_{Re,f} = D_p v' \rho / \mu < 20$, we can estimate the variation of porosity or bed height L as follows. We assume that Eq. (3.1-36) applies over the whole range of fluid velocities, with the first term being neglected. Then, solving for v',

Equation 3.1-39.

$$v' = \frac{D_P^2(\rho_p - \rho) g \phi_S^2}{150\mu} \frac{\varepsilon^3}{1-\varepsilon} = K_1 \frac{\varepsilon^3}{1-\varepsilon}$$

We find that all terms except ε are constant for the particular system, and ε depends upon v'. This equation can be used with liquids to estimate ε with $\varepsilon < 0.80$. However, because of clumping and other factors, errors can occur when used for gases.

The flow rate in a fluidized bed is limited on the one hand by the minimum v'_{mf} and on the other by entrainment of solids from the bed proper. This maximum allowable velocity is approximated as the terminal settling velocity v'_t of the particles. (See Section 13.3 for methods for calculating this settling velocity.) Approximate equations for calculating the operating range are as follows (P2). For fine solids and $N_{Re,f} < 0.4$,

Equation 3.1-40.

$$\frac{v'_t}{v'_{mf}} \cong \frac{90}{1}$$

For large solids and $N_{Re,f} > 1000$,

Equation 3.1-41.

$$\frac{v'_t}{v'_{mf}} \cong \frac{9}{1}$$

EXAMPLE 3.1-7. Expansion of Fluidized Bed

Using the data from Example 3.1-6, estimate the maximum allowable velocity v'_t. Using an operating velocity of 3.0 times the minimum, estimate the voidage of the bed.

Solution: From Example 3.1-6, $N_{Re,mf} = 0.07764$, $v'_{mf} = 0.005029$ m/s, and $\varepsilon_{mf} = 0.42$. Using Eq. (3.1-40), the maximum allowable velocity is

$$v'_t \cong 90(v'_{mf}) = 90(0.005029) = 0.4526 \text{ m/s}$$

Using an operating velocity v' of 2.0 times the minimum,

$$v' = 2.0(v'_{mf}) = 2.0(0.005029) = 0.01006 \text{ m/s}$$

To determine the voidage at this new velocity, we substitute into Eq. (3.1-39) using the known values at minimum fluidizing conditions to determine K_1:

$$0.005029 = K_1 \frac{(0.42)^3}{1 - 0.42}$$

Solving $K_1 = 0.03938$. Then using the operating velocity in Eq. (3.1-39),

$$0.01006 = (0.03938)\frac{\varepsilon^3}{1-\varepsilon}$$

Solving, the voidage of the bed $\varepsilon = 0.503$ at the operating velocity.

Minimum bubbling velocity

The fluidization velocity at which bubbles are first observed is called the *minimum bubbling velocity,* v'_{mb}. For Group B particles, which exhibit bubbling fluidization, v'_{mb} is reasonably close to v'_{mf}. For Group A particles, v'_{mb} is substantially greater than v'_{mf}. The following equation (G3) can be used to calculate v'_{mb}:

Equation 3.1-42.

$$v'_{mb} = 33D_p(\mu/\rho)^{-0.1}$$

where v'_{mb} is minimum bubbling velocity in m/s, μ is viscosity in Pa · s, and ρ is gas density in kg/m^3. If the calculated v'_{mf} is greater than the calculated v'_{mb} by Eq. (3.1-42), then the v'_{mf} should be used as the minimum bubbling velocity (G4).

EXAMPLE 3.1-8. Minimum Bubbling Velocity

Using data from Example 3.1-6, calculate the v'_{mb}.

Solution: Substituting into Eq. (3.1-42),

$$v'_{mb} = 33(0.00012)(1.845\times10^{-5}/2.374)^{-0.1} = 0.01284 \text{ m/s}$$

This is substantially greater than the v'_{mf} of 0.005029 m/s.

MEASUREMENT OF FLOW OF FLUIDS

It is important to be able to measure and control the amount of material entering and leaving a chemical or other processing plant. Since many of the materials are in the form of fluids, they are flowing in pipes or conduits. Many different types of devices are used to measure the flow of fluids. The simplest are those that measure directly the volume of the fluids, such as ordinary gas and water meters and positive-displacement pumps. Current meters make use of an element, such as a propeller or cups on a rotating arm, which rotates at a speed determined by the velocity of the fluid passing through it. Very widely used for fluid metering are the pitot tube, venturi meter, orifice meter, and open-channel weirs.

Pitot Tube

The pitot tube is used to measure the local velocity at a given point in the flow stream and not the average velocity in the pipe or conduit. In Fig. 3.2-1a, a sketch of this simple device is shown. One tube, the impact tube, has its opening normal to the direction of flow, while the static tube has its opening parallel to the direction of flow.

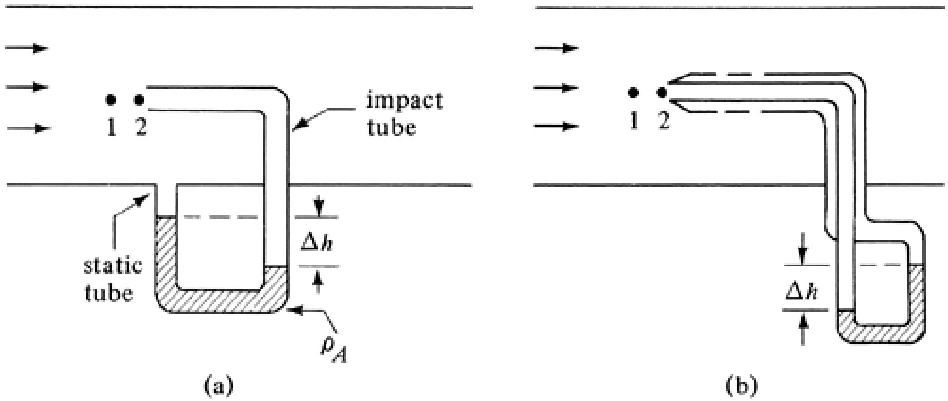

Figure 3.2-1. Diagram of pitot tube: (a) simple tube, (b) tube with static pressure holes.

The fluid flows into the opening at point 2; pressure builds up and then remains stationary at this point, called the *stagnation point.* The difference in the stagnation pressure at point 2 and the static pressure measured by the static tube represents the pressure rise associated with deceleration of the fluid. The manometer measures this small pressure rise. If the fluid is incompressible, we can write the Bernoulli equation (2.7-32) between point 1, where the velocity v_1 is undisturbed before the fluid decelerates, and point 2, where the velocity v_2 is zero:

Equation 3.2-1.

$$\frac{v_1^2}{2} - \frac{v_2^2}{2} + \frac{p_1 - p_2}{\rho} = 0$$

Setting $v_2 = 0$ and solving for v_1,

Equation 3.2-2.

$$v = C_p\sqrt{\frac{2(p_2 - p_1)}{\rho}}$$

where v is the velocity v_1 in the tube at point 1 in m/s, p_2 is the stagnation pressure, ρ is the density of the flowing fluid at the static pressure p_1, and C_p is a dimensionless coefficient to take into account deviations from Eq. (3.2-1) that generally varies between about 0.98 and 1.0. For accurate use, the coefficient should be determined by calibration of the pitot tube. This equation applies to incompressible fluids but can be used to approximate the flow of gases at moderate velocities and pressure changes of about 10% or less of the total pressure. For gases the pressure change is often quite low and, hence, accurate measurement of velocities is difficult.

The value of the pressure drop $p_2 - p_1$ or Δp in Pa is related to Δh, the reading on the manometer, by Eq. (2.2-14) as follows:

Equation 3.2-3.

$$\Delta p = \Delta h(\rho_A - \rho)g$$

where ρ_A is the density of the fluid in the manometer in kg/m^3 and Δh is the manometer reading in m. In Fig. 3.2-1b, a more compact design is shown with concentric tubes. In the outer tube, static pressure holes are parallel to the direction of flow. Further details are given elsewhere (P1).

Since the pitot tube measures velocity at only one point in the flow, several methods can be used to obtain the average velocity in the pipe. In the first method the velocity is measured at the exact center of the tube to obtain v_{max}. Then by using Fig. 2.10-2, the v_{av} can be obtained. Care should be taken to have the pitot tube at least 100 diameters downstream from any pipe obstruction. In the second method, readings are taken at several known positions in the pipe cross section and then, using Eq. (2.6-17), a graphical or numerical integration is performed to obtain v_{av}.

EXAMPLE 3.2-1. Flow Measurement Using a Pitot Tube

A pitot tube similar to Fig. 3.2-1a is used to measure the airflow in a circular duct 600 mm in diameter. The flowing air temperature is 65.6°C. The pitot tube is placed at the center of the duct and the reading Δh on the manometer is 10.7 mm of water. A static-pressure measurement obtained at the pitot tube position is 205 mm of water above atmospheric. The pitot-tube coefficient $C_p = 0.98$.

a. Calculate the velocity at the center and the average velocity.
b. Calculate the volumetric flow rate of the flowing air in the duct.

Solution: For part (a), the properties of air at 65.6°C. from Appendix A.3 are $\mu = 2.03 \times 10^{-5}$ Pa · s, $\rho = 1.043$ kg/m^3 (at 101.325 kPa). To calculate the absolute static pressure, the manometer reading $\Delta h = 0.205$ m of water indicates the pressure above 1 atm abs. Using Eq. (2.2-14), the water density as 1000 kg/m^3, and assuming 1.043 kg/m^3 as the air density,

$$\Delta p = 0.205(1000 - 1.043)9.80665 = 2008 \text{ Pa}$$

Then the absolute static pressure $p_1 = 1.01325 \times 10^5 + 0.02008 \times 10^5 = 1.0333 \times 10^5$ Pa. The correct air density in the flowing air is $(1.0333 \times 10^5/1.01325 \times 10^5)(1.043) = 1.063$ kg/m^3. This correct value, when used instead of 1.043, would have a negligible effect on the recalculation of p_1.

To calculate Δp for the pitot tube, Eq. (3.2-3) is used:

$$\Delta p = \Delta h(\rho_A - \rho)g = \frac{10.7}{1000}(1000 - 1.063)(9.80665) = 104.8 \text{ Pa}$$

Using Eq. (3.2-2), the maximum velocity at the center is

$$v = 0.98\sqrt{\frac{2(104.8)}{1.063}} = 13.76 \text{ m/s}$$

The Reynolds number, using the maximum velocity, is

$$N_{Re} = \frac{D v_{max} \rho}{\mu} = \frac{0.600(13.76)(1.063)}{2.03 \times 10^{-5}} = 4.323 \times 10^5$$

From Fig. 2.10-2, $v_{av}/v_{max} = 0.85$. Then, $v_{av} = 0.85(13.76) = 11.70$ m/s.

To calculate the flow rate for part (b), the cross-sectional area of the duct, $A = (\pi/4)(0.600)^2 = 0.2827$ m^2. The flow rate = 0.2827(11.70) = 3.308 m^3/s.

Venturi Meter

A *venturi meter,* shown in Fig. 3.2-2, is usually inserted directly into a pipeline. A manometer or other device is connected to the two pressure taps shown and measures the pressure difference $p_1 - p_2$ between points 1 and 2. The average velocity at point 1 where the diameter is D_1 m is v_1 m/s, and at point 2 or the throat the velocity is v_2 and the diameter D_2. Since the narrowing down from D_1 to D_2 and the expansion from D_2 back to D_1 is gradual, little frictional loss due to contraction and expansion is incurred.

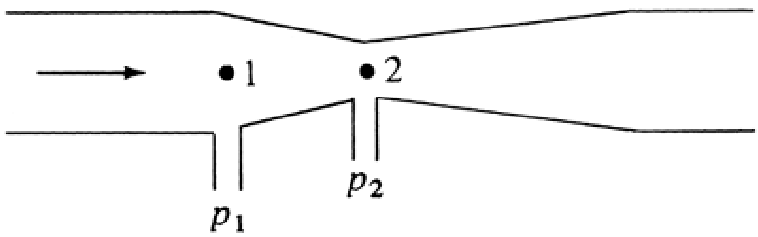

Figure 3.2-2. Venturi flow meter.

To derive the equation for the venturi meter, friction is neglected and the pipe is assumed horizontal. Assuming turbulent flow and writing the mechanical-energy-balance equation (2.7-28) between points 1 and 2 for an incompressible fluid,

Equation 3.2-4.

$$\frac{v_1^2}{2} + \frac{p_1}{\rho} = \frac{v_2^2}{2} + \frac{p_2}{\rho}$$

The continuity equation for constant ρ is

Equation 3.2-5.

$$v_1 \frac{\pi D_1^2}{4} = v_2 \frac{\pi D_2^2}{4}$$

Combining Eqs. (3.2-4) and (3.2-5) and eliminating v_1,

Equation 3.2-6.

$$v_2 = \frac{1}{\sqrt{1-(D_2/D_1)^4}} \sqrt{\frac{2(p_1 - p_2)}{\rho}}$$

To account for the small friction loss, an experimental coefficient C_v is introduced to give

Equation 3.2-7.

$$v_2 = \frac{C_v}{\sqrt{1-(D_2/D_1)^4}} \sqrt{\frac{2(p_1 - p_2)}{\rho}} \quad \text{(SI)}$$

$$v_2 = \frac{C_v}{\sqrt{1-(D_2/D_1)^4}} \sqrt{\frac{2g_c(p_1 - p_2)}{\rho}} \quad \text{(English)}$$

This holds for liquids and very small pressure drops in gases of less than 1%. For many meters and a Reynolds number >10^4 at point 1, C_v is about 0.98 for pipe diameters below 0.2 m and 0.99 for larger sizes. However, these coefficients can vary, and individual calibration is recommended if the manufacturer's calibration is not available.

To calculate the volumetric flow rate, the velocity v_2 is multiplied by the area A_2:

Equation 3.2-8.

$$\text{flow rate} = v_2 \frac{\pi D_2^2}{4} \quad \text{m}^3/\text{s}$$

For the measurement of compressible flow of gases, the adiabatic expansion from p_1 to p_2 pressure must be allowed for in Eq. (3.2-7). A similar equation and the same coefficient C_v are used along with the dimensionless expansion correction factor Y (shown in Fig. 3.2-3 for air) as follows:

Equation 3.2-9.

$$m = \frac{C_v A_2 Y}{\sqrt{1 - (D_2/D_1)^4}} \sqrt{2(p_1 - p_2)\rho_1}$$

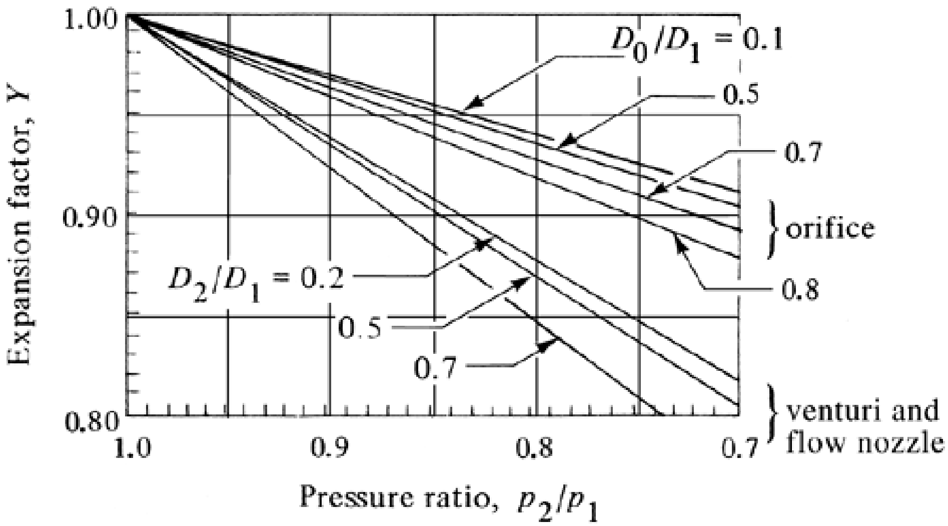

Figure 3.2-3. Expansion factor for air in venturi, flow nozzle, and orifice. [Calculated from equations and data in references (A2, M2, S3).]

where m is flow rate in kg/s, ρ_1 is density of the fluid upstream at point 1 in kg/m^3, and A_2 is cross-sectional area at point 2 in m^2.

The pressure difference $p_1 - p_2$ occurs because the velocity is increased from v_1 to v_2. However, farther down the tube the velocity returns to its original value of v_1 for liquids. Because of frictional losses, some of the difference $p_1 - p_2$ is not fully recovered downstream to the original p_1. In a properly designed venturi meter, the permanent loss is about 10% of the differential $p_1 - p_2$, and this represents power loss. A venturi meter is often used to measure flows in large lines, such as city water systems.

Orifice Meter

For ordinary installations in a process plant the venturi meter has several disadvantages. It occupies a lot of space and is expensive. Also, the throat diameter is fixed, so that if the flow-rate range is changed considerably, inaccurate pressure differences may result. The *orifice meter* overcomes these objections but at the price of a much larger permanent head or power loss.

A typical sharp-edged orifice is shown in Fig. 3.2-4. A machined and drilled plate having a hole of diameter D_0 is mounted between two flanges in a pipe of diameter D_1. Pressure taps at points 1 upstream and 2 downstream measure $p_1 - p_2$. The exact positions of the two taps are somewhat arbitrary: in one type of meter the taps are installed about 1 pipe diameter upstream and 0.3 to 0.8 pipe diameter downstream. The fluid stream, once past the orifice plate, forms a vena contracta or free-flowing jet.

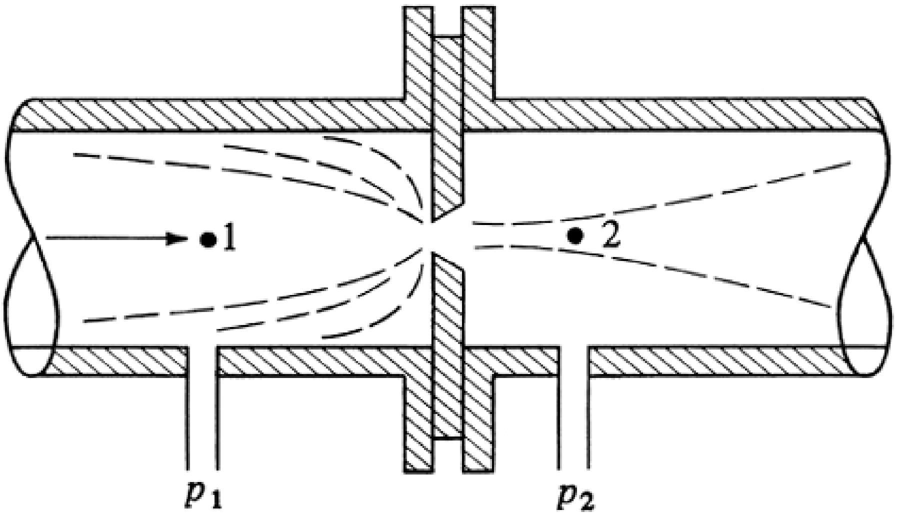

Figure 3.2-4. Orifice flow meter.

The equation for the orifice is similar to Eq. (3.2-7):

Equation 3.2-10.

$$v_0 = \frac{C_0}{\sqrt{1-(D_0/D_1)^4}}\sqrt{\frac{2(p_1-p_2)}{\rho}}$$

where v_0 is the velocity in the orifice in m/s, D_0 is the orifice diameter in m, and C_0 is the dimensionless orifice coefficient. The orifice coefficient C_0 is always determined experimentally. If the N_{Re} at the orifice is above 20000 and D_0/D_1 is less than about 0.5, the value of C_0 is approximately constant and has the value 0.61, which is adequate for design for liquids or gases (M2, P1). Below 20000 the coefficient rises sharply and then drops, and a correlation for C_0 is given elsewhere (P1).

As in the case of the venturi, for the measurement of compressible flow of gases in an orifice, a correction factor Y given in Fig. 3.2-3 for air is used as follows:

Equation 3.2-11.

$$m = \frac{C_0 A_0 Y}{\sqrt{1-(D_0/D_1)^4}}\sqrt{2(p_1-p_2)\rho_1}$$

where m is flow rate in kg/s, ρ_1 is upstream density in kg/m^3, and A_0 is the cross-sectional area of the orifice. For liquids, Y is 1.0.

The permanent pressure loss is much higher than for a venturi because of the eddies formed when the jet expands below the vena contracta. This loss depends on D_0/D_1 and is as follows:

Equation 3.2-12.

$$(p_1 - p_4) = (1-\beta^2)(p_1-p_2)$$

where $\beta = D_0/D_1$ (P1) and p_4 is the fully recovered pressure 4 -8 pipe diameters downstream. For $\beta = \frac{1}{2}$, this power loss is 75% of $p_1 - p_2$.

EXAMPLE 3.2-2. Metering Oil Flow by an Orifice

A sharp-edged orifice having a diameter of 0.0566 m is installed in a 0.1541-m pipe through which oil having a density of 878 kg/m^3 and a viscosity of 4.1 cp is flowing. The measured pressure difference across the orifice is 93.2 kN/m^2. Calculate the volumetric flow rate in m^3/s. Assume that C_0 = 0.61.

Solution:

$$p_1 - p_2 = 93.2 \text{ kN/m}^2 = 9.32 \times 10^4 \text{ N/m}^2$$

$$D_1 = 0.1541 \text{ m} \qquad D_0 = 0.0566 \text{ m} \qquad \frac{D_0}{D_1} = \frac{0.0566}{0.1541} = 0.368$$

Substituting into Eq. (3.2-10).

$$v_0 = \frac{C_0}{\sqrt{1-(D_0/D_1)^4}}\sqrt{\frac{2(p_1-p_2)}{\rho}}$$

$$= \frac{0.61}{\sqrt{1-(0.368)^4}}\sqrt{\frac{2(9.32 \times 10^4)}{878}}$$

$$v_0 = 8.97 \text{ m/s}$$

$$\text{volumetric flow rate} = v_0\frac{\pi D_0^2}{4} = (8.97)\frac{(\pi)(0.0566)^2}{4}$$

$$= 0.02257 \text{ m}^3\text{/s } (0.797 \text{ ft}^3\text{/s})$$

The N_{Re} is calculated see if it is greater than 2 × 10^4 for C_0 = 0.61:

$$\mu = 4.1 \times 1 \times 10^{-3} = 4.1 \times 10^{-3} \text{ kg/m} \cdot \text{s} = 4.1 \times 10^{-3} \text{ Pa} \cdot \text{s}$$

$$N_{Re} = \frac{D_0 v_0 \rho}{\mu} = \frac{0.0566(8.97)(878)}{4.1 \times 10^{-3}} = 1.087 \times 10^5$$

Hence, the Reynolds number is above 2 × 10^4.

Flow-Nozzle Meter

A typical *flow nozzle* is shown in Fig. 3.2-5. It is essentially a short cylinder with the approach being elliptical in shape. This meter has characteristics similar to those of the venturi meter but is shorter and much less expensive. The length of the straight portion of the throat is about one-half the diameter of the throat, D_2. The upstream pressure tap p_1 is 1 pipe diameter from the inlet-nozzle face, and the downstream tap p_2 is $\frac{1}{2}$ pipe diameter from the inlet-nozzle face.

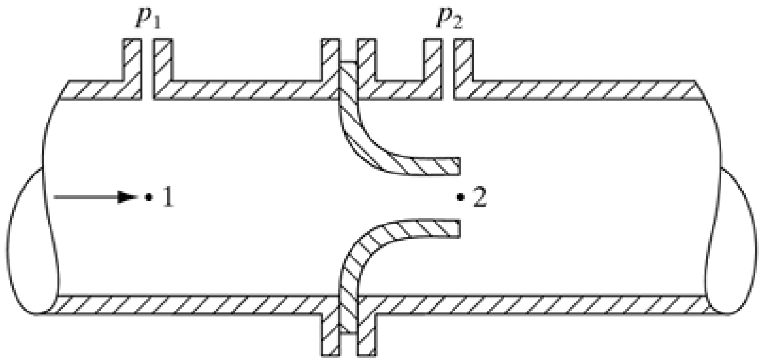

Figure 3.2-5. Flow-nozzle meter.

The equation for flow for liquids is the same as Eq. (3.2-7) for the venturi, with the coefficient C_n for the flow nozzle replacing C_v for the venturi. Also, the equation for compressible flow of gases for the flow nozzle is the same as Eq. (3.2-9) for the venturi, with the coefficient C_n. The expansion factor Y is the same for the flow nozzle and the venturi.

For the flow nozzle the coefficient C_n ranges from 0.95 at a pipe Reynolds number of 10^4, 0.98 at 10^5, and 0.99 at 10^6 or above (P1, S3). The permanent pressure loss ($p_1 - p_4$) is as follows, where p_4 is the final, fully recovered downstream pressure:

Equation 3.2-13.

$$(p_1 - p_4) = \frac{1 - \beta^2}{1 + \beta^2}(p_1 - p_2)$$

where $\beta = D_2/D_1$. This loss is greater than that for venturi meters and less than that for orifice meters. For $\beta = \frac{1}{2}$, this power loss is 60% of $p_1 - p_2$.

Variable-Area Flow Meters (Rotameters)

In Fig. 3.2-6 a variable-area flow meter is shown. The fluid enters at the bottom of the tapered glass tube, flows through the annular area around the tube, and exits at the top. The float remains stationary. The differential head or pressure drop is held constant. At a higher flow rate the float rises and the annular area increases to keep a constant pressure drop. The height of rise in the tube is calibrated with the flow rate, and the relation between the meter reading and the flow rate is approximately linear.

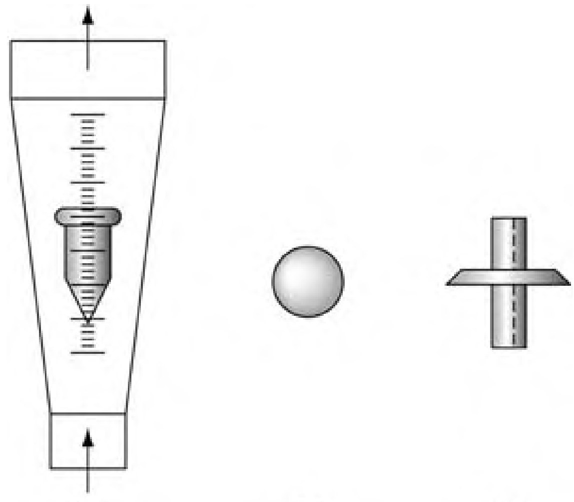

Figure 3.2-6. Rotameter: (a) flow diagram with glass tube, (b) spherical float, (c) viscosity-insensitive float.

For a given float of density ρ_f and a fluid density ρ_A, the mass flow rate m_A is given by

Equation 3.2-14.

$$m_A = q_A \rho_A = K\sqrt{\frac{(\rho_f - \rho_A)\rho_A}{\rho_f}}$$

where q_A, volumetric flow rate, is the reading on the rotameter, and K is a constant which is determined experimentally. If a fluid ρ_B is used instead of ρ_A, at the same height or reading of q_A on the rotameter and assuming K does not vary appreciably, the following approximation can be used:

Equation 3.2-15.

$$\frac{m_A}{m_B} = \frac{q_A \rho_A}{q_B \rho_B} = \sqrt{\frac{(\rho_f - \rho_A)\rho_A}{(\rho_f - \rho_B)\rho_B}}$$

For gases where $\rho_f \gg \rho_A$ and ρ_B, $q_B = q_A\sqrt{\rho_A/\rho_B}$. Note that the reading on the rotameter is taken at the highest and widest point of the float.

Other Types of Flow Meters

Many other types of flow meters are available; the more important ones are discussed briefly as follows:

Turbine- and paddle-wheel meters

A turbine wheel or a paddle wheel is placed inside a pipe, and the rotary speed depends on the flow rate of the fluid. Residential and industrial gas and water meters are often of the rotary wheel type.

Thermal-gas mass flow meters

Gas flowing in a tube is divided into a constant ratio because of laminar flow into a main stream and a small stream in a sensor tube. A small but constant amount of heat is added to the sensor tube flow. By measuring the temperature rise, the output temperature rise can be related to the gas mass flow rate. These meters are mass flow meters and are unaffected by temperature and pressure.

Magnetic flow meters

A magnetic field is generated across the conductive fluid flowing in a pipe. Using Faraday's law of electromagnetic inductance, the induced voltage is directly proportional to the flow velocity (D3). The meter is insensitive to changes in density and viscosity. The meter cannot be used with most hydrocarbons because of their low conductivity.

Coriolis mass flow meter

This meter is insensitive to operating conditions of viscosity, density, type of fluid, and slurries. Fluid from the main flow enters two U-tube side channels (D3). The fluid induces a Coriolis force according to Newton's second law. The tubes then twist slightly, and the measured twist angle is proportional to the mass flow rate.

Vortex-shedding flow meter

When a fluid flows past a blunt object, the fluid forms vortices or eddies (D3). The vortices are counted and the signal is proportional to the flow rate.

Flow in Open Channels and Weirs

In many instances in process engineering and in agriculture, liquids are flowing in open channels rather than closed conduits. To measure the flow rates, weir devices are often used. A *weir* is a dam over which the liquid flows. The two main types of weirs are the rectangular weir and the triangular weir shown in Fig. 3.2-7. The liquid flows over the weir, and the height h_0 (weir head) in m is measured above the flat base or the notch as shown. This head should be measured at a distance of about $3h_0$ m upstream of the weir by a level or float gage.

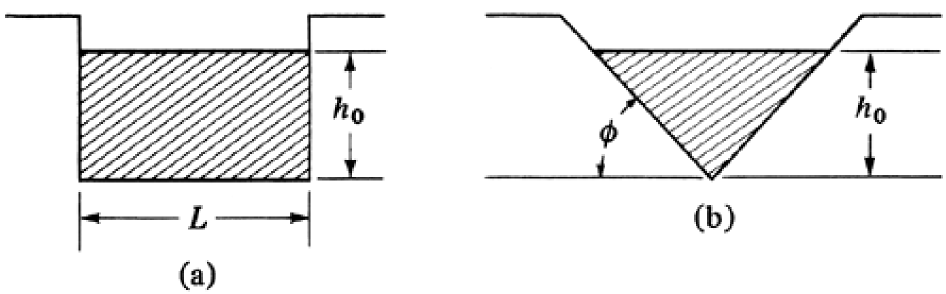

Figure 3.2-7. Types of weirs: (a) rectangular, (b) triangular.

The equation for the volumetric flow rate q in m^3/s for a rectangular weir is given by

Equation 3.2-16.

$$q = 0.415(L - 0.2h_0)h_0^{1.5}\sqrt{2g}$$

where L = crest length in m, g = 9.80665 m/s^2, and h_0 = weir head in m. This is called the *modified Francis weir formula* and it agrees with experimental values within 3% if $L > 2h_0$, velocity upstream < 0.6 m/s, h_0 > 0.09 m, and the height of the crest above the bottom of the channel > $3h_0$. In English units L and h are in ft, q in ft^3/s, and g = 32.174 ft/s^2.

For the triangular notch weir,

Equation 3.2-17.

$$q = \frac{0.31 h_0^{2.5}}{\tan \phi}\sqrt{2g}$$

Both Eqs. (3.2-16) and (3.2-17) apply only to water. For other liquids, see data given elsewhere (P1).

PUMPS AND GAS-MOVING EQUIPMENT

Introduction

In order to make a fluid flow from one point to another in a closed conduit or pipe, it is necessary to have a driving force. Sometimes this force is supplied by gravity, where differences in elevation occur. Usually, the energy or driving force is supplied by a mechanical device such as a pump or blower, which increases the mechanical energy of the fluid. This energy may be used to increase the velocity (move the fluid), the pressure, or the elevation of the fluid, as seen in the mechanical-energy-balance equation (2.7-28), which relates v, p, ρ, and work. The most common methods of adding energy are by positive displacement or centrifugal action.

Generally, the word "pump" designates a machine or device for moving an incompressible liquid. Fans, blowers, and compressors are devices for moving gas (usually air). Fans discharge large volumes of gas at low pressures on the order of several hundred mm of water. Blowers and compressors discharge gases at higher pressures. In pumps and fans the density of the fluid does not change appreciably, and incompressible flow can be assumed. Compressible flow theory is used for blowers and compressors.

Pumps

Power and work required

Using the total mechanical-energy-balance equation (2.7-28) on a pump and piping system, the actual or theoretical mechanical energy W_S J/kg added to the fluid by the pump can be calculated. Example 2.7-5 shows such a case. If η is the fractional efficiency and W_p the shaft work delivered to the pump, Eq. (2.7-30) gives

Equation 3.3-1.

$$W_p = -\frac{W_S}{\eta}$$

The actual or brake power of a pump is as follows:

Equation 3.3-2.

$$\text{brake kW} = \frac{W_p m}{1000} = -\frac{W_S m}{\eta \times 1000} \qquad \text{(SI)}$$

$$\text{brake hp} = \frac{W_p m}{550} = -\frac{W_S m}{\eta \times 550} \qquad \text{(English)}$$

where W_p is J/kg, m is the flow rate in kg/s, and 1000 is the conversion factor W/kW. In English units, W_S is in ft · lb_f/lb_m and m in lb_m/s. The theoretical or fluid power is

Equation 3.3-3.

$$\text{theoretical power} = (\text{brake kW})(\eta)$$

The mechanical energy W_S in J/kg added to the fluid is often expressed as the developed head H of the pump in m of fluid being pumped, where

Equation 3.3-4.

$$-W_S = Hg \qquad \text{(SI)}$$

$$-W_S = H\frac{g}{g_c} \qquad \text{(English)}$$

To calculate the power of a fan where the pressure difference is on the order of a few hundred mm of water, a linear average density of the gas between the inlet and outlet of the fan is used to calculate W_S and brake kW or horsepower.

Electric motor efficiency

Since most pumps are driven by electric motors, the efficiency of the electric motor must be taken into account to determine the total electric power to the motor. Typical efficiencies η_e of electric motors are as follows: 77% for $\frac{1}{2}$-kW motors, 82% for 2 kW, 85% for 5 kW, 88% for 20 kW, 90% for 50 kW, 91% for 100 kW, and 93% for 500 kW and larger. Hence, the total electric power input equals the brake power divided by the electric motor drive efficiency η_e:

Equation 3.3-5.

$$\text{electric power input (kW)} = \frac{\text{brake kW}}{\eta_e} = \frac{-W_S m}{\eta \eta_e \cdot 1000}$$

***Suction lift of pumps* (NPSH)**

The power calculated by Eq. (3.3-4) depends on the differences in pressures and not on the actual pressures being above or below atmospheric pressure. However, the lower limit of the absolute pressure in the suction (inlet) line to the pump is fixed by the vapor pressure of the liquid at the temperature of the liquid in the suction line. If the pressure on the liquid in the suction line drops below the vapor pressure, some of the liquid flashes into vapor (*cavitation*). Then no liquid can be drawn into the pump, and vibration can occur.

To avoid flashes of vapor or cavitation, the pressure at the inlet of the pump must be greater than this vapor pressure and exceed it by a value termed the *net positive suction head required,* or $(\text{NPSH})_R$. Pump manufacturers measure these values experimentally and include them with the pumps furnished.

For water below 100°C at 1750 rpm and centrifugal pumps, typical values of $(\text{NPSH})_R$ are as follows (P4): For pressures 3500 kPa (500 psig) or below: up to 200 gpm, 1.5 m (5 ft); 500 gpm, 2.1 m (7 ft); 1000 gpm, 3 m (10 ft); 2000 gpm, 5.5 m (18 ft). At pressures of 7000 kPa (1000 psig) the values are doubled at 200 gpm or less and at 2000 gpm increased by 20%. At an rpm of 3550, the $(\text{NPSH})_R$ increases by about a factor of 2.2.

To calculate the net positive suction head that will be available $(\text{NPSH})_A$ at the pump suction for the system shown in Fig. 3.3-1, Eq. (3.3-6) can be used:

Equation 3.3-6.

$$g(\text{NPSH})_A = \frac{p_1}{\rho} - \frac{p_{vp}}{\rho} + gz_1 - \frac{v^2}{2} - \sum F \qquad \text{(SI)}$$

$$(\text{NPSH})_A = \frac{p_1}{\rho} - \frac{p_{vp}}{\rho} + \frac{g}{g_c}z_1 - \frac{v^2}{2g_c} - \sum F \qquad \text{(English)}$$

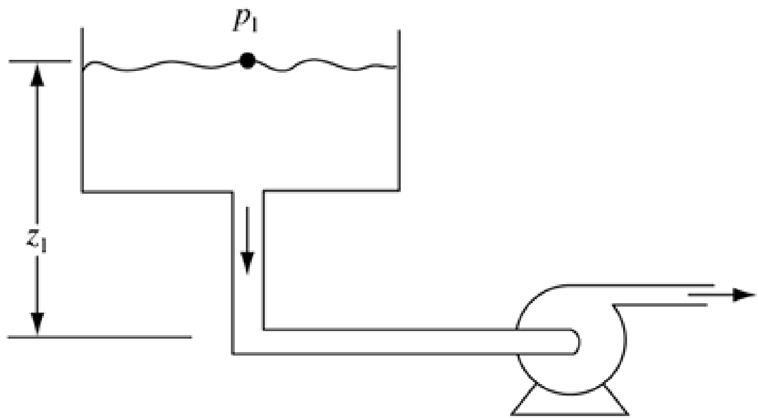

Figure 3.3-1. Diagram for $(\text{NPSH})_A$ available in a pumping system.

where $(\text{NPSH})_A$ is in m (ft), ρ is density of liquid in kg/m^3 (lb$_m$/ft^3), p_1 is pressure above liquid surface in N/m^2 (lb$_f$/ft^2), p_{vp} is vapor pressure of fluid at the given temperature in N/m^2 (lb$_f$/ft^2), z_1 is height of open surface of liquid above pump centerline in m (ft), ΣF is friction loss in suction line to pump from Eq. (2.10-18) in J/kg (ft lb$_f$/lb$_m$), and $v^2/2$ is velocity head in J/kg ($v^2/2g_c$ is ft lb$_f$/lb$_m$). Note that in Eq. (3.3-6) for SI units, the $(\text{NPSH})_A$ in m is multiplied by g to give J/kg.

For cold water and the case where all the terms in Eq. (3.3-6) are small except p_1, at atmospheric pressure the $(\text{NPSH})_A$ is 10.3 m (33.9 ft). However, a practical limit is about 7.5 m (24.6 ft). The available NPSH for a given pump should be at least 1 m (3 ft) more than that required by the manufacturer.

EXAMPLE 3.3-1. $(\text{NPSH})_A$ *Available for Pump*

Water at 50°C is in an open tank at atmospheric pressure. The pump is 3.0 m above the open tank level. The velocity in the pipe is 0.9 m/s. The friction head loss in the pipe has been calculated as 1.0 m. The required $(\text{NPSH})_R$ for this pump is 2.0 m. Calculate the available $(\text{NPSH})_A$.

Solution: From Appendix A.2-3, $\rho = 988.07$ kg/m^3. Also, the vapor pressure $p_{vp} = 12.349$ kPa from A.2-9 and $p_1 = 1.01325 \times 10^5$ Pa. Substituting into Eq. (3.3-6) and noting that z_1 is negative and that the friction loss head of 1.0 m is multiplied by g,

$$9.80665(\text{NPSH})_A = \frac{1.01325 \times 10^5}{988.07} - \frac{12.349 \times 10^3}{988.07} - 9.80665(3.0) - \frac{0.9^2}{2} - 9.80665(1.0)$$

Solving, $(\text{NPSH})_A = 5.14$m

Hence, the available $(\text{NPSH})_A$ of 5.14 m is sufficiently greater than that required of 2.0 m.

Centrifugal pumps

Process industries commonly use centrifugal pumps. They are available in sizes of about 0.004 to 380 m^3/min (1 to 100000 gal/min) and for discharge pressures from a few m of head to 5000 kPa or so. A centrifugal pump in its simplest form consists of an impeller rotating inside a casing. Figure 3.3-2 shows a schematic diagram of a simple centrifugal pump.

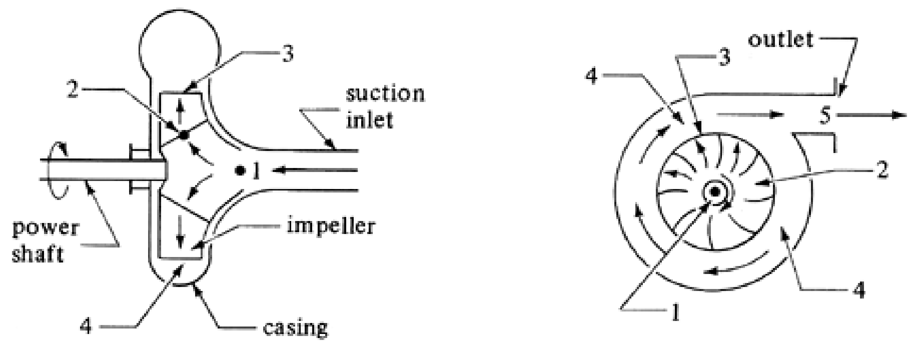

Figure 3.3-2. Simple centrifugal pump.

The liquid enters the pump axially at point 1 in the suction line and then enters the rotating eye of the impeller, where it spreads out radially. On spreading radially it enters the channels between the vanes at point 2 and flows through these channels to point 3 at the periphery of the impeller. From here it is collected in the volute chamber 4 and flows out the pump discharge at 5. The rotation of the impeller imparts a high-velocity head to the fluid, which is changed to a pressure head as the liquid passes into the volute chamber and out the discharge. Some pumps are also made as two-stage or even multistage pumps.

Many complicating factors determine the actual efficiency and performance characteristics of a pump. Hence, the actual experimental performance of the pump is usually employed. The performance is usually expressed by the pump manufacturer in terms of curves called *characteristic curves,* which are usually for water. The head H in m produced will be the same for any liquid of the same viscosity. The pressure produced, $p = H\rho g$, will be in proportion to the density. Viscosities of less than 0.05 Pa · s (50 cp) have little effect on the head produced. The brake kW varies directly as the density.

Pump efficiencies typical of centrifugal pumps at rated capacities are as follows: 50% for 0.075 m^3/min (20 gal/min), 62% for 0.19 m^3/min (50 gal/min), 68% for 0.38 m^3/min (100 gal/min), 75% for 0.76 m^3/min (200 gal/min), 82% for 1.89 m^3/min (500 gal/min), and 85% for 3.8 m^3/min (1000 gal/min).

As rough approximations, the following relationships, called *affinity laws,* can be used for a given pump. The *capacity* q_1 in m^3/s is directly proportional to the rpm N_1 or

Equation 3.3-7.

$$\frac{q_1}{q_2} = \frac{N_1}{N_2}$$

The *head* H_1 is proportional to q_1^2, or

Equation 3.3-8.

$$\frac{H_1}{H_2} = \frac{q_1^2}{q_2^2} = \frac{N_1^2}{N_2^2}$$

The *power consumed* W_1 is proportional to the product of H_1q_1, or

Equation 3.3-9.

$$\frac{W_1}{W_2} = \frac{H_1 q_1}{H_2 q_2} = \frac{N_1^3}{N_2^3}$$

A given pump can be modified when needed for a different capacity by changing the impeller size. Then the *affinity laws* for a constant-rpm N are as follows: The capacity q is proportional to the diameter D, the head H is proportional to D^2, and the brake horsepower W is proportional to D^3.

In most pumps, the speed is generally not varied. Characteristic curves for a typical single-stage centrifugal pump operating at a constant speed are given in Fig. 3.3-3 Most pumps are usually rated on the basis of head and capacity at the point of peak efficiency. The efficiency reaches a peak at about 50 gal/min flow rate. As the discharge rate in gal/min increases, the developed head drops. The brake hp increases, as expected, with flow rate.

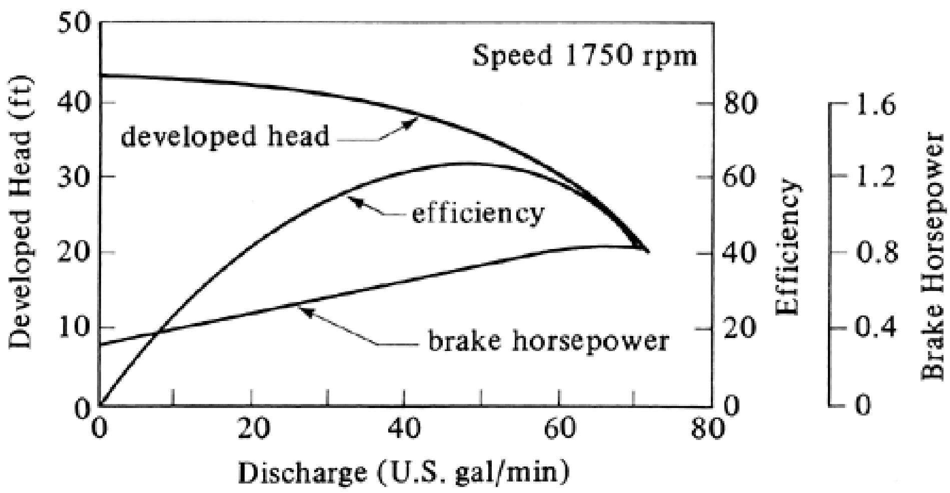

Figure 3.3-3. Characteristic curves for a single-stage centrifugal pump with water. (From W. L. Badger and J. T. Banchero, Introduction to Chemical Engineering. New York: McGraw-Hill Book Company, 1955. With permission.)

EXAMPLE 3.3-2. Calculation of Brake Horsepower of a Pump

In order to see how the brake-hp curve is determined, calculate the brake hp at 40 gal/min flow rate for the pump in Fig. 3.3-3.

Solution: At 40 gal/min, the efficiency η from the curve is about 60% and the head H is 38.5 ft. A flow rate of 40 gal/min of water with a density of 62.4 lb mass/ft^3 is

$$m = \left(\frac{40\ \text{gal/min}}{60\ \text{s/min}}\right)\left(\frac{1\ \text{ft}^3}{7.481\ \text{gal}}\right)\left(62.4\ \frac{\text{lb}_\text{m}}{\text{ft}^3}\right) = 5.56\ \frac{\text{lb}_\text{m}}{\text{s}}$$

The work W_S is as follows, from Eq. (3.3-4):

$$W_S = -H\frac{g}{g_c} = -38.5\ \frac{\text{ft} \cdot \text{lb}_\text{f}}{\text{lb}_\text{m}}$$

The brake hp from Eq. (3.3-2) is

$$\text{brake hp} = \frac{-W_S m}{\eta \cdot 550} = \frac{38.5(5.56)}{0.60(550)} = 0.65\ \text{hp}\ (0.48\ \text{kW})$$

This value agrees with the value on the curve in Fig. 3.3-3.

Positive-displacement pumps

In this class of pumps, a definite volume of liquid is drawn into a chamber and then forced out of the chamber at a higher pressure. There are two main types of positive-displacement pumps. In the *reciprocating pump* the chamber is a stationary cylinder, and liquid is drawn into the cylinder by withdrawal of a piston in the cylinder. Then the liquid is forced out by the piston on the return stroke. In the *rotary pump* the chamber moves from inlet to discharge and back again. In a gear rotary pump two intermeshing gears rotate, and liquid is trapped in the spaces between the teeth and forced out the discharge.

Reciprocating and rotary pumps can be used to very high pressures, whereas centrifugal pumps are limited in their head and are used for lower pressures. Centrifugal pumps deliver liquid at uniform pressure without shocks or pulsations and can handle liquids with large amounts of suspended solids. In general, in chemical and biological processing plants, centrifugal pumps are primarily used.

Equations (3.3-1) through (3.3-5) hold for calculation of the power of positive-displacement pumps. At a constant speed, the flow capacity will remain constant with different liquids. In general, the discharge rate will be directly dependent upon the speed. The power increases directly as the head, and the discharge rate remains nearly constant as the head increases.

Pump efficiencies η of reciprocating pumps used to calculate brake horsepower are as follows: 55% at 2.2 kW (3 hp), 70% at 7.5 kW (10 hp), 77% at 14.9 kW (20 hp), 85% at 37 kW (50 hp), and 90% at 373 kW (500 hp).

Gas-Moving Machinery

Gas-moving machinery comprises mechanical devices used for compressing and moving gases. They are often classified or considered from the standpoint of the pressure heads produced and include fans for low pressures, blowers for intermediate pressures, and compressors for high pressures.

Fans

The commonest method for moving small volumes of gas at low pressures is by means of a *fan.* Large fans are usually centrifugal and their operating principle is similar to that of centrifugal pumps. The discharge heads are low, from about 0.1 m to 1.5 m H_2O. However, in some cases much of the added energy of the fan is converted to velocity energy and a small amount to pressure head.

In a centrifugal fan, the centrifugal force produced by the rotor causes a compression of the gas, called the *static pressure head.* Also, since the velocity of the gas is increased, a velocity head is produced. Both the static-pressure-head increase and velocity-head increase must be included in estimating efficiency and power. Operating efficiencies are in the range 40–70%. The operating pressure of a fan is generally given as inches of water gage and is the sum of the velocity head and the static pressure of the gas leaving the fan. Incompressible flow theory can be used to calculate the power of fans.

When the rpm or speed of centrifugal fans varies, the performance equations are similar to Eqs. (3.3-7)-(3.3-9) for centrifugal pumps.

EXAMPLE 3.3-3. Brake-kW Power of a Centrifugal Fan

It is desired to use 28.32 m^3/min of air (metered at a pressure of 101.3 kPa and 294.1 K) in a process. This amount of air, which is at rest, enters the fan suction at a pressure of 741.7 mm Hg and a temperature of 366.3 K and is discharged at a pressure of 769.6 mm Hg and a velocity of 45.7 m/s. A centrifugal fan having a fan efficiency of 60% is to be used. Calculate the brake-kW power needed.

Solution: Incompressible flow can be assumed, since the pressure drop is only (27.9/741.7)100, or 3.8% of the upstream pressure. The average density of the flowing gas can be used in the mechanical-energy-balance equation.

The density at the suction, point 1, is

$$\rho_1 = \left(28.97\,\frac{\text{kg air}}{\text{kg mol}}\right)\left(\frac{1\ \text{kg mol}}{22.414\ \text{m}^3}\right)\left(\frac{273.2}{366.3}\right)\left(\frac{741.7}{760}\right)$$

$$= 0.940\ \text{kg/m}^3$$

(The molecular weight of 28.97 for air, the volume of 22.414 m^3/kg mol at 101.3 kPa, and 273.2 K were obtained from Appendix A.1.) The density at the discharge, point 2, is

$$\rho_2 = (0.940)\,\frac{769.6}{741.7} = 0.975\ \text{kg/m}^3$$

The average density of the gas is

$$\rho_{\text{av}} = \frac{\rho_1 + \rho_2}{2} = \frac{0.940 + 0.975}{2} = 0.958\ \text{kg/m}^3$$

The mass flow rate of the gas is

$$m = \left(28.32\,\frac{\text{m}^3}{\text{min}}\right)\left(\frac{1\ \text{min}}{60\ \text{s}}\right)\left(\frac{1\ \text{kg mol}}{22.414\ \text{m}^3}\right)\left(\frac{273.2}{294.1}\right)\left(28.97\,\frac{\text{kg}}{\text{kg mol}}\right)$$

$$= 0.5663\ \text{kg/s}$$

The developed pressure head is

$$\frac{p_2 - p_1}{\rho_{\text{av}}} = \frac{(769.6 - 741.7)\ \text{mm Hg}}{760\ \text{mm/atm}}\left(1.01325 \times 10^5\,\frac{\text{N/m}^2}{\text{atm}}\right)\left(\frac{1}{0.958\ \text{kg/m}^3}\right)$$

$$= 3883\ \text{J/kg}$$

The developed velocity head for $v_1 = 0$ is

$$\frac{v_2^2}{2} = \frac{(45.7)^2}{2} = 1044\ \text{J/kg}$$

Writing the mechanical-energy-balance equation (2.7-28),

$$z_1 g + \frac{v_1^2}{2} + \frac{p_1}{\rho} - W_S = z_2 g + \frac{v_2^2}{2} + \frac{p_2}{\rho} + \sum F$$

Setting $z_1 = 0$, $z_2 = 0$, $v_1 = 0$, and $\Sigma F = 0$, and solving for W_S,

$$-W_S = \frac{p_2 - p_1}{\rho_{\text{av}}} + \frac{v_2^2}{2} = 3883 + 1044 = 4927\ \text{J/kg}$$

Substituting into Eq. (3.3-2),

$$\text{brake kW} = \frac{-W_S m}{\eta \cdot 1000} = \frac{4927(0.5663)}{0.60(1000)} = 4.65 \text{ kW } (6.23 \text{ hp})$$

Blowers and compressors

For handling gas volumes at higher pressure rises than fans, several distinct types of equipment are used. *Turboblowers* or *centrifugal compressors* are widely used to move large volumes of gas for pressure rises from about 5 kPa to several thousand kPa. The principles of operation for a turboblower are the same as for a centrifugal pump. The turboblower resembles the centrifugal pump in appearance, the main difference being that the gas in the blower is compressible. The head of the turboblower, as in a centrifugal pump, is independent of the fluid handled. Multistage turboblowers are often used to go to the higher pressures.

Rotary blowers and compressors are machines of the positive-displacement type and are essentially constant-volume flow-rate machines with variable discharge pressure. Changing the speed will change the volume flow rate. Details of construction of the various types (P1) vary considerably, and pressures up to about 1000 kPa can be obtained, depending on the type.

Reciprocating compressers which are of the positive displacement type using pistons are available for higher pressures. Multistage machines are also available for pressures up to 10 000 kPa or more.

Equations for Compression of Gases

In blowers and compressors, pressure changes are large and compressible flow occurs. Since the density changes markedly, the mechanical-energy-balance equation must be written in differential form and then integrated to obtain the work of compression. In compression of gases the static-head terms, velocity-head terms, and friction terms are dropped and only the work term dW and the dp/ρ term remain in the differential form of the mechanical-energy equation; or,

Equation 3.3-10.

$$dW = \frac{dp}{\rho}$$

Integration between the suction pressure p_1 and discharge pressure p_2 gives the work of compression:

Equation 3.3-11.

$$W = \int_{p_1}^{p_2} \frac{dp}{\rho}$$

Isothermal compression

To integrate Eq. (3.3-11) for a perfect gas, either isothermal or adiabatic compression is assumed. For isothermal compression, where the gas is cooled on compression, p/ρ is a constant equal to RT/M, where R = 8314.3 J/kg mol · K in SI units and 1545.3 ft · lb_f/lb mol · °R in English units. Then,

Equation 3.3-12.

$$\frac{p_1}{\rho_1} = \frac{p}{\rho}$$

Solving for ρ in Eq. (3.3-12) and substituting it in Eq. (3.3-11), the work for isothermal compression is

Equation 3.3-13.

$$-W_S = \frac{p_1}{\rho_1}\int_{p_1}^{p_2}\frac{dp}{p} = \frac{p_1}{\rho_1}\ln\frac{p_2}{p_1} = \frac{2.3026RT_1}{M}\log\frac{p_2}{p_1}$$

Also, $T_1 = T_2$, since the process is isothermal.

Adiabatic compression

For adiabatic compression, the fluid follows an isentropic path and

Equation 3.3-14.

$$\frac{p_1}{p} = \left(\frac{\rho_1}{\rho}\right)^{\gamma}$$

where $\gamma = c_p/c_v$, the ratio of heat capacities. By combining Eqs. (3.3-11) and (3.3-14) and integrating,

Equation 3.3-15.

$$-W_S = \frac{\gamma}{\gamma - 1}\frac{RT_1}{M}\left[\left(\frac{p_2}{p_1}\right)^{(\gamma-1)/\gamma} - 1\right]$$

The adiabatic temperatures are related by

Equation 3.3-16.

$$\frac{T_2}{T_1} = \left(\frac{p_2}{p_1}\right)^{(\gamma-1)/\gamma}$$

To calculate the brake power when the efficiency is η,

Equation 3.3-17.

$$\text{brake kW} = \frac{-W_S m}{(\eta)(1000)}$$

where m = kg gas/s and W_S = J/kg.

The values of γ are approximately 1.40 for air, 1.31 for methane, 1.29 for SO_2, 1.20 for ethane, and 1.40 for N_2 (P1). For a given compression ratio, the work for isothermal compression in Eq. (3.3-13) is less than the work for adiabatic compression in Eq. (3.3-15). Hence, cooling is sometimes used in compressors.

EXAMPLE 3.3-4. Compression of Methane

A single-stage compressor is to compress 7.56×10^{-3} kg mol/s of methane gas at 26.7°C and 137.9 kPa abs to 551.6 kPa abs.

a. Calculate the power required if the mechanical efficiency is 80% and the compression is adiabatic.
b. Repeat, but for isothermal compression.

Solution: For part (a), p_1 = 137.9 kPa, p_2 = 551.6 kPa, M = 16.0 kg mass/kg mol, and T_1 = 273.2 + 26.7 = 299.9 K. The mass flow rate per sec is

$$m = (7.56 \times 10^{-3}\ \text{kg mol/s})(16.0\ \text{kg/kg mol}) = 0.121\ \frac{\text{kg}}{\text{s}}$$

Substituting into Eq. (3.3-15) for $\gamma = 1.31$ for methane and $p_2/p_1 = 551.6/137.9 = 4.0/1$,

$$-W_S = \frac{\gamma}{\gamma-1}\frac{RT_1}{M}\left[\left(\frac{p_2}{p_1}\right)^{(\gamma-1)/\gamma} - 1\right]$$

$$= \left(\frac{1.31}{1.31-1}\right)\frac{8314.3(299.9)}{16.0}\left[\left(\frac{4}{1}\right)^{(1.31-1)/1.31} - 1\right]$$

$$= 256\,300 \text{ J/kg}$$

Using Eq. (3.3-17),

$$\text{brake kW} = \frac{-W_S m}{\eta \cdot 1000} = \frac{(256\,300)0.121}{0.80(1000)} = 38.74 \text{ kW } (52.0 \text{ hp})$$

For part (b), using Eq. (3.3-13) for isothermal compression,

$$-W_S = \frac{2.3026RT_1}{M}\log\frac{p_2}{p_1} = \frac{2.3026(8314.3)(299.9)}{16.0}\log\frac{4}{1}$$

$$= 216\,000 \text{ J/kg}$$

$$\text{brake kW} = \frac{-W_S m}{\eta \cdot 1000} = \frac{(216\,000)0.121}{0.80(1000)} = 32.67 \text{ kW } (43.8 \text{ hp})$$

Hence, isothermal compression uses 15.8% less power.

Polytropic compression

In large compressors neither isothermal nor adiabatic compression is achieved. This polytropic path is

Equation 3.3-18.

$$\frac{p_1}{p} = \left(\frac{\rho_1}{\rho}\right)^n$$

For isothermal compression $n = 1.0$ and for adiabatic, $n = \gamma$. The value of n is found by measuring the pressure p_1 and density ρ_1 at the inlet and p_2 and ρ_2 at the discharge and substituting these values into Eq. (3.3-18).

Multistage compression ratios

Water cooling is used between each stage in multistage compressors to reduce the outlet temperature to near the inlet temperature for minimum power requirement. The compression ratios should be the same for each stage so that the total power is a minimum. This gives the same power in each stage. Hence, for n stages, the compression ratio (p_b/p_a) for each stage is

Equation 3.3-19.

$$\frac{p_b}{p_a} = \left(\frac{p_n}{p_1}\right)^{1/n}$$

where p_1 is the inlet pressure and p_n the outlet pressure from n stages. For two stages, the compression ratio is $\sqrt{p_n/p_1}$.

AGITATION AND MIXING OF FLUIDS AND POWER REQUIREMENTS

Purposes of Agitation

In the chemical and other processing industries, many operations are dependent to a great extent on effective agitation and mixing of fluids. Generally, *agitation* refers to forcing a fluid by mechanical means to flow in a circulatory or other pattern inside a vessel. *Mixing* usually implies the taking of two or more separate phases, such as a fluid and a powdered solid or two fluids, and causing them to be randomly distributed through one another.

There are a number of purposes for agitating fluids, some of which are briefly summarized:

1. Blending of two miscible liquids, such as ethyl alcohol and water.
2. Dissolving solids in liquids, such as salt in water.
3. Dispersing a gas in a liquid as fine bubbles, such as oxygen from air in a suspension of microorganisms for fermentation or for the activated sludge process in waste treatment.
4. Suspending of fine solid particles in a liquid, as in the catalytic hydrogenation of a liquid, where solid catalyst particles and hydrogen bubbles are dispersed in the liquid.
5. Agitation of the fluid to increase heat transfer between the fluid and a coil or jacket in the vessel wall.

Equipment for Agitation

Generally, liquids are agitated in a cylindrical vessel which can be closed or open to the air. The height of liquid is approximately equal to the tank diameter. An impeller mounted on a shaft is driven by an electric motor. A typical agitator assembly is shown in Fig. 3.4-1.

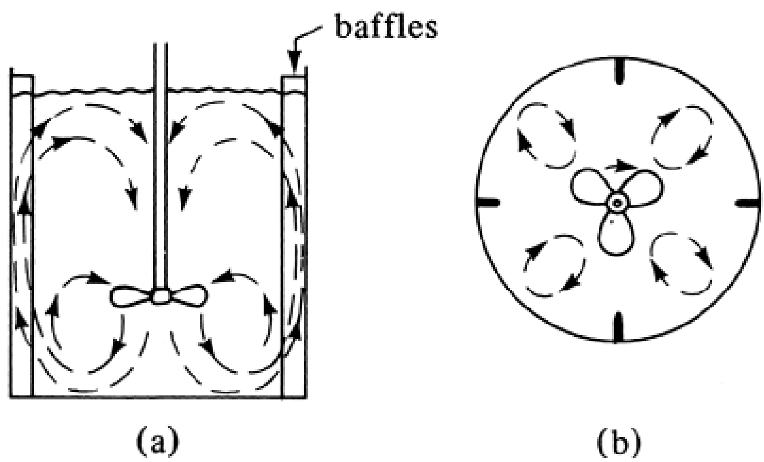

Figure 3.4-1. Baffled tank and three-blade propeller agitator with axial-flow pattern: (a) side view, (b) bottom view.

Three-blade propeller agitator

There are several types of agitators that are widely used. A common type, shown in Fig. 3.4-1, is a three-bladed marine-type propeller similar to the propeller blade used in driving boats. The propeller can be a side-entering type in a tank or be clamped on the side of an open vessel in an off-center position. These propellers turn at high speeds of 400 to 1750 rpm (revolutions per minute) and are used for liquids of low viscosity. The flow pattern in a baffled tank with a propeller positioned on the center of the tank is shown in Fig. 3.4-1. This type of flow pattern is called *axial flow* since the fluid flows axially down the center axis or propeller shaft and up on the sides of the tank as shown.

Paddle agitators

Various types of paddle agitators are often used at low speeds, between about 20 and 200 rpm. Two-bladed and four-bladed flat paddles are often used, as shown in Fig. 3.4-2a. The total length of the paddle impeller is usually 60–80% of the tank diameter and the width of the blade $\frac{1}{6}$ to $\frac{1}{10}$ of its length. At low speeds mild agitation is obtained in an unbaffled vessel. At higher speeds baffles are used, since, without baffles, the liquid is simply swirled around with little actual mixing. The paddle agitator is ineffective for suspending solids, since good radial flow is present but little vertical or axial flow. An anchor or gate paddle, shown in Fig. 3.4-2b, is often used. It sweeps or scrapes the tank walls and sometimes the tank bottom. It is used with viscous liquids where deposits on walls can occur and to improve heat transfer to the walls. However, it is a poor mixer. Paddle agitators are often used to process starch pastes, paints, adhesives, and cosmetics.

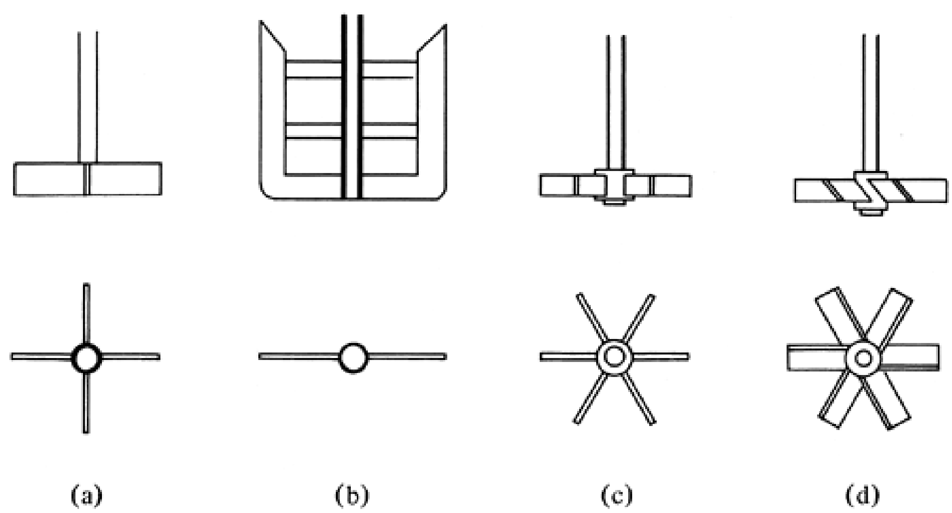

Figure 3.4-2. Various types of agitators: (a) four-blade paddle, (b) gate or anchor paddle, (c) six-blade open turbine, (d) pitched-blade (45°) turbine.

Turbine agitators

Turbines that resemble multibladed paddle agitators with shorter blades are used at high speeds for liquids with a very wide range of viscosities. The diameter of a turbine is normally between 30 and 50% of the tank diameter. The turbines usually have four or six blades. Figure 3.4-3 shows a flat six-blade turbine agitator with disk. In Fig. 3.4-2c a flat six-blade open turbine is shown. The turbines with flat blades give radial flow, as shown in Fig. 3.4-3. They are also useful for good gas dispersion; the gas is introduced just below the impeller at its axis and is drawn up to the blades and chopped into fine bubbles. In the pitched-blade turbine shown in Fig. 3.4-2d, with the blades at 45°, some axial flow is imparted so that a combination of axial and radial flow is present. This type is useful in suspending solids since the currents flow downward and then sweep up the solids.

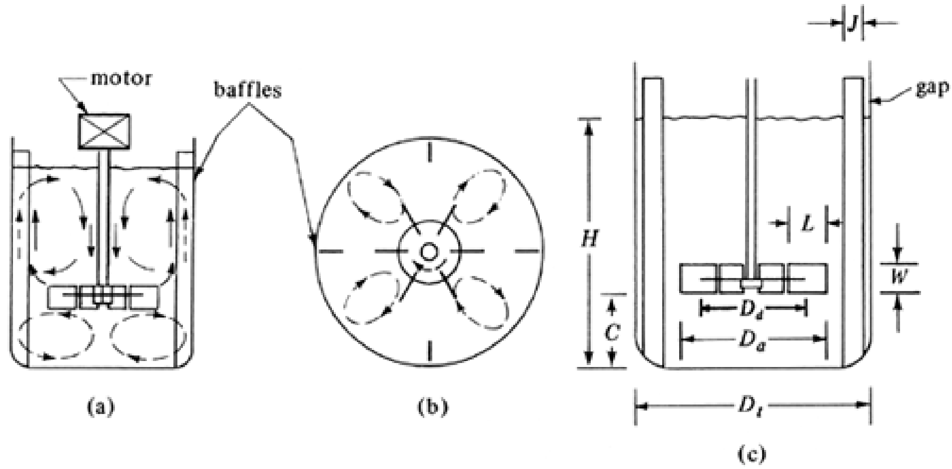

Figure 3.4-3. Baffled tank with six-blade turbine agitator with disk showing flow patterns: (a) side view, (b) bottom view, (c) dimensions of turbine and tank.

Often a pitched-blade turbine with only four blades is used in suspension of solids. A high-efficiency, three-blade impeller (B6, F2) shown in Fig. 3.4-4a is similar to a four-blade pitched turbine; however, it features a larger pitch angle of 30–60° at the hub and a smaller angle of 10–30° at the tip. This axial-flow impeller produces more fluid motion and mixing per unit of power and is very useful in suspension of solids.

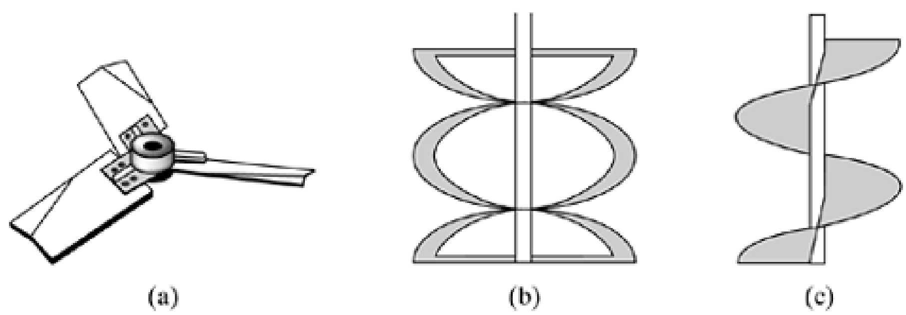

*Figure 3.4-4. Other types of agitators: (a) high-efficiency, three-blade impeller, (b) double-helical-ribbon, (c) helical-screw. [Reprinted with permission from André Bakker and Lewis E. Gates, Chem. Eng. Progr., **91** (Dec.), 25 (1995). Copyright by the American Institute of Chemical Engineers.]*

Helical-ribbon agitators

This type of agitator is used in highly viscous solutions and operates at a low RPM in the *laminar* region. The ribbon is formed in a helical path and is attached to a central shaft. The liquid moves in a tortuous flow path down the center and up along the sides in a twisting motion. Similar types are the double-helical-ribbon agitator shown in Fig. 3.4-4b and the helical-screw impeller shown in Fig. 3.4-4c.

Agitator selection and viscosity ranges

The viscosity of the fluid is one of several factors affecting the selection of the type of agitator. Indications of the viscosity ranges of these agitators are as follows. Propellers are used for fluid viscosities below about 3 Pa · s (3000 cp); turbines can be used below about 100 Pa · s (100 000 cp); modified paddles such as anchor agitators can be used above 50 Pa · s to about 500 Pa · s (500 000 cp); helical and ribbon-type agitators are often used above this range to about 1000 Pa · s and have been used up to 25 000 Pa · s. For viscosities greater than about 2.5 to 5 Pa · s (5000 cp) and above, baffles are not needed since little swirling is present above these viscosities.

Flow Patterns in Agitation

The flow patterns in an agitated tank depend upon the fluid properties, the geometry of the tank, the types of baffles in the tank, and the agitator itself. If a propeller or other agitator is mounted vertically in the center of a tank with no baffles, a swirling flow pattern usually develops. Generally, this is undesirable, because of excessive air entrainment, development of a large vortex, surging, and the like, especially at high speeds. To prevent this, an angular off-center position can be used with propellors with small horsepower. However, for vigorous agitation at higher power, unbalanced forces can become severe and limit the use of higher power.

For vigorous agitation with vertical agitators, baffles are generally used to reduce swirling and still promote good mixing. Baffles installed vertically on the walls of the tank are shown in Fig. 3.4-3. Usually four baffles are sufficient, with their width being about $\frac{1}{12}$ of the tank diameter for turbines and propellers. The turbine impeller drives the liquid radially against the wall, where it divides with one portion flowing upward near the surface and back to the impeller from above and the other flowing downward. Sometimes, in tanks with large liquid depths much greater than the tank diameter, two or three impellers are mounted on the same shaft, each acting as a separate mixer. The bottom impeller is about 1.0 impeller diameter above the tank bottom.

In an agitation system, the volume flow rate of fluid moved by the impeller, or circulation rate, is important in sweeping out the whole volume of the mixer in a reasonable time. Also, turbulence in the moving stream is important for mixing, since it entrains the material from the bulk liquid in the tank into the flowing stream. Some agitation systems require high turbulence with low circulation rates, others low turbulence with high circulation rates. This often depends on the types of fluids being mixed and on the amount of mixing needed.

Typical "Standard" Design of Turbine

The turbine agitator shown in Fig. 3.4-3 is the most commonly used agitator in the process industries. For design of an ordinary agitation system, this type of agitator is often used in the initial design. The geometric proportions of the agitation system which are considered as a typical "standard" design are given in Table 3.4-1. These relative proportions are the basis for the major correlations of agitator performance in numerous publications. (See Fig. 3.4-3c for nomenclature.)

Table 3.4-1. Geometric Proportions for a "Standard" Agitation System

$\frac{D_a}{D_t} = 0.3 \text{ to } 0.5$		$\frac{H}{D_t} = 1$	$\frac{C}{D_t} = \frac{1}{3}$
$\frac{W}{D_a} = \frac{1}{5}$	$\frac{D_d}{D_a} = \frac{2}{3}$	$\frac{L}{D_a} = \frac{1}{4}$	$\frac{J}{D_t} = \frac{1}{12}$

In some cases $W/D_a = \frac{1}{8}$ for agitator correlations. The number of baffles is four in most uses. The clearance or gap between the baffles and the wall is usually 0.10–0.15 J to ensure that liquid does not form stagnant pockets next to the baffle and wall. In a few correlations the ratio of baffle to tank diameter is $J/D_t = \frac{1}{10}$ instead of $\frac{1}{12}$.

Power Used in Agitated Vessels

In the design of an agitated vessel, an important factor is the power required to drive the impeller. Since the power required for a given system cannot be predicted theoretically, empirical correlations have been developed to predict the power required. The presence or absence of turbulence can be correlated with the impeller Reynolds number N'_{Re}, defined as

Equation 3.4-1.

$$N'_{\mathrm{Re}} = \frac{D_a^2 N \rho}{\mu}$$

where D_a is the impeller (agitator) diameter in m, N is rotational speed in rev/s, ρ is fluid density in kg/m^3, and μ is viscosity in kg/m · s. The flow is laminar in the tank for $N'_{\mathrm{Re}} < 10$, turbulent for $N'_{\mathrm{Re}} > 10^4$, and for a range between 10 and 10^4, the flow is transitional, being turbulent at the impeller and laminar in remote parts of the vessel.

Power consumption is related to fluid density ρ, fluid viscosity μ, rotational speed N, and impeller diameter D_a by plots of power number N_p versus N'_{Re}. The power number is

Equation 3.4-2.

$$N_p = \frac{P}{\rho N^3 D_a^5} \qquad \text{(SI)}$$

$$N_p = \frac{P g_c}{\rho N^3 D_a^5} \qquad \text{(English)}$$

where P = power in J/s or W. In English units, P = ft · lb$_f$/s.

Figure 3.4-5 is a correlation (B3, R1) for frequently used impellers with Newtonian liquids contained in baffled, cylindrical vessels. Dimensional measurements of baffle, tank, and impeller sizes are given in Fig. 3.4-3c. These curves may also be used for the same impellers in unbaffled tanks when N'_{Re} is 300 or less (B3, R1). When N'_{Re} is above 300, the power consumption for an unbaffled vessel is considerably less than for a baffled vessel. Curves for other impellers are also available (B3, R1).

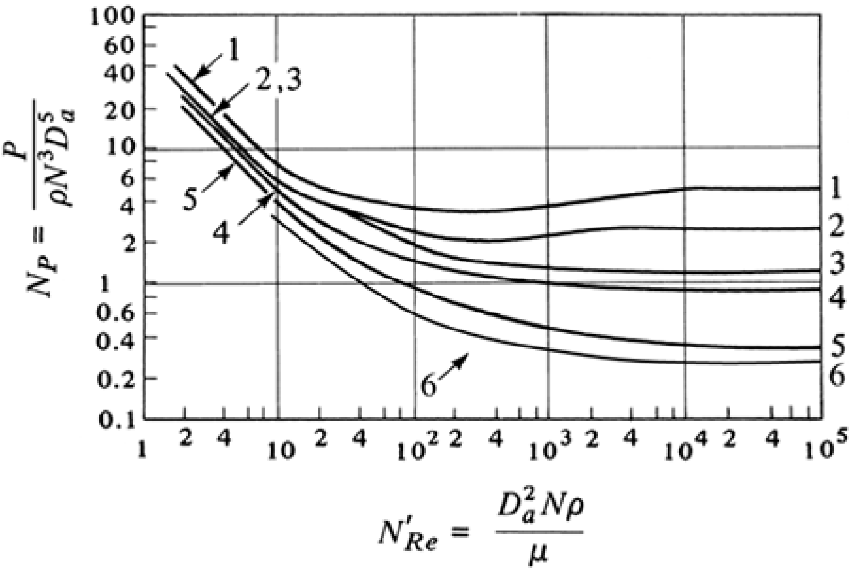

Curve 1. Flat six-blade turbine with disk (like Fig. 3.4-3 but six blades); $D_a/W = 5$; four baffles each $D_t/J = 12$.

Curve 2. Flat six-blade open turbine (like Fig. 3.4-2c); $D_a/W = 8$; four baffles each $D_t/J = 12$.

Curve 3. Six-blade open turbine (pitched-blade) but blades at 45° (like Fig. 3.4-2d); $D_a/W = 8$; four baffles each $D_t/J = 12$.

Curve 4. Propeller (like Fig. 3.4-1); pitch = $2D_a$; four baffles each $D_t/J = 10$; also holds for same propeller in angular off-center position with no baffles.

Curve 5. Propeller; pitch = D_a; four baffles each $D_t/J = 10$; also holds for same propeller in angular off-center position with no baffles.

Curve 6. High-efficiency impeller (like Fig. 3-4-4a); four baffles each $D_t/J = 12$.

[Curves 1, 2, and 3 reprinted with permission from R. L. Bates. P. L. Fondy, and R. R. Corpstein, Ind. Eng. Chem. Proc. Des. Dev., 2, 310 (1963). Copyright by the American Chemical Society. Curves 4 and 5 from J. H. Rushton, E. W. Costich, and H. J. Everett, Chem. Eng. Progr., 46, 395, 467 (1950). With permission.]

Figure 3.4-5. Power correlations for various impellers and baffles (see Fig. 3.4-3c for dimension D_a, D_t, J, and W).

The power-number curve for N_p for the high-efficiency, three-blade impeller is shown as curve 6 in Fig. 3-4-5.

EXAMPLE 3.4-1. Power Consumption in an Agitator

A flat-blade turbine agitator with disk having six blades is installed in a tank similar to Fig. 3.4-3. The tank diameter D_t is 1.83 m, the turbine diameter D_a is 0.61 m, $D_t = H$, and the width W is 0.122 m. The tank contains four baffles, each having a width J of 0.15 m. The turbine is operated at 90 rpm and the liquid in the tank has a viscosity of 10 cp and a density of 929 kg/m^3.

a. Calculate the required kW of the mixer.

b. For the same conditions, except for the solution having a viscosity of 100 000 cp, calculate the required kW.

Solution:

For part (a) the following data are given: $D_a = 0.61$ m, $W = 0.122$ m, $D_t = 1.83$ m, $J = 0.15$ m, $N = 90/60 = 1.50$ rev/s, $\rho = 929$ kg/m^3, and

$$\mu = (10.0\ \text{cp})(1 \times 10^{-3}) = 0.01\ \frac{\text{kg}}{\text{m}\cdot\text{s}} = 0.01\ \text{Pa}\cdot\text{s}$$

Using Eq. (3.4-1), the Reynolds number is

$$N'_{\text{Re}} = \frac{D_a^2 N\rho}{\mu} = \frac{(0.61)^2(1.50)929}{0.01} = 5.185 \times 10^4$$

Using curve 1 in Fig. 3.4-5, since $D_a/W = 5$ and $D_t/J = 12$, $N_P = 5$ for $N'_{\text{Re}} = 5.185 \times 10^4$. Solving for P in Eq. (3.4-2) and substituting known values,

$$P = N_P \rho N^3 D_a^5 = 5(929)(1.50)^3(0.61)^5$$

$$= 1324\ \text{J/s} = 1.324\ \text{kW}\ (1.77\ \text{hp})$$

For part (b),

$$\mu = 100\,000(1 \times 10^{-3}) = 100\ \frac{\text{kg}}{\text{m}\cdot\text{s}}$$

$$N'_{\text{Re}} = \frac{(0.61)^2(1.50)929}{100} = 5.185$$

This is in the laminar flow region. From Fig. 3.4-5, $N_P = 14$.

$$P = 14(929)(1.50)^3(0.61)^5 = 3707\ \text{J/s} = 3.71\ \text{kW}\ (4.98\ \text{hp})$$

Hence, a 10 000-fold increase in viscosity only increases the power from 1.324 to 3.71 kW.

Variations of various geometric ratios from the "standard" design can have different effects on the power number N_P in the turbulent region of the various turbine agitators as follows (B3):

1. For the flat six-blade open turbine, $N_P \propto (W/D_a)^{1.0}$.
2. For the flat six-blade open turbine, varying D_a/D_t from 0.25 to 0.50 has practically no effect on N_P.
3. With two six-blade open turbines installed on the same shaft and the spacing between the two impellers (vertical distance between the bottom edges of the two turbines) being at least equal to D_a, the total power is 1.9 times a single flat-blade impeller. For two six-blade pitched-blade (45°) turbines, the power is also about 1.9 times that of a single pitched-blade impeller.
4. A baffled, vertical square tank or a horizontal cylindrical tank has the same power number as a vertical cylindrical tank. However, marked changes in the flow patterns occur.

The power number for a plain anchor-type agitator similar to Fig. 3.4-2b but without the two horizontal crossbars is as follows for $N'_{\text{Re}} < 100$ (H2):

Equation 3.4-3.

$$N_P = 215(N'_{\text{Re}})^{-0.955}$$

where $D_a/D_t = 0.90$, $W/D_t = 0.10$, and $C/D_t = 0.05$.

The power number for a helical-ribbon agitator for very viscous liquids for $N'_{\text{Re}} < 20$ is as follows (H2, P3):

Equation 3.4-4.

$$N_p = 186(N'_{\mathrm{Re}})^{-1} \qquad \text{(agitator pitch/tank diameter = 1.0)}$$

Equation 3.4-5.

$$N_p = 290(N'_{\mathrm{Re}})^{-1} \qquad \text{(agitator pitch/tank diameter = 0.5)}$$

The typical dimensional ratios used are $D_a/D_t = 0.95$, with some ratios as low as 0.75, and $W/D_t = 0.095$. The agitator pitch is the vertical distance of a single flight of the helix in a 360° rotation (B6).

Agitator Scale-Up

Introduction

In the process industries, experimental data are often available for a laboratory-size or pilot-unit-size agitation system, and it is desired to scale up the results to design a full-scale unit. Since the processes to be scaled up are very diverse, no single method can handle all types of scale-up problems, and many approaches to scale-up exist. Geometric similarity is, of course, important and simplest to achieve. Kinematic similarity can be defined in terms of ratios of velocities or of times (R2). Dynamic similarity requires fixed ratios of viscous, inertial, or gravitational forces. Even if geometric similarity is achieved, dynamic and kinematic similarity often cannot be obtained at the same time. Hence, it is frequently up to the designer to rely on judgment and experience in the scale-up.

In many cases, the main objectives usually present in an agitation process are as follows: *equal liquid motion,* such as in liquid blending, where the liquid motion or corresponding velocities are approximately the same in both cases; *equal suspension of solids,* where the levels of suspension are the same; and *equal rates of mass transfer,* where mass transfer is occurring between a liquid and a solid phase, liquid-liquid phases, and so on, and the rates are the same.

Scale-up procedure

A suggested step-by-step procedure to follow in the scale-up is detailed as follows for scaling up from the initial conditions, where the geometric sizes given in Table 3.4-1 are D_{a1}, D_{T1}, H_1, W_1, and so on, to the final conditions of D_{a2}, D_{T2}, and so on.

1. Calculate the scale-up ratio R. Assuming that the original vessel is a standard cylinder with $D_{T1} = H_1$, the volume V_1 is

   Equation 3.4-6.

   $$V_1 = \left(\frac{\pi D_{T1}^2}{4}\right)(H_1) = \left(\frac{\pi D_{T1}^3}{4}\right)$$

Then the ratio of the volumes is

Equation 3.4-7.

$$\frac{V_2}{V_1} = \frac{\pi D_{T2}^3/4}{\pi D_{T1}^3/4} = \frac{D_{T2}^3}{D_{T1}^3}$$

The scale-up ratio is then

Equation 3.4-8.

$$R = \left(\frac{V_2}{V_1}\right)^{1/3} = \frac{D_{T2}}{D_{T1}}$$

2. Using this value of R, apply it to all of the dimensions in Table 3.4-1 to calculate the new dimensions. For example,

Equation 3.4-9.

$$D_{a2} = RD_{a1}, \qquad J_2 = RJ_1, \ldots$$

3. Then a scale-up rule must be selected and applied to determine the agitator speed N_2 to be used to duplicate the small-scale results using N_1. This equation is as follows (R2):

Equation 3.4-10.

$$N_2 = N_1\left(\frac{1}{R}\right)^n = N_1\left(\frac{D_{T1}}{D_{T2}}\right)^n$$

where $n = 1$ for equal liquid motion, $n = \frac{3}{4}$ for equal suspension of solids, and $n = \frac{2}{3}$ for equal rates of mass transfer (which is equivalent to equal power per unit volume). This value of n is based on empirical and theoretical considerations.

4. Knowing N_2, the power required can be determined using Eq. (3.4-2) and Fig. 3.4-5.

EXAMPLE 3.4-2. Derivation of Scale-Up Rule Exponent

For the scale-up-rule exponent n in Eq. (3.4-10), show the following for turbulent agitation:

a. That when $n = \frac{2}{3}$, the power per unit volume is constant in the scale-up.
b. That when $n = 1.0$, the tip speed is constant in the scale-up.

Solution: For part (a), from Fig. 3.4-5, N_P is constant for the turbulent region. From Eq. (3.4-2),

Equation 3.4-11.

$$P_1 = N_P \rho N_1^3 D_{a1}^5$$

Then for equal power per unit volume, $P_1/V_1 = P_2/V_2$, or, using Eq. (3.4-6),

Equation 3.4-12.

$$\frac{P_1}{V_1} = \frac{P_1}{\pi D_{T1}^3/4} = \frac{P_2}{V_2} = \frac{P_2}{\pi D_{T2}^3/4}$$

Substituting P_1 from Eq. (3.4-11) together with a similar equation for P_2 into Eq. (3.4-12) and combining with Eq. (3.4-8).

Equation 3.4-13.

$$N_2 = N_1\left(\frac{1}{R}\right)^{2/3}$$

For part (b), using Eq. (3.4-10) with $n = 1.0$, rearranging, and multiplying by π,

Equation 3.4-14.

$$N_2 = N_1\left(\frac{D_{T1}}{D_{T2}}\right)^{1.0}$$

Equation 3.4-15.

$$\pi D_{T2} N_2 = \pi D_{T1} N_1$$

where $\pi D_{T2} N_2$ is the tip speed in m/s.

To aid the designer of new agitation systems as well as serve as a guide for evaluating existing systems, some approximate guidelines are given as follows for liquids of normal viscosities (M2): for mild agitation and blending, 0.1 to 0.2 kW/m^3 of fluid (0.0005 to 0.001 hp/gal); for vigorous agitation, 0.4 to 0.6 kW/m^3 (0.002 to 0.003 hp/gal); for intense agitation or where mass transfer is important, 0.8 to 2.0 kW/m^3 (0.004 to 0.010 hp/gal). This power in kW is the actual power delivered to the fluid as given in Fig. 3.4-5 and Eq. (3.4-2). This does not include the power used in the gear boxes and bearings. Typical efficiencies of electric motors are given in Section 3.3B. As an approximation, the power lost in the gear boxes and bearings and in inefficiency of the electric motor is about 30 to 40% of P, the actual power input to the fluid.

EXAMPLE 3.4-3. Scale-Up of Turbine Agitation System

An existing agitation system is the same as given in Example 3.4-1a for a flat-blade turbine with a disk and six blades. The given conditions and sizes are D_{T1} = 1.83 m, D_{a1} = 0.61 m, W_1 = 0.122 m, J_1 = 0.15 m, N_1 = 90/60 = 1.50 rev/s, ρ = 929 kg/m^3, and μ = 0.01 Pa · s. It is desired to scale up these results for a vessel whose volume is 3.0 times as large. Do this for the following two process objectives:

a. Where equal rate of mass transfer is desired.
b. Where equal liquid motion is needed.

***Solution*:** Since $H_1 = D_{T1}$ = 1.83 m, the original tank volume $V_1 = (\pi D_{T1}^2/4)(H_1) = \pi(1.83)^3/4$ = 4.813 m^3. Volume V_2 = 3.0(4.813) = 14.44 m^3. Following the steps in the scale-up procedure, and using Eq. (3.4-8),

$$R = \left(\frac{V_2}{V_1}\right)^{1/3} = \left(\frac{14.44}{4.813}\right)^{1/3} = 1.442$$

The dimensions of the larger agitation system are as follows: D_{T2} **= RD_{T1} = 1.442(1.83) = 2.64 m, D_{a2} = 1.442(0.61) = 0.880 m, W_2 = 1.442(0.122) = 0.176 m, and J_2 = 1.442(0.15) = 0.216 m.**

For part (a), for equal mass transfer, $n = \frac{2}{3}$ in Eq. (3.4-10).

$$N_2 = N_1\left(\frac{1}{R}\right)^{2/3} = (1.50)\left(\frac{1}{1.442}\right)^{2/3} = 1.175 \text{ rev/s (70.5 rpm)}$$

Using Eq. (3.4-1),

$$N'_{\text{Re}} = \frac{D_a^2 N\rho}{\mu} = \frac{(0.880)^2(1.175)929}{0.01} = 8.453 \times 10^4$$

Using N_P = 5.0 in Eq. (3.4-2),

$$P_2 = N_P \rho N_2^3 D_{a2}^5 = 5.0(9.29)(1.175)^3(0.880)^5 = 3977 \text{ J/s} = 3.977 \text{ kW}$$

The power per unit volume is

$$\frac{P_1}{V_1} = \frac{1.324}{4.813} = 0.2752 \text{ kW/m}^3$$

$$\frac{P_2}{V_2} = \frac{3.977}{14.44} = 0.2752 \text{ kW/m}^3$$

The value of 0.2752 kW/m^3 is somewhat lower than the approximate guidelines of 0.8 to 2.0 for mass transfer.

For part (b), for equal liquid motion, $n = 1.0$.

$$N_2 = (1.50)\left(\frac{1}{1.442}\right)^{1.0} = 1.040 \text{ rev/s}$$

$$P_2 = 5.0(929)(1.040)^3(0.880)^5 = 2757 \text{ J/s} = 2.757 \text{ kW}$$

$$\frac{P_2}{V_2} = \frac{2.757}{14.44} = 0.1909 \text{ kW/m}^3$$

Mixing Times of Miscible Liquids

In one method used to study the blending or mixing time for two miscible liquids, an amount of HCl acid is added to an equivalent of NaOH and the time required for the indicator to change color is noted. This is a measure of molecule-molecule mixing. Other experimental methods are also used. Rapid mixing takes place near the impeller, with slower mixing, which depends on the pumping circulation rate, in the outer zones.

In Fig. 3.4-6, a correlation of mixing time is given for a turbine agitator (B5, M5, N1). The dimensionless mixing factor f_t is defined as

Equation 3.4-16.

$$f_t = t_T \frac{(ND_a^2)^{2/3} g^{1/6} D_a^{1/2}}{H^{1/2} D_t^{3/2}}$$

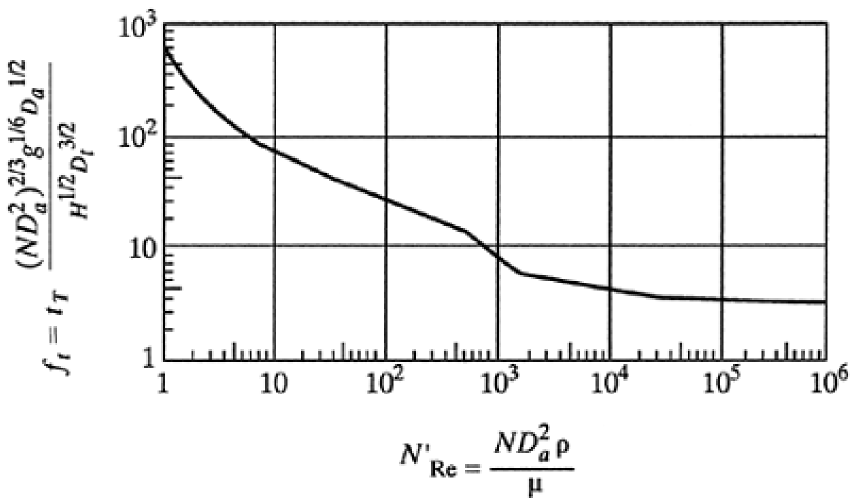

*Figure 3.4-6. Correlation of mixing time for miscible liquids using a turbine in a baffled tank (for a plain turbine, turbine with disk, and pitched-blade turbine). [From "Flow Patterns and Mixing Rates in Agitated Vessels" by K. W. Norwood and A. B. Metzner, A.I.Ch.E.J., **6**, 432 (1960). Reproduced by permission of the American Institute of Chemical Engineers, 1960.]*

where t_T is the mixing time in seconds. For $N'_{Re} > 1000$, since f_t is approximately constant, then $t_T N^{2/3}$ is constant. For some other mixers it has been shown that $t_T N$ is approximately constant. For scaling up from vessel 1 to another size vessel 2 with similar geometry and with the same power/unit volume in the turbulent region, the mixing times are related by

Equation 3.4-17.

$$\frac{t_{T_2}}{t_{T_1}} = \left(\frac{D_{a_2}}{D_{a_1}}\right)^{11/18}$$

Hence, the mixing time increases for the larger vessel. For scaling up while keeping the same mixing time, the power/unit volume *P/V* increases markedly:

Equation 3.4-18.

$$\frac{(P_2/V_2)}{(P_1/V_1)} = \left(\frac{D_{a_2}}{D_{a_1}}\right)^{11/4}$$

Usually, in scaling up to large-size vessels, a somewhat larger mixing time is used so that the power/unit volume does not increase markedly.

The mixing time for a helical-ribbon agitator is as follows for N'_{Re} < 20 (H2):

Equation 3.4-19.

$$N t_T = 126 \qquad \text{(agitator pitch/tank diameter = 1.0)}$$

Equation 3.4-20.

$$N t_T = 90 \qquad \text{(agitator pitch/tank diameter = 0.5)}$$

For very viscous liquids the helical-ribbon mixer gives a much smaller mixing time than a turbine for the same power/unit volume (M5). For nonviscous liquids, however, it gives longer times.

For a propellor agitator in a baffled tank, a mixing-time correlation is given by Biggs (B5), and that for an unbaffled tank by Fox and Gex (F1).

For a high-efficiency impeller in a baffled tank, mixing-time correlations are given by reference (F2), which shows that mixing times are lower than for pitched-blade agitators.

EXAMPLE 3.4-4. Scale-Up of Mixing Time in a Turbine Agitation System.

Using the existing conditions for the turbine with a disk as in Example 3.4-1, part (a), do as follows:

a. Calculate the mixing time.
b. Calculate the mixing time for a smaller vessel with a similar geometric ratio, where D_t is 0.30 m instead of 1.83 m. Do this for the same power per unit volume as used in part (a).
c. Using the same mixing time calculated for the smaller vessel in part (b), calculate the new power per unit volume for the larger vessel in part (a).

Solution: In part (a), D_t = 1.83 m, D_a = 0.61 m, $D_t = H$, N = 90/60 = 1.50 rev/s, ρ = 929 kg/m^3, μ = 10 cp = 0.01 Pa · s. From Example 3.4-1, N'_{Re} = 5.185 × 10^4, N_p = 5, P_1 = 1.324 kW. For the tank volume,

$$V_1 = \frac{\pi(1.83)^2(1.83)}{4} = 4.813 \text{ m}^3$$

The power per unit volume is

$$\frac{P_1}{V_1} = \frac{1.324}{4.813} = 0.2751 \text{ kW/m}^3$$

From Fig. 3.4-6 for N'_{Re} = 5.185 × 10^4, f_t = 4.0. Substituting into Eq. (3.4-16),

$$f_t = 4.0 = \frac{t_T (N_1 D_{a1}^2)^{2/3} g^{1/6} D_{a1}^{1/2}}{H_1^{1/2} D_{t1}^{3/2}}$$

$$= \frac{t_T (1.5 \times 0.61^2)^{2/3} (9.80665)^{1/6} (0.61)^{1/2}}{(1.83^{1/2})(1.83)^{3/2}}$$

$$t_T = 17.30 \text{ s}$$

For part (b), the scale-down ratio R from Eq. (3.4-8) is

$$R = D_{T2}/D_{T1} = 0.30/1.83 = 0.1639$$

$$D_{a2} = RD_{a1} = 0.1639(0.61) = 0.1000 \text{ m}$$

Also, $H_2 = D_{T2}$ = 0.300 m. Using the same $P_1/V_1 = P_2/V_2$ = 0.2751 kW/m^3 in the turbulent region, and Eq. (3.4-17),

$$\frac{t_{T2}}{t_{T1}} = \left(\frac{D_{a2}}{D_{a1}}\right)^{11/18}$$

$$t_{T2} = 17.30\left(\frac{0.100}{0.61}\right)^{11/18}$$

Hence, t_{T2} = 5.73 s. This shows that the larger vessel has a marked increase in mixing time from 5.73 to 17.30 s for equal power per unit volume.

For part (c), using the same mixing time of 5.73 s for the smaller vessel, the power per unit volume of the larger vessel is calculated from Eq. (3.4-18) for equal mixing times:

$$\frac{P_2/V_2}{P_1/V_1} = \left(\frac{D_{a2}}{D_{a1}}\right)^{11/4}$$

$$\frac{0.2751}{P_1/V_1} = \left(\frac{0.1000}{0.6100}\right)^{11/4}$$

Solving, P_1/V_1 = 39.73 kW/m^3. This, of course, is a very large and impractical increase.

Flow Number and Circulation Rate in Agitation

An agitator acts like a centrifugal pump impeller without a casing and gives a flow at a certain pressure head. This circulation rate Q in m^3/s from the edge of the impeller is the flow rate perpendicular to the impeller discharge area. Fluid velocities have been measured in mixers and have been used to calculate the circulation rates. Data for baffled vessels have been correlated using the dimensionless flow number N_Q (U1):

Equation 3.4-21.

$$N_Q = \frac{Q}{ND_a^3}$$

$N_Q = 0.5$ marine propeller (pitch = diameter)

$N_Q = 0.75$ six-blade turbine with disk ($W/D_a = \frac{1}{5}$)

$N_Q = 0.5$ six-blade turbine with disk ($W/D_a = \frac{1}{8}$)

$N_Q = 0.75$ pitched-blade turbine ($W/D_a = \frac{1}{5}$)

Special Agitation Systems

Suspension of solids

In some agitation systems a solid is suspended in the agitated liquid. Examples are when a finely dispersed solid is to be dissolved in the liquid, microorganisms are suspended in fermentation, a homogeneous liquid-solid mixture is to be produced for feed to a process, and a suspended solid is used as a catalyst to speed up a reaction. The suspension of solids is somewhat similar to a fluidized bed. In the agitated system, circulation currents of the liquid keep the particles in suspension. The amount and type of agitation needed depend mainly on the terminal settling velocity of the particles, which can be calculated using the equations in Section 14.3. Empirical equations for predicting the power required to suspend particles are given in references (M2, W1). Equations for pitched-blade turbines and high-efficiency impellers are given by Corpstein et al. (C4).

Dispersion of gases and liquids in liquids

In gas-liquid dispersion processes, the gas is introduced below the impeller, which chops the gas into very fine bubbles. The type and degree of agitation affect the size of the bubbles and the total interfacial area. Typical of such processes are aeration in sewage treatment plants, hydrogenation of liquids by hydrogen gas in the presence of a catalyst, absorption of a solute from the gas by the liquid, and fermentation. Correlations are available for predicting the bubble size, holdup, and kW power needed (C3, L1, Z1). For liquids dispersed in immiscible liquids, see reference (T1). The power required for the agitator in gas-liquid dispersion systems can be as much as 10 to 50% less than that required when no gas is present (C3, T2).

Motionless mixers

Mixing of two fluids can be accomplished in motionless mixers in a pipe with no moving parts. In such commercial devices, stationary elements inside a pipe successively divide portions of the stream and then recombine these portions.

Laminar-flow mixers are used to mix highly viscous mixtures. One type of static mixer has a series of fixed helical elements as shown in Fig. 3.4-7. (Note that most mixers have from six to 20 elements.) In the first element, the flow is split into two semicircular channels and the helical shape gives the streams a 180° twist. The next and successive elements are placed at 90° relative to each other and split the flows into two for each element. Each split in flow creates more interfacial area between layers. When these layers become sufficiently thin, molecular diffusion will eliminate concentration differences remaining. When each element divides the flow into two flow channels (M6),

Equation 3.4-22.

$$\frac{d}{D} = \frac{1}{2^n}$$

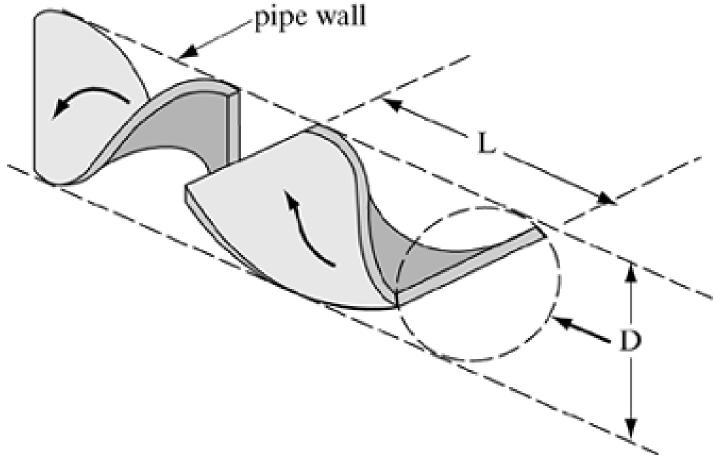

Figure 3.4-7. Two-element helical motionless mixer with element length L and pipe diameter D (M2, M6).

where *n* is the number of elements in series, *d* is the maximum striation thickness, and *D* is pipe diameter. When *n* = 20, then about 10^6 divisions occur and *d* is a very small thickness, which enhances the rate of diffusion.

In another commercial type of static mixer (K3), the stream is divided four times for each element. Each element has interacting bars or corrugated sheets placed lengthwise in the pipe and at a 45° angle to the pipe axis. The lengths *L* of the various types of elements vary from about 1.0 to 1.5 times the pipe diameter. These mixers are also used in turbulent-flow mixing.

In laminar flow with helical mixers the pressure drop (and, hence, power required) is approximately six times as large as that in the empty pipe. In turbulent flow, because of energy losses due to changes of direction, the pressure drop can be up to several hundred times as large (M6, P1). The power loss is typically about 10% of the power of a dynamic mixer (K3). Motionless mixers are also used for heat transfer, chemical reactions, and dispersion of gases in liquids.

Mixing of Powders, Viscous Materials, and Pastes

Powders

In mixing of solid particles or powders it is necessary to displace parts of the powder mixture with respect to other parts. The simplest class of devices suitable for gentle blending is the tumbler. However, it is not usually used for breaking up agglomerates. A common type of tumbler is the *double-cone blender,* in which two cones are mounted with their open ends fastened together and rotated, as shown in Fig. 3.4-8a. Baffles can also be used internally. If an internal rotating device is also used in the double cone, agglomerates can also be broken up. Other geometries used are a cylindrical drum with internal baffles or twin-shell V type. Tumblers used specifically for breaking up agglomerates are rotating cylindrical or conical shells charged with metal or porcelain steel balls or rods.

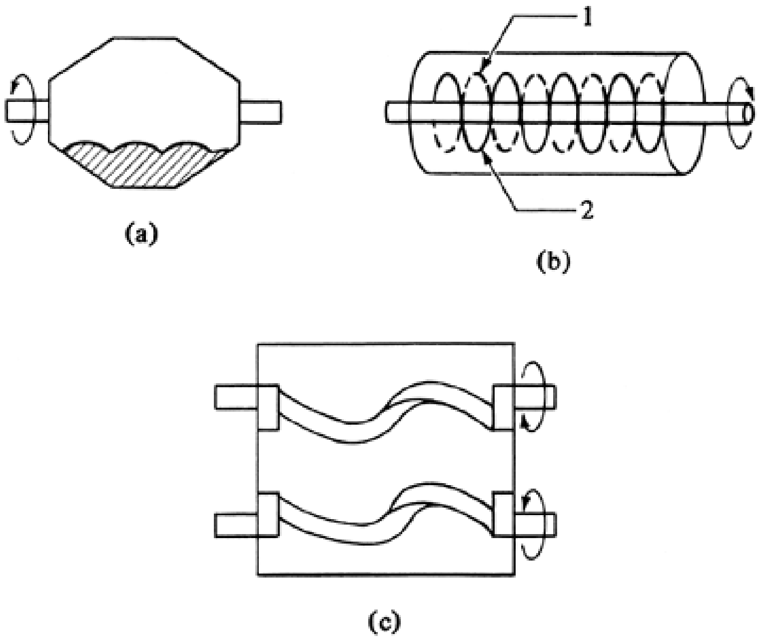

Figure 3.4-8. Mixers for powders and pastes: (a) double-cone powder mixer, (b) ribbon powder mixer with two ribbons, (c) kneader mixer for pastes.

Another class of devices for blending solids is the *stationary shell device,* in which the container is stationary and the material displacement is accomplished by single or multiple rotating inner devices. In the ribbon mixer in Fig. 3.4-8b, a shaft with two open helical screws numbers 1 and 2 attached to it rotates. One screw is left-handed and one right-handed. As the shaft rotates, sections of powder move in opposite directions and mixing occurs. Other types of internal rotating devices are available for special situations (P1). Also, in some devices both the shell and the internal device rotate.

Dough, pastes, and viscous materials

In the mixing of dough, pastes, and viscous materials, large amounts of powder are required as the material is divided, folded, or recombined, and as different parts of the material are displaced relative to each other so that fresh surfaces recombine as often as possible. Some machines may require jacketed cooling to remove the heat generated.

The first type of device for this purpose is somewhat similar to those for agitating fluids, with an impeller slowly rotating in a tank. The impeller can be a close-fitting anchor agitator as in Fig. 3.4-2b, where the outer sweep assembly may have scraper blades. A gate impeller can also be used which has horizontal and vertical bars that cut the paste at various levels and at the wall, which may have stationary bars. A modified gate mixer is the shear-bar mixer, which contains vertical rotating bars or paddles passing between vertical stationary fingers. Other modifications of these types are those where the can or container will rotate as well as the bars and scrapers. These are called *change-can mixers.*

The most commonly used mixer for heavy pastes and dough is the *double-arm kneader mixer.* The mixing action is bulk movement, smearing, stretching, dividing, folding, and re-combining. The most widely used design employs two contrarotating arms of sigmoid shape which may rotate at different speeds, as shown in Fig. 3.4-8c.

NON-NEWTONIAN FLUIDS

Types of Non-Newtonian Fluids

As discussed in Section 2.4, Newtonian fluids are those which follow Newton's law, Eq. (3.5-1):

Equation 3.5-1.

$$\tau = -\mu \frac{dv}{dr} \qquad \text{(SI)}$$

$$\tau = -\frac{\mu}{g_c}\frac{dv}{dr} \qquad \text{(English)}$$

where μ is the viscosity and is a constant independent of shear rate. In Fig. 3.5-1 a plot is shown of shear stress τ versus shear rate $-dv/dr$. The line for a Newtonian fluid is straight, the slope being μ.

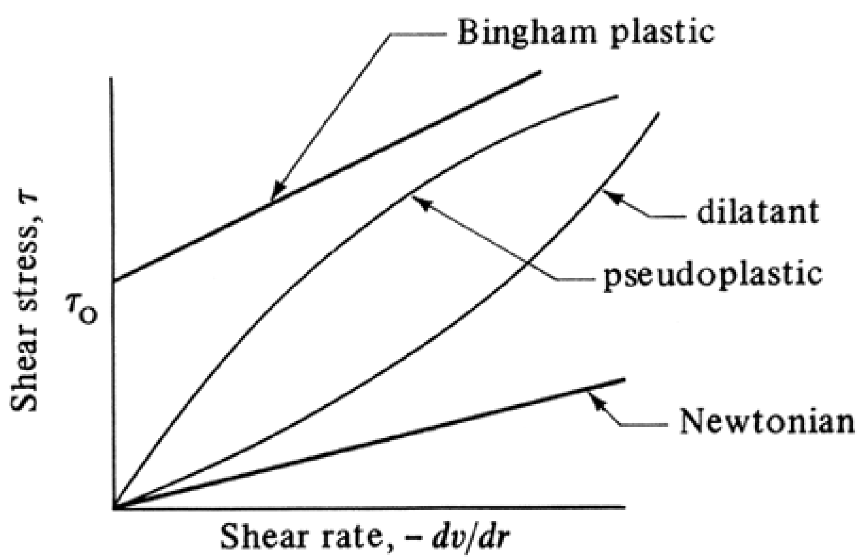

Figure 3.5-1. Shear diagram for Newtonian and time-independent non-Newtonian fluids.

If a fluid does not follow Eq. (3.5-1), it is a non-Newtonian fluid. Then a plot of τ versus $-dv/dr$ is not linear through the origin for these fluids. Non-Newtonian fluids can be divided into two broad categories on the basis of their shear-stress/shear-rate behavior: those whose shear stress is independent of time or duration of shear (time-independent) and those whose shear stress is dependent on time or duration of shear (time-dependent). In addition to unusual shear-stress behavior, some non-Newtonian fluids also exhibit elastic (rubberlike) behavior, which is a function of time and results in their being called *viscoelastic fluids.* These fluids exhibit normal stresses perpendicular to the direction of flow in addition to the usual tangential stresses. Most of the emphasis here will be put on the time-independent class, which includes the majority of non-Newtonian fluids.

Time-Independent Fluids

Bingham plastic fluids

These are the simplest because, as shown in Fig. 3.5-1, they differ from Newtonian only in that the linear relationship does not go through the origin. A finite shear stress τ_C (called *yield stress*) in N/m^2 is needed to initiate flow. Some fluids have a finite yield (shear) stress τ_O, but the plot of τ versus $-dv/dr$ is curved upward or downward. However, this departure from exact Bingham plasticity is often small. Examples of fluids with a yield stress are drilling muds, peat slurries, margarine, chocolate mixtures, greases, soap, grain-water suspensions, toothpaste, paper pulp, and sewage sludge.

Pseudoplastic fluids

The majority of non-Newtonian fluids are in this category and include polymer solutions or melts, greases, starch suspensions, mayonnaise, biological fluids, detergent slurries, dispersion media in certain pharmaceuticals, and paints. The shape of the flow curve is shown in Fig. 3.5-1, and it generally can be represented by a power-law equation (sometimes called the *Ostwald-de Waele equation):*

Equation 3.5-2.

$$\tau = K\left(-\frac{dv}{dr}\right)^n \qquad (n < 1)$$

where K is consistency index in N · s^n/m^2 or lb$_f$ · s^{n}ft^2, and n is the flow behavior index, dimensionless. The apparent viscosity μ_a in Eq. (3.5-3) is obtained from Eqs. (3.5-1) and (3.5-2) and decreases with increasing shear rate:

Equation 3.5-3.

$$\mu_a = K\left(-\frac{dv}{dr}\right)^{n-1}$$

Dilatant fluids

These fluids are far less common than pseudoplastic fluids, and their flow behavior (Fig. 3.5-1) shows an increase in apparent viscosity with increasing shear rate. The power-law equation (3.5-2) is often applicable, but with $n > 1$:

Equation 3.5-4.

$$\tau = K\left(-\frac{dv}{dr}\right)^n \qquad (n > 1)$$

For a Newtonian fluid, $n = 1$. Solutions showing dilatancy are some corn flour-sugar solutions, wet beach sand, starch in water, potassium silicate in water, and some solutions containing high concentrations of powder in water.

Time-Dependent Fluids

Thixotropic fluids

These fluids exhibit a reversible decrease in shear stress with time at a constant rate of shear. This shear stress approaches a limiting value that depends on the shear rate. Examples include some polymer solutions, shortening, some food materials, and paints. At present the theory for time-dependent fluids is still not completely developed.

Rheopectic fluids

These fluids are quite rare in occurrence and exhibit a reversible increase in shear stress with time at a constant rate of shear. Examples are bentonite clay suspensions, certain sols, and gypsum suspensions. In design procedures for thixotropic and rheopectic fluids for steady flow in pipes, the limiting flow-property values at a constant rate of shear are sometimes used (S2, W3).

Viscoelastic Fluids

Viscoelastic fluids exhibit elastic recovery from the deformations that occur during flow. They show both viscous and elastic properties. Part of the deformation is recovered upon removal of the stress. Examples are flour dough, napalm, polymer melts, and bitumens.

Laminar Flow of Time-Independent Non-Newtonian Fluids

Flow properties of a fluid

In determining the flow properties of a time-independent non-Newtonian fluid, a capillary-tube viscometer is often used. The pressure drop ΔP N/m^2 for a given flow rate q m^3/s is measured in a straight tube of length L m and diameter D m. This is repeated for different flow rates or average velocities V m/s. If the fluid is time-independent, these flow data can be used to predict the flow in any other pipe size.

A plot of $D\Delta p/4L$, which is τ_w, the shear stress at the wall in N/m^2, versus $8V/D$, which is proportional to the shear rate at the wall, is shown in Fig. 3.5-2 for a power-law fluid following Eq. (3.5-5):

Equation 3.5-5.

$$\tau_w = \frac{D\,\Delta p}{4L} = K'\left(\frac{8V}{D}\right)^{n'}$$

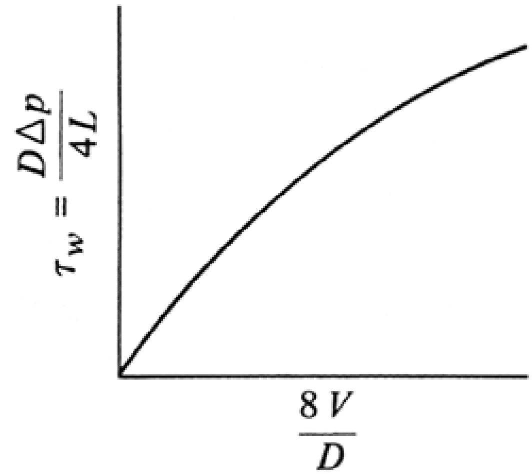

Figure 3.5-2. General flow curve for a power-law fluid in laminar flow in a tube.

where n' is the slope of the line when the data are plotted on logarithmic coordinates and K' has units of $N \cdot s^{n'}/m^2$. For $n' = 1$, the fluid is Newtonian; for $n' < 1$, pseudoplastic, or Bingham plastic if the curve does not go through the origin; and for $n' > 1$, dilatant. The K', the consistency index in Eq. (3.5-5), is the value of $D\Delta p/4L$ for $8V/D = 1$. The shear rate at the wall, $(-dv/dr)_w$, is

Equation 3.5-6.

$$\left(-\frac{dv}{dr}\right)_w = \left(\frac{3n' + 1}{4n'}\right)\left(\frac{8V}{D}\right)$$

Also, $K' = \mu$ for Newtonian fluids.

Equation (3.5-5) is simply another statement of the power-law model of Eq. (3.5-2) applied to flow in round tubes, and is more convenient to use for pipe-flow situations (D2). Hence, Eq. (3.5-5) defines the flow characteristics just as completely as Eq. (3.5-2). It has been found experimentally (M3) that for most fluids K' and n' are constant over wide ranges of $8V/D$ or $D\Delta p/4L$. For some fluids this is not the case, and K' and n' vary. Then the particular values of K' and n' used must be valid for the actual $8V/D$ or $D\Delta p/4L$ with which one is dealing in a design problem. This method using flow in a pipe or tube is often used to determine the flow properties of a non-Newtonian fluid.

In many cases the flow properties of a fluid are determined using a rotational viscometer. The flow properties K and n in Eq. (3.5-2) are determined in this manner. A discussion of the rotational viscometer is given in Section 3.5I.

When the flow properties are constant over a range of shear stresses that occurs for many fluids, the following equations hold (M3):

Equation 3.5-7.

$$n' = n$$

Equation 3.5-8.

$$K' = K\left(\frac{3n' + 1}{4n'}\right)^{n'}$$

Often a generalized viscosity coefficient γ is defined as

Equation 3.5-9.

$$\gamma = K'8^{n'-1} \qquad \text{(SI)}$$

$$\gamma = g_c K'8^{n'-1} \qquad \text{(English)}$$

where γ has units of $N \cdot s^{n'}/m^2$ or $lb_m/ft \cdot s^{2-n'}$

Typical flow-property constants (rheological constants) for some fluids are given in Table 3.5-1. Some data give γ values instead of K' values, but Eq. (3.5-9) can be used to convert these values if necessary. In some cases in the literature, K or K' values are given as $dyn \cdot s^{n'}/cm^2$ or $lb_f \cdot s^{n'}/ft^2$. From Appendix A.1, the conversion factors are

$$1\ lb_f \cdot s^{n'}/ft^2 = 47.880\ N \cdot s^{n'}/m^2$$

$$1\ dyn \cdot s^{n'}/cm^2 = 2.0886 \times 10^{-3}\ lb_f \cdot s^{n'}/ft^2$$

Table 3.5-1. Flow-Property Constants for Non-Newtonian Fluids

	Flow-Property Constants			
Fluid	n'	$\gamma\left(\frac{N \cdot s^{n'}}{m^2}\right)$	$K\left(\frac{N \cdot s^{n'}}{m^2}\right)$	**Ref.**
1.5% carboxymethylcellulose in water	0.554	1.369		(S1)
3.0% CMC in water	0.566	4.17		(S1)
4% paper pulp in water	0.575	9.12		(A1)
14.3% clay in water	0.350	0.0512		(W2)
10% napalm in kerosene	0.520	1.756		(S1)
25% clay in water	0.185	0.3036		(W2)
Applesauce, brand A (297 K), density = 1.10 g/cm³	0.645		0.500	(C1)
Banana purée, brand A (297 K), density = 0.977 g/cm³	0.458		6.51	(C1)
Honey (297 K)	1.00		5.61	(C1)
Cream, 30% fat (276 K)	1.0		0.01379	(M4)
Tomato concentrate, 5.8% total solids (305 K)	0.59		0.2226	(H1)

Equations for flow in a tube

In order to predict the frictional pressure drop Δp in laminar flow in a tube, Eq. (3.5-5) is solved for Δp ($p_0 - p_L$):

Equation 3.5-10.

$$\Delta p = \frac{K'4L}{D}\left(\frac{8V}{D}\right)^{n'}$$

If the average velocity is desired, Eq. (3.5-5) can be rearranged to give

Equation 3.5-11.

$$V = \frac{D}{8}\left(\frac{\Delta p\, D}{K'4L}\right)^{1/n'}$$

If the equations are desired in terms of *K* instead of *K′*, Eqs. (3.5-7) and (3.5-8) can be substituted into (3.5-10) and (3.5-11). Substituting Eqs. (3.5-7) and (3.5-8) into Eq. (3.5-11) and noting that $V = v_{x\,\text{av}}$,

Equation 3.5-12.

$$V = v_{x\text{av}} = \left(\frac{n}{3n+1}\right)\left(\frac{p_0 - p_L}{2KL}\right)^{1/n} R_0^{(n+1)/n}$$

The flow must be laminar. The generalized Reynolds number has been defined as

Equation 3.5-13.

$$N_{\text{Re,gen}} = \frac{D^{n'}V^{2-n'}\rho}{\gamma} = \frac{D^{n'}V^{2-n'}\rho}{K'8^{n'-1}} = \frac{D^{n}V^{2-n}\rho}{K8^{n-1}\left(\dfrac{3n+1}{4n}\right)^{n}} \qquad \text{(SI)}$$

Friction factor method

Alternatively, using the Fanning friction factor method given in Eqs. (2.10-5)–(2.10-7) for Newtonian fluids, but using the generalized Reynolds numbers,

Equation 3.5-14.

$$f = \frac{16}{N_{\text{Re,gen}}}$$

Equation 3.5-15.

$$\Delta p = 4f\rho\frac{L}{D}\frac{V^2}{2} \qquad \text{(SI)}$$

$$\Delta p = 4f\rho\frac{L}{D}\frac{V^2}{2g_c} \qquad \text{(English)}$$

EXAMPLE 3.5-1. Pressure Drop of Power-Law Fluid in Laminar Flow

A power-law fluid having a density of 1041 kg/m^3 is flowing through 14.9 m of a tubing having an inside diameter of 0.0524 m at an average velocity of 0.0728 m/s. The rheological or flow properties of the fluid are $K' = 15.23$ N · s$^{n'}$/m^2 (0.318 lb$_f$ · s$^{n'}$/ft^2) and $n' = 0.40$.

a. Calculate the pressure drop and friction loss using Eq. (3.5-10) for laminar flow. Check the generalized Reynolds number to make sure that the flow is laminar.
b. Repeat part (a) but use the friction factor method.

***Solution*:** The known data are as follows: $K' = 15.23$, $n' = 0.40$, $D = 0.0524$ m, $V = 0.0728$ m/s, $L = 14.9$ m, and $\rho = 1041$ kg/m^3. For part (a), using Eq. (3.5-10),

$$\Delta p = \frac{K'4L}{D}\left(\frac{8V}{D}\right)^{n'} = \frac{15.23(4)(14.9)}{0.0524}\left(\frac{8\times 0.0728}{0.0524}\right)^{0.4} = 45\,390 \text{ N/m}^2$$

Also, to calculate the friction loss,

$$F_f = \frac{\Delta p}{\rho} = \frac{45\,390}{1041} = 43.60 \text{ J/kg}$$

Using Eq. (3.5-13),

$$N_{\text{Re,gen}} = \frac{D^{n'}V^{2-n'}\rho}{K'g^{n'-1}} = \frac{(0.0524)^{0.40}(0.0728)^{1.60}(1041)}{15.23(8)^{-0.6}} = 1.106$$

Hence, the flow is laminar.

For part (b), using Eq. (3.5-14)

$$f = \frac{16}{N_{\text{Re,gen}}} = \frac{16}{1.106} = 14.44$$

Substituting into Eq. (3.5-15),

$$\Delta p = 4f\rho\frac{L}{D}\frac{V^2}{2} = 4(14.44)(1041)\frac{14.9}{0.0524}\frac{(0.0728)^2}{2}$$

$$= 45.39\,\frac{\text{kN}}{\text{m}^2}\left(946\,\frac{\text{lb}_f}{\text{ft}^2}\right)$$

Friction Losses in Contractions, Expansions, and Fittings in Laminar Flow

Since non-Newtonian power-law fluids flowing in conduits are often in laminar flow because of their usually high effective viscosity, losses in sudden changes of velocity and fittings are important in laminar flow.

Kinetic energy in laminar flow

In application of the total mechanical-energy balance in Eq. (2.7-28), the average kinetic energy per unit mass of fluid is needed. For fluids, this is (S2)

Equation 3.5-16.

$$\text{average kinetic energy/kg} = \frac{V^2}{2\alpha}$$

For Newtonian fluids, $\alpha = \frac{1}{2}$ for laminar flow. For power-law non-Newtonian fluids,

Equation 3.5-17.

$$\alpha = \frac{(2n+1)(5n+3)}{3(3n+1)^2}$$

For example, if $n = 0.50$, $\alpha = 0.585$. If $n = 1.00$, $\alpha = \frac{1}{2}$. For turbulent flow for Newtonian and non-Newtonian flow, $\alpha = 1.0$(D1).

Losses in contractions and fittings

Skelland (S2) and Dodge and Metzner (D2) state that when a fluid leaves a tank and flows through a sudden contraction to a pipe of diameter D_2 or flows from a pipe of diameter D_1 through a sudden contraction to a pipe of D_2, a vena contracta is usually formed downstream from the contraction. General indications are that the frictional pressure losses for pseudoplastic and Bingham plastic fluids are very similar to those for Newtonian fluids at the same generalized Reynolds numbers in laminar and turbulent flow for contractions as well as for fittings and valves.

For contraction losses, Eq. (2.10-16) can be used, where $\alpha = 1.0$ for turbulent flow; and for laminar flow Eq. (3.5-17) can be used to determine α, since n is not 1.00.

For fittings and valves, friction losses should be determined using Eq. (2.10-17) and values from Table 2.10-1.

Losses in sudden expansion

For the friction loss for a non-Newtonian fluid in laminar flow through a sudden expansion from D_1 to D_2 diameter, Skelland (S2) gives

Equation 3.5-18.

$$h_{ex} = \frac{3n+1}{2n+1} V_1^2 \left[\frac{n+3}{2(5n+3)} \left(\frac{D_1}{D_2}\right)^4 - \left(\frac{D_1}{D_2}\right)^2 + \frac{3(3n+1)}{2(5n+3)} \right]$$

where h_{ex} is the friction loss in J/kg. In English units Eq. (3.5-18) is divided by g_c and h_{ex} is in ft · lb_f/lb_m.

Equation (2.10-15) for laminar flow with $\alpha = \frac{1}{2}$ for a Newtonian fluid gives values reasonably close to those of Eq. (3.5-18) for $n = 1$ (Newtonian fluid). For turbulent flow the friction loss can be approximated by Eq. (2.10-15), with $\alpha = 1.0$ for non-Newtonian fluids (S2).

Turbulent Flow and Generalized Friction Factors

In turbulent flow of time-independent fluids the Reynolds number at which turbulent flow occurs varies with the flow properties of the non-Newtonian fluid. In a comprehensive study Dodge and Metzner (D2) derived a theoretical equation for turbulent flow of non-Newtonian fluids through smooth, round tubes. The final equation is plotted in Fig. 3.5-3, where the Fanning friction factor is plotted versus the generalized Reynolds number, $N_{Re,gen}$, given in Eq. (3.5-13). Power-law fluids with flow-behavior indexes n' between 0.36 and 1.0 were experimentally studied at Reynolds numbers up to 3.5×10^4 and the derivation was confirmed.

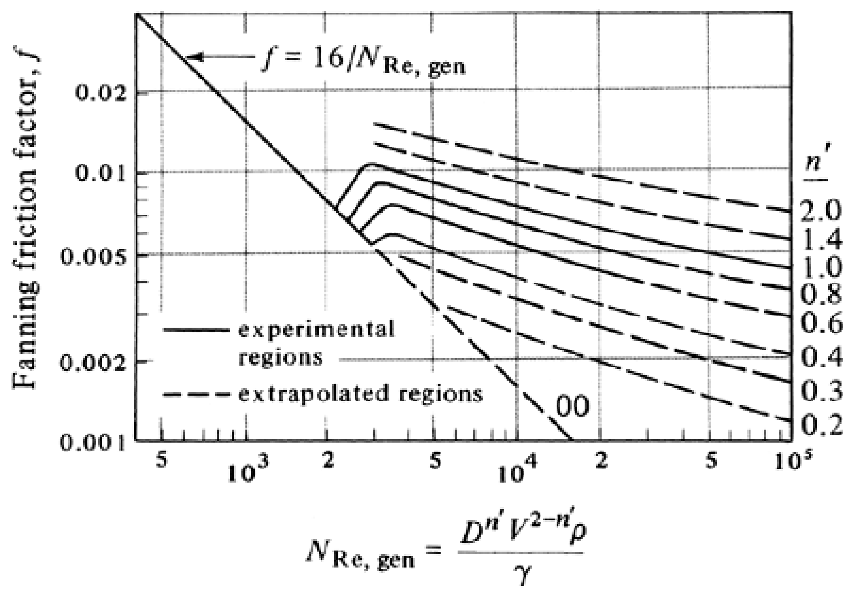

*Figure 3.5-3. Fanning friction factor versus generalized Reynolds number for time-independent non-Newtonian and Newtonian fluids flowing in smooth tubes. [From D. W. Dodge and A. B. Metzner, A.I.Ch.E. J., **5**, 189 (1959). With permission.]*

The curves for different n' values break off from the laminar line at different Reynolds numbers to enter the transition region. For n' = 1.0 (Newtonian), the transition region starts at $N_{Re,gen}$ = 2100. Since many non-Newtonian power-law fluids have high effective viscosities, they are often in laminar flow. The correlation for a smooth tube also holds for a rough pipe in laminar flow.

For rough commercial pipes with various values of roughness ε/D, Fig. 3.5-3 cannot be used for turbulent flow, since it is derived for smooth tubes. The functional dependence of the roughness values ε/D on n' requires experimental data which are not yet available. Metzner and Reed (M3, S3) recommend use of the existing relationship, Fig. 2.10-3, for Newtonian fluids in rough tubes using the generalized Reynolds number $N_{Re,gen}$. This is somewhat conservative, since preliminary data indicate that friction factors for pseudoplastic fluids may be slightly smaller than for Newtonian fluids. This is also consistent with Fig. 3.5-3 for smooth tubes, which indicates lower f values for fluids with n' below 1.0 (S2).

EXAMPLE 3.5-2. Turbulent Flow of Power-Law Fluid

A pseudoplastic fluid that follows the power law, having a density of 961 kg/m^3, is flowing through a smooth, circular tube having an inside diameter of 0.0508 m at an average velocity of 6.10 m/s. The flow properties of the fluid are n' = 0.30 and K' = 2.744 N · s$^{n'}$/m^2. Calculate the frictional pressure drop for a tubing 30.5 m long.

Solution: The data are as follows: K' = 2.744, n' = 0.30, D = 0.0508 m, V = 6.10 m/s, ρ = 961 kg/m^3, and L = 30.5 m. Using the general Reynolds-number equation (3.5-13),

$$N_{\text{Re,gen}} = \frac{D^{n'}V^{2-n'}\rho}{K'8^{n'-1}} = \frac{(0.0508)^{0.3}(6.10)^{1.7}(961)}{2.744(8^{-0.7})}$$

$$= 1.328 \times 10^4$$

Hence, the flow is turbulent. Using Fig. 3.5-3 for $N_{Re,gen}$ = 1.328 × 10^4 and n' = 0.30, f = 0.0032.

Substituting into Eq. (3.5-15),

$$\Delta p = 4f\rho \frac{L}{D}\frac{V^2}{2} = 4(0.0032)(961)\left(\frac{30.5}{0.0508}\right)\frac{(6.10)^2}{2}$$

$$= 137.4\ \text{kN/m}^2\ (2870\ \text{lb}_f/\text{ft}^2)$$

Velocity Profiles for Non-Newtonian Fluids

Pseudoplastic and dilatant fluids

For pipe flow, Eq. (3.5-2) can be written as

Equation 3.5-19.

$$\tau_{rx} = K\left(\frac{-dv_x}{dr}\right)^n$$

Equation (2.9-6) holds for all fluids:

Equation 2.9-6.

$$\tau_{rx} = \frac{(p_0 - p_L)r}{2L}$$

which relates τ_{rx} with the radial distance r from the center. Equating the above two equations and integrating between $r = r$ and $r = R_0$ where $v_x = 0$,

Equation 3.5-20.

$$v_x = \frac{n}{n+1}\left(\frac{p_0 - p_L}{2KL}\right)^{1/n} R_0^{(n+1)/n}\left[1 - \left(\frac{r}{R_0}\right)^{(n+1)/n}\right]$$

At $r = 0$, $v_x = v_{x\,max}$ and Eq. (3.5-20) becomes

Equation 3.5-21.

$$v_x = v_{x\,\max}\left[1 - \left(\frac{r}{R_0}\right)^{(n+1)/n}\right]$$

The average velocity $v_{x\,av}$ is given by Eq. (3.5-12):

Equation 3.5-12.

$$v_{x\,\text{av}} = \left(\frac{n}{3n+1}\right)\left(\frac{p_0 - p_L}{2KL}\right)^{1/n} R_0^{(n+1)/n}$$

Dividing Eq. (3.5-20) by (3.5-12),

Equation 3.5-22.

$$\frac{v_x}{v_{x\,\text{av}}} = \frac{3n+1}{n+1}\left[1 - \left(\frac{r}{R_0}\right)^{(n+1)/n}\right]$$

Using Eq. (3.5-22), the velocity profile can be calculated for laminar flow of a Newtonian fluid for $n = 1$ to show the parabolic profile in Fig. 3.5-4. The velocity profiles for pseudoplastic fluids $(n < 1)$ show a flatter profile compared to the velocity profile for a Newtonian fluid. For extreme pseudoplastic behavior for $n = 0$, plug flow is obtained across the entire pipe. For dilatant behavior $(n > 1)$ the velocity profile is more pointed and narrower. For extreme dilatant fluids $(n = \infty)$ the velocity profile is a linear function of the radius.

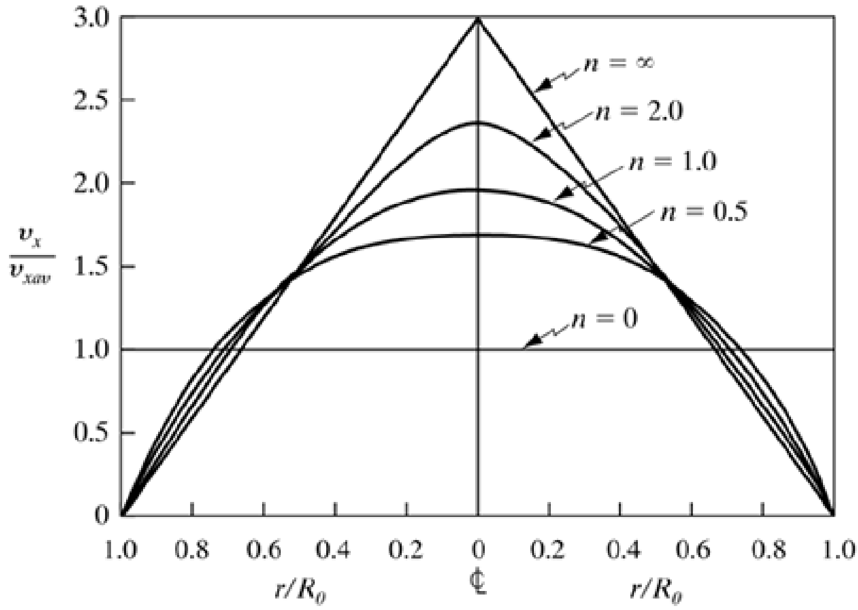

Figure 3.5-4. Dimensionless velocity profile $v_x/v_{x\,av}$ for power-law non-Newtonian fluids.

Bingham plastic fluids

For Bingham plastic fluids a finite yield stress τ_0 in N/m^2 is needed to initiate flow, as given in Eq. (3.5-23):

Equation 3.5-23.

$$\tau_{rx} = \tau_0 + \mu\left(-\frac{dv_x}{dr}\right)$$

The velocity profile for this fluid is more complex than that for non-Newtonian fluids. This velocity profile for Bingham plastic fluids is shown in Fig. 3.5-5. Note the plug-flow region $r = 0$ to $r = r_0$. In this region $dv_x/dr = 0$ because the momentum flux or shear stress τ_{rx} is less than the yield value τ_0.

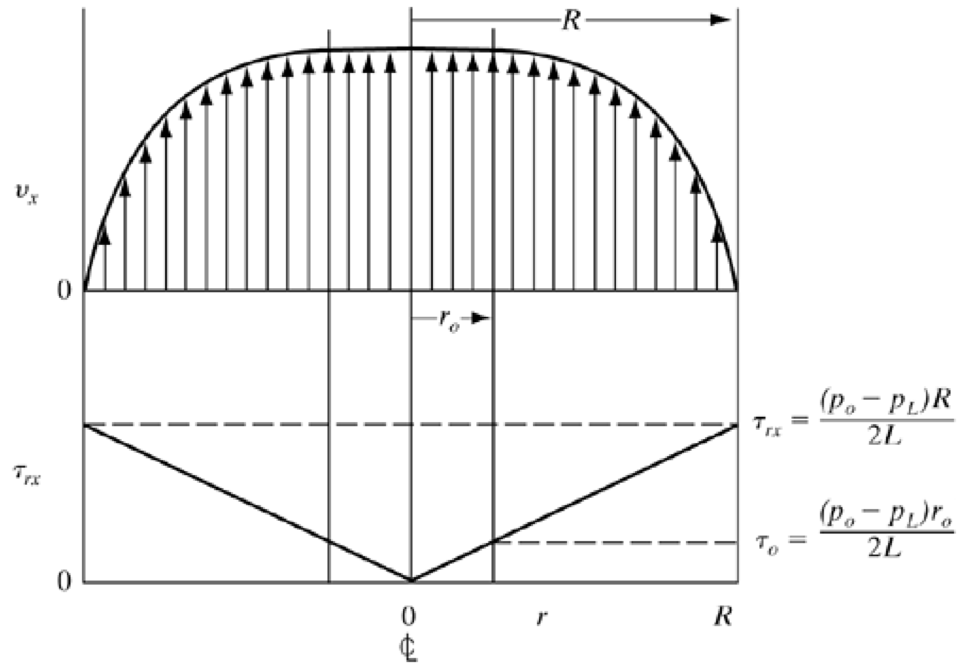

Figure 3.5-5. Velocity profile and shear diagram for flow of a Bingham plastic fluid in a pipe.

In Table 3.5-2 some typical values for the rheological constants for Bingham plastic fluids are given.

Table 3.5-2. Rheological Constants for Bingham Plastic Fluids

Fluid	τ_0, N/m^2	μ, Pa · s	*Ref.*
Coal slurry (ρ = 1500 kg/m^3)	2.0	0.03	(D4)
Molten chocolate (100°F)	20	2.0	(D4)
Printing pigment in varnish (10% by wt)	0.4	0.25	(C5)

To derive the equation for pipe flow, note that Eq. (2.9-6) holds for all fluids:

Equation 2.9-6.

$$\tau_{rx} = \frac{(p_0 - p_L)r}{2L}$$

Substituting Eq. (2.9-6) into (3.5-23),

Equation 3.5-24.

$$\frac{(p_0 - p_L)r}{2L} = \tau_0 + \mu\left(-\frac{dv_x}{dr}\right)$$

Rearranging and integrating, where $v_x = v_x$ at $r = r$ and $v_x = 0$ at $r = R$,

Equation 3.5-25.

$$v_x = \left(\frac{p_0 - p_L}{4\mu L}\right)R^2\left[1 - \left(\frac{r}{R}\right)^2\right] - \frac{\tau_0}{\mu}R\left[1 - \frac{r}{R}\right]$$

The equation holds for the region where $r > r_0$ and up to $r = R$. For the plug-flow region $r \le r_0$, $dv_x/dr = 0$. In this region, using Eq. (2.9-6) and setting $\tau_{rx} = \tau_0$ at r_0,

Equation 3.5-26.

$$\tau_0 = \frac{(p_0 - p_L)r_0}{2L}$$

Substituting Eq. (3.5-26) into (3.5-25) for $r = r_0$, where plug flow occurs,

Equation 3.5-27.

$$v_x = \left(\frac{p_0 - p_L}{4\mu L}\right)R^2\left[1 - \frac{r_0}{R}\right]^2$$

To obtain the flow rate Q in m^3/s, the following integral must be evaluated:

Equation 3.5-28.

$$Q = 2\pi\int_0^{r_0} v_x r\, dr + 2\pi\int_{r_0}^{R} v_x r\, dr$$

Substituting Eq. (3.5-27) into the first part of Eq. (3.5-28) and (3.5-25) into the last part and integrating,

Equation 3.5-29.

$$Q = \frac{\pi(p_0 - p_L)R^4}{8\mu L}\left[1 - \frac{4}{3}\frac{\tau_0}{\tau_R} + \frac{1}{3}\left(\frac{\tau_0}{\tau_R}\right)^4\right]$$

where $\tau_R = (p_0 - p_L)R/2L$, the momentum flux at the wall. This is the Buckingham-Reiner equation. When τ_0 is zero, Eq. (3.5-29) reduces to the Hagen-Poiseuille Eq. (2.9-11) for Newtonian fluids.

EXAMPLE 3.5-3. Flow Rate of a Bingham Plastic Fluid

A printing-pigment solution with properties similar to those in Table 3.5-2 is flowing in a 1.0-cm-diameter pipe which is 10.2 m long. A pressure driving force of 4.35 kN/m^2 is being used. Calculate the flow rate Q in m^3/s.

Solution. From Table 3.5-2, $\tau_0 = 0.4$ N/m^2 and $\mu = 0.25$ Pa · s. Also, $(p_0 - p) = 4.35$ kN/m^2 = 4350 N/m^2, L = 10.2 m, R = 1.0/2 cm = 0.005 m. Substituting into Eq. (3.5-26),

$$\tau_0 = 0.4 \text{ N/m}^2 = \frac{(p_0 - p_L)r_0}{2L} = \frac{(4350)r_0}{2(10.2)}$$

Solving,

$$r_0 = \frac{0.400(2)(10.2)}{4350} = 0.001876 \text{ m} = 0.1876 \text{ cm}$$

Substituting into the following for τ_R,

$$\tau_R = \frac{(p_0 - p_L)R}{2L} = \frac{(4350)(0.005)}{2(10.2)} = 1.066 \text{ N/m}^2$$

Finally, substituting into Eq. (3.5-29),

$$Q = \frac{\pi(4350)(0.005)^4}{8(0.25)(10.2)}\left[1 - \frac{4}{3}\frac{0.4}{1.066} + \frac{1}{3}\left(\frac{0.4}{1.066}\right)^4\right]$$

$$Q = 2.120 \times 10^{-7}\ \text{m}^3/\text{s}$$

$$v_{x\,\text{av}} = \frac{Q}{\pi R^2} = \frac{2.120 \times 10^{-7}}{\pi(0.005)^2} = 2.700 \times 10^{-3}\ \text{m/s}$$

Determination of Flow Properties of Non-Newtonian Fluids Using Rotational Viscometer

The flow-property or rheological constants of non-Newtonian fluids can be measured using pipe flow, as discussed in Section 3.5E. Another, more important method for measuring flow properties is by using a rotating concentric-cylinder viscometer, first described by Couette in 1890. In this device a concentric rotating cylinder (spindle) spins at a constant rotational speed inside another cylinder. Generally, there is a very small gap between the walls. This annulus is filled with the fluid. The torque needed to maintain this constant rotation rate of the inner spindle is measured by means of a torsion wire from which the spindle is suspended. A typical commercial instrument of this type is the Brookfield viscometer. Some types rotate the outer cylinder.

The shear stress at the wall of the bob or spindle is given by

Equation 3.5-30.

$$\tau_w = \frac{T}{2\pi R_b^2 L}$$

where τ_w is the shear stress at the wall, N/m^2 or kg/s^2 · m; T is the measured torque, kg · m^2/s^2; R_b is the radius of the spindle, m; and L is the effective length of the spindle, m. Note that Eq. (3.5-30) holds for Newtonian and non-Newtonian fluids.

The shear rate at the surface of the spindle for non-Newtonian fluids is as follows (M6) for $0.5 < R_b/R_c < 0.99$:

Equation 3.5-31.

$$\left(-\frac{dv}{dr}\right)_w = \frac{2\omega}{n[1 - (R_b/R_c)^{2/n}]}$$

where R_c is the radius of the outer cylinder or container, m; and ω is the angular velocity of the spindle, rad/s. Also, $\omega = 2\pi N/60$, when N is the RPM. Results calculated using Eq. (3.5-31) give values very close to those using the more complicated equation of Krieger and Maron (K2), also given in (P4, S2).

The power-law equation is given as

Equation 3.5-2.

$$\tau = K\left(-\frac{dv}{dr}\right)^n$$

where $K = \text{N} \cdot \text{s}^n/\text{m}^2$, $\text{kg} \cdot \text{s}^{n-2}/\text{m}$. Substituting Eqs. (3.5-30) and (3.5-31) into (3.5-2) gives

Equation 3.5-32.

$$T = 2\pi R_b^2 LK\left[\frac{2}{n[1-(R_b/R_c)^{2/n}]}\right]^n \omega^n$$

or,

Equation 3.5-33.

$$T = A\omega^n$$

where

Equation 3.5-34.

$$A = 2\pi R_b^2 LK\left[\frac{2}{n[1-(R_b/R_c)^{2/n}]}\right]^n$$

Experimental data are obtained by measuring the torque T at different values of ω for a given fluid. The flow-property constants may be evaluated by plotting log T versus log ω. The parameter n is the slope of the straight line and the intercept is log A. The consistency factor K is now easily evaluated from Eq. (3.5-34).

Various special cases can be derived for Eq. (3.5-31):

***Newtonian fluid.* (n = 1)**

Equation 3.5-35.

$$\left(-\frac{dv}{dr}\right)_w = \frac{2\omega}{1-(R_b/R_c)^2}$$

***Very large gap* ($R_b/R_c < 0.1$)**

This is the case of a spindle immersed in a large beaker of test fluid. Equation (3.5-31) becomes

Equation 3.5-36.

$$\left(-\frac{dv}{dr}\right)_w = \frac{2\omega}{n}$$

Substituting Eqs. (3.5-30) and (3.5-36) into (3.5-2),

Equation 3.5-37.

$$T = 2\pi R_b^2 LK\left(\frac{2}{n}\right)^n \omega^n$$

Again, as before, the flow-property constants can be evaluated by plotting log T versus log ω.

***Very narrow gap* ($R_b/R_c > 0.99$)**

This is similar to flow between parallel plates. Taking the shear rate at radius $(R_b + R_c)/2$,

Equation 3.5-38.

$$\left(-\frac{dv}{dr}\right)_w \cong \frac{\Delta v}{\Delta r} = \frac{2\omega}{1-(R_b/R_c)^2}$$

This equation, then, is the same as Eq. (3.5-35).

Power Requirements in Agitation and Mixing of Non-Newtonian Fluids

For correlating the power requirements in agitation and mixing of non-Newtonian fluids, the power number N_P is defined by Eq. (3.4-2), which is also the equation used for Newtonian fluids. However, the definition of the Reynolds number is much more complicated than for Newtonian fluids, since the apparent viscosity is not constant for non-Newtonian fluids but varies with the shear rates or velocity gradients in the vessel. Several investigators (G1, M1) have used an average apparent viscosity μ_a, which is used in the Reynolds number as follows:

Equation 3.5-39.

$$N'_{\mathrm{Re},n} = \frac{D_a^2 N\rho}{\mu_a}$$

The average apparent viscosity can be related to the average shear rate or average velocity gradient by the following method. For a power-law fluid,

Equation 3.5-40.

$$\tau = K\left(-\frac{dv}{dy}\right)_{\mathrm{av}}^n$$

For a Newtonian fluid,

Equation 3.5-41.

$$\tau = \mu_a\left(-\frac{dv}{dy}\right)_{\mathrm{av}}$$

Combining Eqs. (3.5-40) and (3.5-41),

Equation 3.5-42.

$$\mu_a = K\left(-\frac{dv}{dy}\right)_{\mathrm{av}}^{n-1}$$

Metzner and others (G1, M1) found experimentally that the average shear rate $(dv/dy)_{\mathrm{av}}$ for pseudoplastic liquids ($n < 1$) varies approximately as follows with the rotational speed:

Equation 3.5-43.

$$\left(\frac{dv}{dy}\right)_{\mathrm{av}} = 11N$$

Hence, combining Eqs. (3.5-42) and (3.5-43),

Equation 3.5-44.

$$\mu_a = (11N)^{n-1}K$$

Substituting into Eq. (3.5-39),

Equation 3.5-45.

$$N'_{\mathrm{Re},n} = \frac{D_a^2 N^{2-n} \rho}{11^{n-1} K}$$

Equation (3.5-45) has been used to correlate data for a flat six-blade turbine with disk in pseudoplastic liquids, and the dashed curve in Fig. 3.5-6 shows the correlation (M1). The solid curve applies to Newtonian fluids (R1). Both sets of data were obtained for four baffles with $D_t/J = 10$, $D_a/W = 5$, and $L/W = \frac{5}{4}$. However, since it has been shown that the difference in results for $D_t/J = 10$ and $D_t/J = 12$ is very slight (R1), this Newtonian line can be considered the same as curve 1 in Fig. 3.4-5. The curves in Fig. 3.5-6 show that the results are identical for the Reynolds number range 1–2000, except that they differ only in the Reynolds number range 10–100, where the pseudoplastic fluids use less power than the Newtonian fluids. The flow patterns for the pseudoplastic fluids show much greater velocity-gradient changes than do the Newtonian fluids in the agitator. The fluid far from the impeller may be moving in slow laminar flow with a high apparent viscosity. Data for fan turbines and propellers are also available (M1).

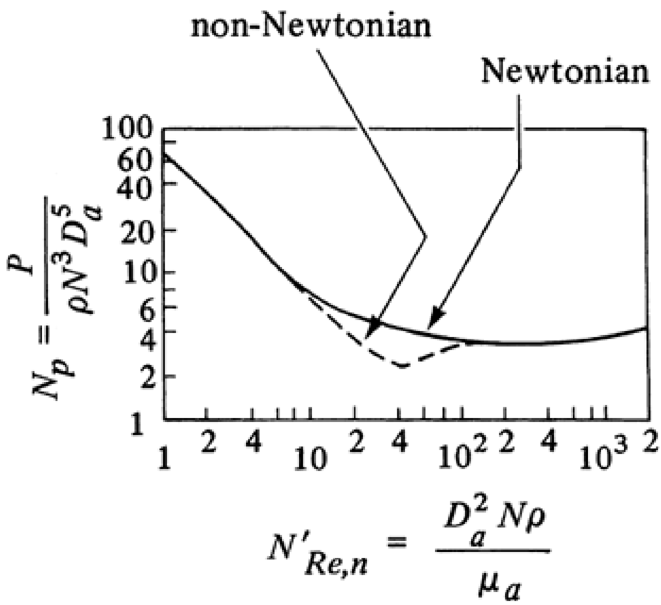

Figure 3.5-6. Power correlation in agitation for a flat, six-blade turbine with disk in pseudoplastic non-Newtonian and Newtonian fluids (G1, M1, R1): $D_a/W = 5$, $L/W = 5/4$, $D_t/J = 10$.

DIFFERENTIAL EQUATIONS OF CONTINUITY

Introduction

In Sections 2.6, 2.7, and 2.8, overall mass, energy, and momentum balances allowed us to solve many elementary problems in fluid flow. These balances were done on an arbitrary finite volume sometimes called a *control volume.* In these total-energy, mechanical-energy, and momentum balances, we only needed to know the state of the inlet and outlet streams and the exchanges with the surroundings.

These overall balances were powerful tools in solving various flow problems because they did not require knowledge of what goes on inside the finite control volume. Also, in the simple shell-momentum balances made in Section 2.9, expressions were obtained for the velocity distribution and pressure drop. However, to advance in our study of these flow systems, we must investigate in greater detail what goes on inside this finite control volume. To do this, we now use a differential element for a control volume. The differential balances will be somewhat similar to the overall and shell balances, but now we shall make the balance in a single phase and integrate to the phase boundary using the boundary conditions. In the balances done earlier, a balance was made for each new system studied. It is not necessary to formulate new balances for each new flow problem. It is often easier to start with the differential equations for the conservation of mass (equation of continuity) and the conservation of momentum in general form. Then these equations are simplified by discarding unneeded terms for each particular problem.

For nonisothermal systems, a general differential equation for conservation of energy will be considered in Chapter 5. Also, in Chapter 7, a general differential equation of continuity for a binary mixture will be derived. The differential-momentum-balance equation to be derived is based on Newton's second law and allows us to determine the way velocity varies with position and time as well as the pressure drop in laminar flow. The equation of momentum balance can be used for turbulent flow with certain modifications.

Often these conservation equations are called *equations of change,* since they describe the variations in the properties of the fluid with respect to position and time. Before we derive these equations, a brief review of the different types of derivatives with respect to time which occur in these equations and a brief description of vector notation will be given.

Types of Time Derivatives and Vector Notation

Partial time derivative

Various types of time derivatives are used in the derivations to follow. The most common type of derivative is the partial time derivative. For example, suppose that we are interested in the mass concentration or density ρ in kg/m^3 in a flowing stream as a function of position x, y, z and time t. The partial time derivative of ρ is $\partial\rho/\partial t$. This is the local change of density with time at a fixed point x, y, z.

Total time derivative

Suppose that we want to measure the density in the stream while we are moving about in the stream with velocities in the x, y, and z directions of dx/dt, dy/dt, and dz/dt, respectively. The total derivative $d\rho/dt$ is

Equation 3.6-1.

$$\frac{d\rho}{dt} = \frac{\partial\rho}{\partial t} + \frac{\partial\rho}{\partial x}\frac{dx}{dt} + \frac{\partial\rho}{\partial y}\frac{dy}{dt} + \frac{\partial\rho}{\partial z}\frac{dz}{dt}$$

This means that the density is a function of t and of the velocity components dx/dt, dy/dt, and dz/dt at which the observer is moving.

Substantial time derivative

Another useful type of time derivative is obtained if the observer floats along with the velocity v of the flowing stream and notes the change in density with respect to time. This is called the derivative that follows the motion, or the *substantial time derivative, $D\rho/Dt$:*

Equation 3.6-2.

$$\frac{D\rho}{Dt} = \frac{\partial\rho}{\partial t} + v_x\frac{\partial\rho}{\partial x} + v_y\frac{\partial\rho}{\partial y} + v_z\frac{\partial\rho}{\partial z} = \frac{\partial\rho}{\partial t} + (\boldsymbol{v}\cdot\boldsymbol{\nabla}\rho)$$

where v_x, v_y, and v_z are the velocity components of the stream velocity v, which is a vector. This substantial derivative is applied to both scalar and vector variables. The term $(v \cdot \nabla\rho)$ will be discussed in part 6 of Section 3.6B.

Scalars

The physical properties encountered in momentum, heat, and mass transfer can be placed in several categories: scalars, vectors, and tensors. Scalars are quantities such as concentration, temperature, length, volume, time, and energy. They have magnitude but no direction and are considered to be zero-order tensors. The common mathematical algebraic laws hold for the algebra of scalars. For example, $bc = cd$, $b(cd) = (bc)d$, and so on.

Vectors

Velocity, force, momentum, and acceleration are considered vectors since they have magnitude and direction. They are regarded as first-order tensors and are written in boldface letters in this text, such as v for velocity. The addition of two vectors $B + C$ by parallelogram construction and the subtraction of two vectors $B - C$ are shown in Fig. 3.6-1. The vector B is represented by its three projections B_x, B_y, and B_z on the x, y, and z axes, and

Equation 3.6-3.

$$\boldsymbol{B} = \boldsymbol{i}B_x + \boldsymbol{j}B_y + \boldsymbol{k}B_z$$

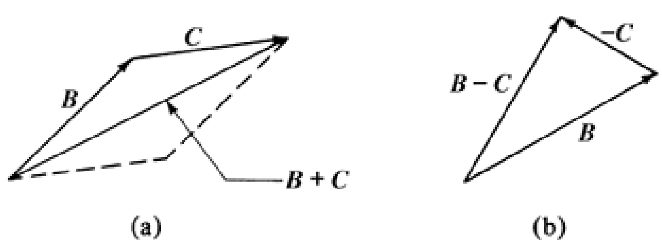

*Figure 3.6-1. Addition and subtraction of vectors: (a) addition of vectors, **B + C**; (b) subtraction of vectors, **B - C**.*

where i, j, and k are unit vectors along the axes x, y, and z, respectively.

In multiplying a scalar quantity r or s by a vector B, the following hold:

Equation 3.6-4.

$$r\boldsymbol{B} = \boldsymbol{B}r$$

Equation 3.6-5.

$$(rs)\boldsymbol{B} = r(s\boldsymbol{B})$$

Equation 3.6-6.

$$r\boldsymbol{B} + s\boldsymbol{B} = (r + s)\boldsymbol{B}$$

The following also hold:

Equation 3.6-7.

$$(\boldsymbol{B} \cdot \boldsymbol{C}) = (\boldsymbol{C} \cdot \boldsymbol{B})$$

Equation 3.6-8.

$$\boldsymbol{B} \cdot (\boldsymbol{C} + \boldsymbol{D}) = (\boldsymbol{B} \cdot \boldsymbol{C}) + (\boldsymbol{B} \cdot \boldsymbol{D})$$

Equation 3.6-9.

$$(\boldsymbol{B} \cdot \boldsymbol{C})\boldsymbol{D} \neq \boldsymbol{B}(\boldsymbol{C} \cdot \boldsymbol{D})$$

Equation 3.6-10.

$$(\boldsymbol{B} \cdot \boldsymbol{C}) = BC \cos\phi_{BC}$$

where ϕ_{BC} is the angle between two vectors and is <180°.

Second-order tensors τ arise primarily in momentum transfer and have nine components. They are discussed elsewhere (B2).

Differential operations with scalars and vectors

The gradient or "grad" of a scalar field is

Equation 3.6-11.

$$\boldsymbol{\nabla}\rho = \boldsymbol{i}\frac{\partial \rho}{\partial x} + \boldsymbol{j}\frac{\partial \rho}{\partial y} + \boldsymbol{k}\frac{\partial \rho}{\partial z}$$

where ρ is a scalar such as density.

The divergence or "div" of a vector v is

Equation 3.6-12.

$$(\boldsymbol{\nabla} \cdot \boldsymbol{v}) = \frac{\partial v_x}{\partial x} + \frac{\partial v_y}{\partial y} + \frac{\partial v_z}{\partial z}$$

where v is a function of v_x, v_y, and v_z.

The Laplacian of a scalar field is

Equation 3.6-13.

$$\boldsymbol{\nabla}^2\rho = \frac{\partial^2 \rho}{\partial x^2} + \frac{\partial^2 \rho}{\partial y^2} + \frac{\partial^2 \rho}{\partial z^2}$$

Other operations that may be useful are

Equation 3.6-14.

$$\boldsymbol{\nabla} rs = r\boldsymbol{\nabla} s + s\boldsymbol{\nabla} r$$

Equation 3.6-15.

$$(\boldsymbol{\nabla} \cdot s\boldsymbol{v}) = (\boldsymbol{\nabla} s \cdot \boldsymbol{v}) + s(\boldsymbol{\nabla} \cdot \boldsymbol{v})$$

Equation 3.6-16.

$$(\boldsymbol{v} \cdot \boldsymbol{\nabla} s) = v_x \frac{\partial s}{\partial x} + v_y \frac{\partial s}{\partial y} + v_z \frac{\partial s}{\partial z}$$

Differential Equation of Continuity

Derivation of equation of continuity

A mass balance will be made for a pure fluid flowing through a stationary volume element $\Delta x\,\Delta y\,\Delta z$ which is fixed in space as in Fig. 3.6-2. The mass balance for the fluid with a concentration of ρ kg/m^3 is

Equation 3.6-17.

$$(\text{rate of mass in}) - (\text{rate of mass out}) = (\text{rate of mass accumulation})$$

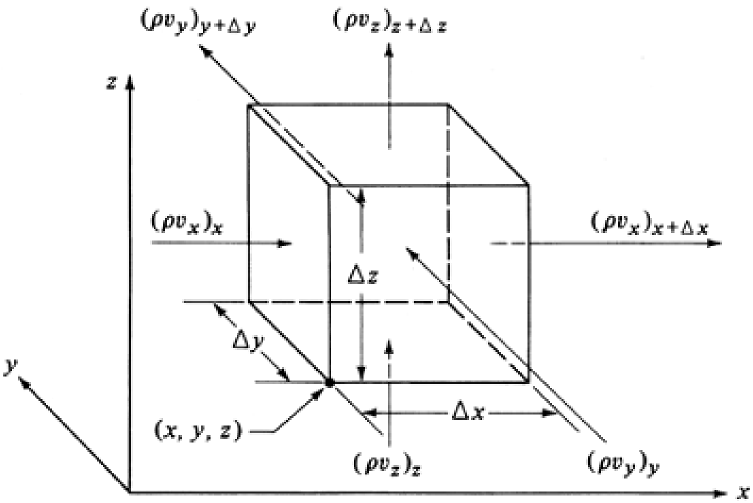

Figure 3.6-2. Mass balance for a pure fluid flowing through a fixed volume Δx Δy Δz in space.

In the x direction the rate of mass entering the face at x having an area of $\Delta y\,\Delta z$ m^2 is $(\rho v_x)_x\,\Delta y\,\Delta z$ kg/s and that leaving at $x + \Delta x$ is $(\rho v_x)_{x+\Delta x}\,\Delta y\,\Delta z$. The term (ρv_x) is a mass flux in kg/s · m^2. Mass entering and mass leaving in the y and z directions are also shown in Fig. 3.6-2.

The rate of mass accumulation in the volume $\Delta x\,\Delta y\,\Delta z$ is

Equation 3.6-18.

$$\text{rate of mass accumulation} = \Delta x\ \Delta y\ \Delta z \frac{\partial \rho}{\partial t}$$

Substituting all these expressions into Eq. (3.6-17) and dividing both sides by $\Delta x\,\Delta y\,\Delta z$,

Equation 3.6-19.

$$\frac{[(\rho v_x)_x - (\rho v_x)_{x+\Delta x}]}{\Delta x} + \frac{[(\rho v_y)_y - (\rho v_y)_{y+\Delta y}]}{\Delta y} + \frac{[(\rho v_z)_z - (\rho v_z)_{z+\Delta z}]}{\Delta z} = \frac{\partial \rho}{\partial t}$$

Taking the limit as Δx, Δy, and Δz approach zero, we obtain the equation of continuity or conservation of mass for a pure fluid:

Equation 3.6-20.

$$\frac{\partial \rho}{\partial t} = -\left[\frac{\partial(\rho v_x)}{\partial x} + \frac{\partial(\rho v_y)}{\partial y} + \frac{\partial(\rho v_z)}{\partial z}\right] = -(\nabla \cdot \rho \boldsymbol{v})$$

The vector notation on the right side of Eq. (3.6-20) comes from the fact that v is a vector. Equation (3.6-20) tells us how density ρ changes with time at a fixed point resulting from the changes in the mass velocity vector ρv.

We can convert Eq. (3.6-20) into another form by carrying out the actual partial differentiation:

Equation 3.6-21.

$$\frac{\partial \rho}{\partial t} = -\rho\left(\frac{\partial v_x}{\partial x} + \frac{\partial v_y}{\partial y} + \frac{\partial v_z}{\partial z}\right) - \left(v_x \frac{\partial \rho}{\partial x} + v_y \frac{\partial \rho}{\partial y} + v_z \frac{\partial \rho}{\partial z}\right)$$

Rearranging Eq. (3.6-21),

Equation 3.6-22.

$$\frac{\partial \rho}{\partial t} + v_x \frac{\partial \rho}{\partial x} + v_y \frac{\partial \rho}{\partial y} + v_z \frac{\partial \rho}{\partial z} = -\rho\left(\frac{\partial v_x}{\partial x} + \frac{\partial v_y}{\partial y} + \frac{\partial v_z}{\partial z}\right)$$

The left-hand side of Eq. (3.6-22) is the same as the substantial derivative in Eq. (3.6-2). Hence, Eq. (3.6-22) becomes

Equation 3.6-23.

$$\frac{D\rho}{Dt} = -\rho\left(\frac{\partial v_x}{\partial x} + \frac{\partial v_y}{\partial y} + \frac{\partial v_z}{\partial z}\right) = -\rho(\nabla \cdot \boldsymbol{v})$$

Equation of continuity for constant density

Often in engineering with liquids that are relatively incompressible, the density ρ is essentially constant. Then ρ remains constant for a fluid element as it moves along a path following the fluid motion, or $D\rho/Dt = \mathbf{0}$. Hence, Eq. (3.6-23) becomes, for a fluid of constant density at steady or unsteady state,

Equation 3.6-24.

$$(\nabla \cdot \boldsymbol{v}) = \frac{\partial v_x}{\partial x} + \frac{\partial v_y}{\partial y} + \frac{\partial v_z}{\partial z} = 0$$

At steady state, $\partial \mathbf{p}/\partial t = \mathbf{0}$ in Eq. (3.6-22).

EXAMPLE 3.6-1. Flow over a Flat Plate

An incompressible fluid flows past one side of a flat plate. The flow in the *x* direction is parallel to the flat plate. At the leading edge of the plate the flow is uniform at the free stream velocity v_{x0}. There is no velocity in the z direction. The *y* direction is the perpendicular distance from the plate. Analyze this case using the equation of continuity.

***Solution*:** For this case where ρ is constant, Eq. (3.6-24) holds:

Equation 3.6-24.

$$\frac{\partial v_x}{\partial x} + \frac{\partial v_y}{\partial y} + \frac{\partial v_z}{\partial z} = 0$$

Since there is no velocity in the *z* direction, we obtain

Equation 3.6-25.

$$\frac{\partial v_x}{\partial x} = -\frac{\partial v_y}{\partial y}$$

At a given small value of *y* close to the plate, the value of v_x must decrease from its free stream velocity v_{x0} as it passes the leading edge in the *x* direction because of fluid friction. Hence, $\partial v_x/\partial x$ is negative. Then from Eq. (3.6-25), $\partial v_y/\partial y$ is positive and there is a component of velocity away from the plate.

Continuity equation in cylindrical and spherical coordinates

It is often convenient to use cylindrical coordinates to solve the equation of continuity if fluid is flowing in a cylinder. The coordinate system as related to rectangular coordinates is shown in Fig. 3.6-3a. The relations between rectangular *x, y, z* and cylindrical *r, θ, z* coordinates are

Equation 3.6-26.

$$x = r\cos\theta \qquad y = r\sin\theta \qquad z = z$$

$$r = +\sqrt{x^2 + y^2} \qquad \theta = \tan^{-1}\frac{y}{x}$$

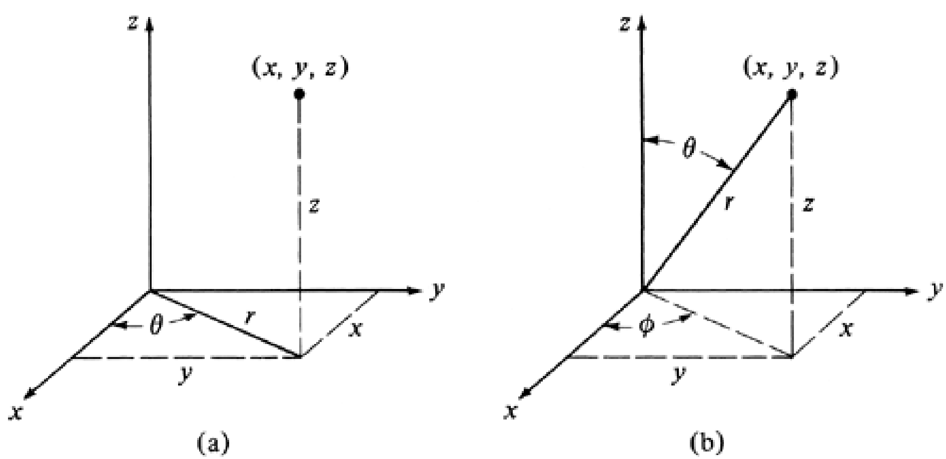

Figure 3.6-3. Curvilinear coordinate systems: (a) cylindrical coordinates, (b) spherical coordinates.

Using the relations from Eq. (3.6-26) with Eq. (3.6-20), the equation of continuity in cylindrical coordinates is

Equation 3.6-27.

$$\frac{\partial \rho}{\partial t} + \frac{1}{r}\frac{\partial(\rho r v_r)}{\partial r} + \frac{1}{r}\frac{\partial(\rho v_\theta)}{\partial \theta} + \frac{\partial(\rho v_z)}{\partial z} = 0$$

For spherical coordinates the variables *r, θ*, and *φ* are related to *x, y, z* by the following, as shown in Fig. 3.6-3b:

Equation 3.6-28.

$$x = r\sin\theta\cos\phi \qquad y = r\sin\theta\sin\phi \qquad z = r\cos\theta$$

$$r = +\sqrt{x^2 + y^2 + z^2} \qquad \theta = \tan^{-1}\frac{\sqrt{x^2 + y^2}}{z} \qquad \phi = \tan^{-1}\frac{y}{x}$$

The equation of continuity in spherical coordinates becomes

Equation 3.6-29.

$$\frac{\partial \rho}{\partial t} + \frac{1}{r^2}\frac{\partial(\rho r^2 v_r)}{\partial r} + \frac{1}{r \sin\theta}\frac{\partial(\rho v_\theta \sin\theta)}{\partial \theta} + \frac{1}{r\sin\theta}\frac{\partial(\rho v_\phi)}{\partial \phi} = 0$$

DIFFERENTIAL EQUATIONS OF MOMENTUM TRANSFER OR MOTION

Derivation of Equations of Momentum Transfer

The *equation of motion* is really the conservation-of-momentum equation (2.8-3), which we can write as

Equation 3.7-1.

$$\begin{pmatrix}\text{rate of}\\ \text{momentum in}\end{pmatrix} - \begin{pmatrix}\text{rate of}\\ \text{momentum out}\end{pmatrix} + \begin{pmatrix}\text{sum of forces}\\ \text{acting on system}\end{pmatrix} = \begin{pmatrix}\text{rate of momentum}\\ \text{accumulation}\end{pmatrix}$$

We will make a balance on an element as in Fig. 3.6-2. First we shall consider only the *x* component of each term in Eq. (3.6-30). The *y* and z components can be described in an analogous manner.

The rate at which the *x* component of momentum enters the face at *x* in the *x* direction by convection is $(\rho v_x v_x)_x \Delta y \Delta z$, and the rate at which it leaves at $x + \Delta x$ is $(\rho v_x v_x)_{x+\Delta x} \Delta y \Delta z$. The quantity (ρv_x) is the concentration in momentum/m^3 or (kg · m/s)/m^3, and it is multiplied by v_x to give the momentum flux as momentum/s · m^2.

The *x* component of momentum entering the face at *y* is $(\rho v_y v_x)_y \Delta x \Delta z$, and leaving at $y + \Delta y$ it is $(\rho v_y v_x)_{y+\Delta y} \Delta x \Delta z$. For the face at *z* we have $(\rho v_z v_x)_z \Delta x \Delta y$ entering, and at $z + \Delta z$ we have $(\rho v_z v_x)_{z+\Delta z} \Delta x \Delta y$ leaving. Hence, the net convective *x* momentum flow into the volume element $\Delta x \Delta y \Delta z$ is

Equation 3.7-2.

$$[(\rho v_x v_x)_x - (\rho v_x v_x)_{x+\Delta x}]\Delta y\, \Delta z + [(\rho v_y v_x)_y - (\rho v_y v_x)_{y+\Delta y}]\Delta x\, \Delta z + [(\rho v_z v_x)_z - (\rho v_z v_x)_{z+\Delta z}]\Delta x\, \Delta y$$

Momentum flows in and out of the volume element by the mechanisms of convection or bulk flow as given in Eq. (3.7-2) and also by molecular transfer (by virtue of the velocity gradients in laminar flow). The rate at which the x component of momentum enters the face at x by molecular transfer is $(\tau_{xx})_x \Delta y \Delta z$, and the rate at which it leaves the surface at x + Ax is $(\tau_{xx})_{x+\Delta x} \Delta y \Delta z$. The rate at which it enters the face at *y* is $(\tau_{yx})_y \Delta x \Delta z$, and it leaves at $y + \Delta y$ at a rate of $(\tau_{yx})_{y+\Delta y} \Delta x \Delta z$. Note that τ_{yx} is the flux of *x* momentum through the face perpendicular to the *y* axis. Writing a similar equation for the remaining faces, the net x component of momentum by molecular transfer is

Equation 3.7-3.

$$[(\tau_{xx})_x - (\tau_{xx})_{x+\Delta x}]\Delta y\, \Delta z + [(\tau_{yx})_y - (\tau_{yx})_{y+\Delta y}]\Delta x\, \Delta z + [(\tau_{zx})_z - (\tau_{zx})_{z+\Delta z}]\Delta x\, \Delta y$$

These molecular fluxes of momentum may be considered as shear stresses and normal stresses. Hence, τ_{yx} is the x-direction shear stress on the y face and τ_{zx} the shear stress on the z face. Also, τ_{xx} is the normal stress on the x face.

The net fluid-pressure force acting on the element in the x direction is the difference between the forces acting at x and $x + \Delta x$:

Equation 3.7-4.

$$(p_x - p_{x+\Delta x})\Delta y \, \Delta z$$

The gravitational force g_x acting on a unit mass in the x direction is multiplied by the mass of the element to give

Equation 3.7-5.

$$\rho g_x \, \Delta x \, \Delta y \, \Delta z$$

where g_x is the x component of the gravitational vector g.

The rate of accumulation of x momentum in the element is

Equation 3.7-6.

$$\Delta x \, \Delta y \, \Delta z \frac{\partial(\rho v_x)}{\partial t}$$

Substituting Eqs. (3.7-2)-(3.7-6) into (3.7-1), dividing by $\Delta x \, \Delta y \, \Delta z$, and taking the limit as Δx, Δy, and Δz approach zero, we obtain the x component of the differential equation of motion:

Equation 3.7-7.

$$\frac{\partial(\rho v_x)}{\partial t} = -\left[\frac{\partial(\rho v_x v_x)}{\partial x} + \frac{\partial(\rho v_y v_x)}{\partial y} + \frac{\partial(\rho v_z v_x)}{\partial z}\right] - \left(\frac{\partial \tau_{xx}}{\partial x} + \frac{\partial \tau_{yx}}{\partial y} + \frac{\partial \tau_{zx}}{\partial z}\right) - \frac{\partial p}{\partial x} + \rho g_x$$

The y and z components of the differential equation of motion are, respectively,

Equation 3.7-8.

$$\frac{\partial(\rho v_y)}{\partial t} = -\left[\frac{\partial(\rho v_x v_y)}{\partial x} + \frac{\partial(\rho v_y v_y)}{\partial y} + \frac{\partial(\rho v_z v_y)}{\partial z}\right] - \left(\frac{\partial \tau_{xy}}{\partial x} + \frac{\partial \tau_{yy}}{\partial y} + \frac{\partial \tau_{zy}}{\partial z}\right) - \frac{\partial p}{\partial y} + \rho g_y$$

Equation 3.7-9.

$$\frac{\partial(\rho v_z)}{\partial t} = -\left[\frac{\partial(\rho v_x v_z)}{\partial x} + \frac{\partial(\rho v_y v_z)}{\partial y} + \frac{\partial(\rho v_z v_z)}{\partial z}\right] - \left(\frac{\partial \tau_{xz}}{\partial x} + \frac{\partial \tau_{yz}}{\partial y} + \frac{\partial \tau_{zz}}{\partial z}\right) - \frac{\partial p}{\partial z} + \rho g_z$$

We can use Eq. (3.6-20), which is the continuity equation, and Eq. (3.7-7) to obtain an equation of motion for the *x* component and also do the same for the *y* and *z* components as follows:

Equation 3.7-10.

$$\rho\left(\frac{\partial v_x}{\partial t} + v_x\frac{\partial v_x}{\partial x} + v_y\frac{\partial v_x}{\partial y} + v_z\frac{\partial v_x}{\partial z}\right) = -\left[\frac{\partial \tau_{xx}}{\partial x} + \frac{\partial \tau_{yx}}{\partial y} + \frac{\partial \tau_{zx}}{\partial z}\right] + \rho g_x - \frac{\partial p}{\partial x}$$

Equation 3.7-11.

$$\rho\left(\frac{\partial v_y}{\partial t} + v_x\frac{\partial v_y}{\partial x} + v_y\frac{\partial v_y}{\partial y} + v_z\frac{\partial v_y}{\partial z}\right) = -\left[\frac{\partial \tau_{xy}}{\partial x} + \frac{\partial \tau_{yy}}{\partial y} + \frac{\partial \tau_{zy}}{\partial z}\right] + \rho g_y - \frac{\partial p}{\partial y}$$

Equation 3.7-12.

$$\rho\left(\frac{\partial v_z}{\partial t} + v_x\frac{\partial v_z}{\partial x} + v_y\frac{\partial v_z}{\partial y} + v_z\frac{\partial v_z}{\partial z}\right) = -\left[\frac{\partial \tau_{xz}}{\partial x} + \frac{\partial \tau_{yz}}{\partial y} + \frac{\partial \tau_{zz}}{\partial z}\right] + \rho g_z - \frac{\partial p}{\partial z}$$

Adding vectorially, we obtain an equation of motion for a pure fluid:

Equation 3.7-13.

$$\rho\frac{D\boldsymbol{v}}{Dt} = -(\boldsymbol{\nabla}\cdot\boldsymbol{\tau}) - \boldsymbol{\nabla}p + \rho\boldsymbol{g}$$

We should note that Eqs. (3.7-7)-(3.7-13) are valid for any continuous medium.

Equations of Motion for Newtonian Fluids with Varying Density and Viscosity

In order to use Eqs. (3.7-7)-(3.7-13) to determine velocity distributions, expressions must be used for the various stresses in terms of velocity gradients and fluid properties. For Newtonian fluids the expressions for the stresses τ_{xx}, τ_{yx}, τ_{zx}, and so on, have been related to the velocity gradients and the fluid viscosity μ (B1, B2, D1) and are as follows:

Shear-stress components for Newtonian fluids in rectangular coordinates

Equation 3.7-14.

$$\tau_{xx} = -2\mu\frac{\partial v_x}{\partial x} + \frac{2}{3}\mu(\boldsymbol{\nabla}\cdot\boldsymbol{v})$$

Equation 3.7-15.

$$\tau_{yy} = -2\mu\frac{\partial v_y}{\partial y} + \frac{2}{3}\mu(\boldsymbol{\nabla}\cdot\boldsymbol{v})$$

Equation 3.7-16.

$$\tau_{zz} = -2\mu\frac{\partial v_z}{\partial z} + \frac{2}{3}\mu(\boldsymbol{\nabla}\cdot\boldsymbol{v})$$

Equation 3.7-17.

$$\tau_{xy} = \tau_{yx} = -\mu\left(\frac{\partial v_x}{\partial y} + \frac{\partial v_y}{\partial x}\right)$$

Equation 3.7-18.

$$\tau_{yz} = \tau_{zy} = -\mu\left(\frac{\partial v_y}{\partial z} + \frac{\partial v_z}{\partial y}\right)$$

Equation 3.7-19.

$$\tau_{zx} = \tau_{xz} = -\mu\left(\frac{\partial v_z}{\partial x} + \frac{\partial v_x}{\partial z}\right)$$

Equation 3.7-20.

$$(\nabla \cdot v) = \left(\frac{\partial v_x}{\partial x} + \frac{\partial v_y}{\partial y} + \frac{\partial v_z}{\partial z}\right)$$

Shear-stress components for Newtonian fluids in cylindrical coordinates

Equation 3.7-21.

$$\tau_{rr} = -\mu\left[2\frac{\partial v_r}{\partial r} - \frac{2}{3}(\nabla \cdot v)\right]$$

Equation 3.7-22.

$$\tau_{\theta\theta} = -\mu\left[2\left(\frac{1}{r}\frac{\partial v_\theta}{\partial \theta} + \frac{v_r}{r}\right) - \frac{2}{3}(\nabla \cdot v)\right]$$

Equation 3.7-23.

$$\tau_{zz} = -2\mu\frac{\partial v_z}{\partial z} + \frac{2}{3}\mu(\nabla \cdot v)$$

Equation 3.7-24.

$$\tau_{r\theta} = \tau_{\theta r} = -\mu\left[r\frac{\partial(v_\theta/r)}{\partial r} + \frac{1}{r}\frac{\partial v_r}{\partial \theta}\right]$$

Equation 3.7-25.

$$\tau_{\theta z} = \tau_{z\theta} = -\mu\left[\frac{\partial v_\theta}{\partial z} + \frac{1}{r}\frac{\partial v_z}{\partial \theta}\right]$$

Equation 3.7-26.

$$\tau_{zr} = \tau_{rz} = -\mu\left[\frac{\partial v_z}{\partial r} + \frac{\partial v_r}{\partial z}\right]$$

Equation 3.7-27.

$$(\nabla \cdot v) = \frac{1}{r}\frac{\partial(rv_r)}{\partial r} + \frac{1}{r}\frac{\partial v_\theta}{\partial \theta} + \frac{\partial v_z}{\partial z}$$

Shear-stress components for Newtonian fluids in spherical coordinates

Equation 3.7-28.

$$\tau_{rr} = -\mu\left[2\frac{\partial v_r}{\partial r} - \frac{2}{3}(\nabla \cdot v)\right]$$

Equation 3.7-29.

$$\tau_{\theta\theta} = -\mu\left[2\left(\frac{1}{r}\frac{\partial v_\theta}{\partial \theta} + \frac{v_r}{r}\right) - \frac{2}{3}(\nabla \cdot v)\right]$$

Equation 3.7-30.

$$\tau_{\phi\phi} = -\mu\left[2\left(\frac{1}{r\sin\theta}\frac{\partial v_\phi}{\partial \phi} + \frac{v_r}{r} + \frac{v_\theta \cot\theta}{r}\right) - \frac{2}{3}(\nabla \cdot v)\right]$$

Equation 3.7-31.

$$\tau_{r\theta} = \tau_{\theta r} = -\mu\left[r\frac{\partial(v_\theta/r)}{\partial r} + \frac{1}{r}\frac{\partial v_r}{\partial \theta}\right]$$

Equation 3.7-32.

$$\tau_{\theta\phi} = \tau_{\phi\theta} = -\mu\left[\frac{\sin\theta}{r}\frac{\partial(v_\phi/\sin\theta)}{\partial \theta} + \frac{1}{r\sin\theta}\frac{\partial v_\theta}{\partial \phi}\right]$$

Equation 3.7-33.

$$\tau_{\phi r} = \tau_{r\phi} = -\mu\left[\frac{1}{r\sin\theta}\frac{\partial v_r}{\partial \phi} + r\frac{\partial(v_\phi/r)}{\partial r}\right]$$

Equation 3.7-34.

$$(\nabla \cdot v) = \frac{1}{r^2}\frac{\partial(r^2 v_r)}{\partial r} + \left[\frac{1}{r\sin\theta}\frac{\partial(v_\theta \sin\theta)}{\partial \theta} + \frac{1}{r\sin\theta}\frac{\partial v_\phi}{\partial \phi}\right]$$

Equation of motion for Newtonian fluids with varying density and viscosity

After Eqs. (3.7-14)-(3.7-20) for shear-stress components are substituted into Eq. (3.7-10) for the *x* component of momentum, we obtain the general equation of motion for a Newtonian fluid with varying density and viscosity:

Equation 3.7-35.

$$\rho\frac{Dv_x}{Dt} = \frac{\partial}{\partial x}\left[2\mu\frac{\partial v_x}{\partial x} - \frac{2}{3}\mu(\nabla \cdot v)\right] + \frac{\partial}{\partial y}\left[\mu\left(\frac{\partial v_x}{\partial y} + \frac{\partial v_y}{\partial x}\right)\right]$$
$$+ \frac{\partial}{\partial z}\left[\mu\left(\frac{\partial v_z}{\partial x} + \frac{\partial v_x}{\partial z}\right)\right] - \frac{\partial p}{\partial x} + \rho g_x$$

Similar equations are obtained for the *y* and *z* components of momentum.

Equations of Motion for Newtonian Fluids with Constant Density and Viscosity

The equations above are seldom used in their complete forms. When the density ρ and the viscosity μ are constant where $(\nabla \cdot v) = 0$, the equations are simplified and we obtain the equations of motion for Newtonian fluids. These equations are also called the *Navier-Stokes equations.*

Equation of motion in rectangular coordinates

For Newtonian fluids for constant ρ and μ for the x component, y component, and z component we obtain, respectively,

Equation 3.7-36.

$$\rho\left(\frac{\partial v_x}{\partial t} + v_x\frac{\partial v_x}{\partial x} + v_y\frac{\partial v_x}{\partial y} + v_z\frac{\partial v_x}{\partial z}\right) = \mu\left(\frac{\partial^2 v_x}{\partial x^2} + \frac{\partial^2 v_x}{\partial y^2} + \frac{\partial^2 v_x}{\partial z^2}\right) - \frac{\partial p}{\partial x} + \rho g_x$$

Equation 3.7-37.

$$\rho\left(\frac{\partial v_y}{\partial t} + v_x\frac{\partial v_y}{\partial x} + v_y\frac{\partial v_y}{\partial y} + v_z\frac{\partial v_y}{\partial z}\right) = \mu\left(\frac{\partial^2 v_y}{\partial x^2} + \frac{\partial^2 v_y}{\partial y^2} + \frac{\partial^2 v_y}{\partial z^2}\right) - \frac{\partial p}{\partial y} + \rho g_y$$

Equation 3.7-38.

$$\rho\left(\frac{\partial v_z}{\partial t} + v_x\frac{\partial v_z}{\partial x} + v_y\frac{\partial v_z}{\partial y} + v_z\frac{\partial v_z}{\partial z}\right) = \mu\left(\frac{\partial^2 v_z}{\partial x^2} + \frac{\partial^2 v_z}{\partial y^2} + \frac{\partial^2 v_z}{\partial z^2}\right) - \frac{\partial p}{\partial z} + \rho g_z$$

Combining the three equations for the three components, we obtain

Equation 3.7-39.

$$\rho\frac{D\mathbf{v}}{Dt} = -\nabla p + \rho\mathbf{g} + \mu\nabla^2\mathbf{v}$$

Equation of motion in cylindrical coordinates

These equations are as follows for Newtonian fluids for constant ρ and μ for the r, θ, and z components, respectively:

Equation 3.7-40.

$$\rho\left(\frac{\partial v_r}{\partial t} + v_r\frac{\partial v_r}{\partial r} + \frac{v_\theta}{r}\frac{\partial v_r}{\partial \theta} - \frac{v_\theta^2}{r} + v_z\frac{\partial v_r}{\partial z}\right)$$
$$= -\frac{\partial p}{\partial r} + \mu\left[\frac{\partial}{\partial r}\left(\frac{1}{r}\frac{\partial(rv_r)}{\partial r}\right) + \frac{1}{r^2}\frac{\partial^2 v_r}{\partial \theta^2} - \frac{2}{r^2}\frac{\partial v_\theta}{\partial \theta} + \frac{\partial^2 v_r}{\partial z^2}\right] + \rho g_r$$

Equation 3.7-41.

$$\rho\left(\frac{\partial v_\theta}{\partial t} + v_r\frac{\partial v_\theta}{\partial r} + \frac{v_\theta}{r}\frac{\partial v_\theta}{\partial \theta} + \frac{v_r v_\theta}{r} + v_z\frac{\partial v_\theta}{\partial z}\right)$$
$$= -\frac{1}{r}\frac{\partial p}{\partial \theta} + \mu\left[\frac{\partial}{\partial r}\left(\frac{1}{r}\frac{\partial(rv_\theta)}{\partial r}\right) + \frac{1}{r^2}\frac{\partial^2 v_\theta}{\partial \theta^2} + \frac{2}{r^2}\frac{\partial v_r}{\partial \theta} + \frac{\partial^2 v_\theta}{\partial z^2}\right] + \rho g_\theta$$

Equation 3.7-42.

$$\rho\left(\frac{\partial v_z}{\partial t} + v_r\frac{\partial v_z}{\partial r} + \frac{v_\theta}{r}\frac{\partial v_z}{\partial \theta} + v_z\frac{\partial v_z}{\partial z}\right) = -\frac{\partial p}{\partial z} + \mu\left[\frac{1}{r}\frac{\partial}{\partial r}\left(r\frac{\partial v_z}{\partial r}\right) + \frac{1}{r^2}\frac{\partial^2 v_z}{\partial \theta^2} + \frac{\partial^2 v_z}{\partial z^2}\right] + \rho g_z$$

Equation of motion in spherical coordinates

The equations for Newtonian fluids are given below for constant ρ and μ for the r, θ, and ϕ components, respectively:

Equation 3.7-43.

$$\rho\left(\frac{\partial v_r}{\partial t} + v_r\frac{\partial v_r}{\partial r} + \frac{v_\theta}{r}\frac{\partial v_r}{\partial \theta} + \frac{v_\phi}{r\sin\theta}\frac{\partial v_r}{\partial \phi} - \frac{v_\theta^2 + v_\phi^2}{r}\right) = -\frac{\partial p}{\partial r} + \mu\left(\nabla^2 v_r - \frac{2}{r^2}v_r - \frac{2}{r^2}\frac{\partial v_\theta}{\partial \theta} - \frac{2}{r^2}v_\theta\cot\theta - \frac{2}{r^2\sin\theta}\frac{\partial v_\phi}{\partial \phi}\right) + \rho g_r$$

Equation 3.7-44.

$$\rho\left(\frac{\partial v_\theta}{\partial t} + v_r\frac{\partial v_\theta}{\partial r} + \frac{v_\theta}{r}\frac{\partial v_\theta}{\partial \theta} + \frac{v_\phi}{r\sin\theta}\frac{\partial v_\theta}{\partial \phi} + \frac{v_r v_\theta}{r} - \frac{v_\phi^2\cot\theta}{r}\right) = -\frac{1}{r}\frac{\partial p}{\partial \theta} + \mu\left(\nabla^2 v_\theta + \frac{2}{r^2}\frac{\partial v_r}{\partial \theta} - \frac{v_\theta}{r^2\sin^2\theta} - \frac{2}{r^2}\frac{\cos\theta}{\sin^2\theta}\frac{\partial v_\phi}{\partial \phi}\right) + \rho g_\theta$$

Equation 3.7-45.

$$\rho\left(\frac{\partial v_\phi}{\partial t} + v_r\frac{\partial v_\phi}{\partial r} + \frac{v_\theta}{r}\frac{\partial v_\phi}{\partial \theta} + \frac{v_\phi}{r\sin\theta}\frac{\partial v_\phi}{\partial \phi} + \frac{v_\phi v_r}{r} + \frac{v_\theta v_\phi}{r}\cot\theta\right) = -\frac{1}{r\sin\theta}\frac{\partial p}{\partial \phi} + \mu\left(\nabla^2 v_\phi - \frac{v_\phi}{r^2\sin^2\theta} + \frac{2}{r^2\sin\theta}\frac{\partial v_r}{\partial \phi} + \frac{2\cos\theta}{r^2\sin^2\theta}\frac{\partial v_\theta}{\partial \phi}\right) + \rho g_\phi$$

where in the three equations above,

Equation 3.7-46.

$$\nabla^2 = \frac{1}{r^2}\frac{\partial}{\partial r}\left(r^2\frac{\partial}{\partial r}\right) + \frac{1}{r^2\sin\theta}\frac{\partial}{\partial \theta}\left(\sin\theta\frac{\partial}{\partial \theta}\right) + \frac{1}{r^2\sin^2\theta}\left(\frac{\partial^2}{\partial \phi^2}\right)$$

Significant advantages and uses arise in the transformation from rectangular coordinates to cylindrical coordinates. For example, in Eq. (3.7-40) the term $\rho v_\theta^2/r$ is the centrifugal force. This gives the force in the r direction (radial) resulting from the motion of the fluid in the θ direction. Note that this term is obtained automatically from the transformation from rectangular to cylindrical coordinates. It does not have to be added to the equation on physical grounds.

The Coriolis force $\rho v_r v_\theta/r$ also arises automatically in the transformation of coordinates in Eq. (3.7-41). It is the effective force in the θ direction when there is flow in both the r and the θ directions, as in the case of flow near a rotating disk.

USE OF DIFFERENTIAL EQUATIONS OF CONTINUITY AND MOTION

Introduction

The purpose and uses of the differential equations of motion and continuity, as mentioned previously, are to apply these equations to any viscous-flow problem. For a given specific problem, the terms that are zero or near zero are simply discarded and the remaining equations used to solve for the velocity, density, and pressure distributions. Of course, it is necessary to know the initial conditions and the boundary conditions to solve the equations. Several examples will be given to illustrate the general methods used.

We will consider cases for flow in specific geometries that can easily be described mathematically, such as flow between parallel plates and in cylinders.

Differential Equations of Continuity and Motion for Flow between Parallel Plates

Two examples will be considered, one for horizontal plates and one for vertical plates.

EXAMPLE 3.8-1. Laminar Flow Between Horizontal Parallel Plates

Derive the equation giving the velocity distribution at steady state for laminar flow of a constant-density fluid with constant viscosity flowing between two flat and parallel plates. The velocity profile desired is at a point far from the inlet or outlet of the channel. The two plates will be considered to be fixed and of infinite width, with the flow driven by the pressure gradient in the x direction.

Solution: Assuming that the channel is horizontal, Fig. 3.8-1 shows the axes selected, with flow in the x direction and the width in the z direction. The velocities v_y and v_z are then zero. The plates are a distance $2y_0$ apart.

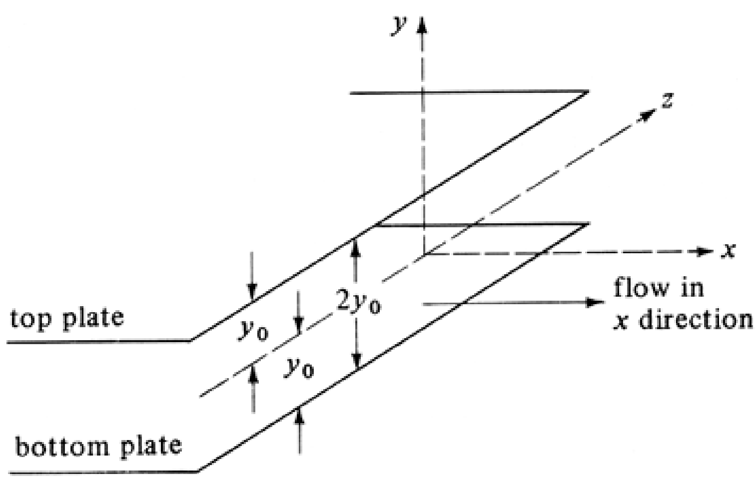

Figure 3.8-1. Flow between two parallel plates in Example 3.8-1.

The continuity equation (3.6-24) for constant density is

Equation 3.6-24.

$$\frac{\partial v_x}{\partial x} + \frac{\partial v_y}{\partial y} + \frac{\partial v_z}{\partial z} = 0$$

Since v_y and v_z are zero, Eq. (3.6-24) becomes

Equation 3.8-1.

$$\frac{\partial v_x}{\partial x} = 0$$

The Navier-Stokes equation for the x component is

Equation 3.7-36.

$$\rho\left(\frac{\partial v_x}{\partial t} + v_x\frac{\partial v_x}{\partial x} + v_y\frac{\partial v_x}{\partial y} + v_z\frac{\partial v_x}{\partial z}\right) = \mu\left(\frac{\partial^2 v_x}{\partial x^2} + \frac{\partial^2 v_x}{\partial y^2} + \frac{\partial^2 v_x}{\partial z^2}\right) - \frac{\partial p}{\partial x} + \rho g_x$$

Also, $\partial v_x/\partial t = 0$ for steady state, $v_y = 0$, $v_z = 0$, $\partial v_x/\partial x = 0$, $\partial^2 v_x/\partial x^2 = 0$. We can see that $\partial v_x/\partial z = 0$, since there is no change of v_x with z. Then $\partial^2 v_x/\partial z^2 = 0$. Making these substitutions into Eq. (3.7-36), we obtain

Equation 3.8-2.

$$\frac{\partial p}{\partial x} - \rho g_x = \mu\frac{\partial^2 v_x}{\partial y^2}$$

In fluid-flow problems we will be concerned with gravitational force only in the vertical direction for g_x, which is g, the gravitational force, in m/s^2. We shall combine the static pressure p and the gravitational force and call them simply p, as follows (note that $g_x = 0$ for the present case of a horizontal pipe but is not zero for the general case of a nonhorizontal pipe):

Equation 3.8-3.

$$p = p + \rho g h$$

where h is the distance upward from any chosen reference plane (h is in the direction opposed to gravity). Then Eq. (3.8-2) becomes

Equation 3.8-4.

$$\frac{\partial p}{\partial x} = \mu\frac{\partial^2 v_x}{\partial y^2}$$

We can see that p is not a function of z. Also, assuming that $2y_0$ is small, p is not a function of y. (Some references avoid this problem and simply use p as a dynamic pressure, which is rigorously correct since dynamic pressure gradients cause flow. In a fluid at rest, the total pressure gradient is the hydrostatic pressure gradient, and the dynamic pressure gradient is zero.) Also, $\partial p/\partial x$ is a constant in this problem, since v_x is not a function of x. Then Eq. (3.8-4) becomes an ordinary differential equation:

Equation 3.8-5.

$$\frac{d^2 v_x}{dy^2} = \frac{1}{\mu}\frac{dp}{dx} = \text{const}$$

Integrating Eq. (3.8-5) once, using the condition $dv_x/dy = 0$ at $y = 0$ for symmetry,

Equation 3.8-6.

$$\frac{dv_x}{dy} = \left(\frac{1}{\mu}\frac{dp}{dx}\right)y$$

Integrating again, using $v_x = 0$ at $y = y_0$,

Equation 3.8-7.

$$v_x = \frac{1}{2\mu}\frac{dp}{dx}(y^2 - y_0^2)$$

The maximum velocity in Eq. (3.8-7) occurs when $y = 0$, giving

Equation 3.8-8.

$$v_{x\max} = \frac{1}{2\mu}\frac{dp}{dx}(-y_0^2)$$

Combining Eqs. (3.8-7) and (3.8-8),

Equation 3.8-9.

$$v_x = v_{x\max}\left[1 - \left(\frac{y}{y_0}\right)^2\right]$$

Hence, a parabolic velocity profile is obtained. This result was also obtained in Eq. (2.9-9) when using a shell-momentum balance.

The results obtained in Example 3.8-1 could also have been obtained by making a force balance on a differential element of fluid and using the symmetry of the system to omit certain terms.

EXAMPLE 3.8-2. Laminar Flow Between Vertical Plates with One Plate Moving

A Newtonian fluid is confined between two parallel and vertical plates as shown in Fig. 3.8-2 (W6). The surface on the left is stationary and the other is moving vertically at a constant velocity v_0. Assuming that the flow is laminar, solve for the velocity profile.

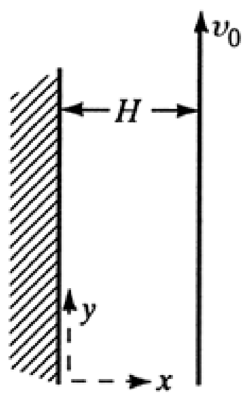

Figure 3.8-2. Flow between vertical parallel plates in Example 3.8-2.

Solution: The equation to use is the Navier-Stokes equation for the y coordinate, Eq. (3.7-37):

Equation 3.7-37.

$$\rho\left(\frac{\partial v_y}{\partial t} + v_x\frac{\partial v_y}{\partial x} + v_y\frac{\partial v_y}{\partial y} + v_z\frac{\partial v_y}{\partial z}\right) = \mu\left(\frac{\partial^2 v_y}{\partial x^2} + \frac{\partial^2 v_y}{\partial y^2} + \frac{\partial^2 v_y}{\partial z^2}\right) - \frac{\partial p}{\partial y} + \rho g_y$$

At steady state, $\partial v_y/\partial t = 0$. The velocities v_x and $v_z = 0$. Also, $\partial v_y/\partial y = 0$ from the continuity equation, $\partial v_y/\partial z = 0$, and $\rho g_y = -\rho g$. The partial derivatives become derivatives and Eq. (3.7-37) becomes

Equation 3.8-10.

$$\mu \frac{d^2 v_y}{dx^2} - \frac{dp}{dy} - \rho g = 0$$

This is similar to Eq. (3.8-2) in Example 3.8-1. The pressure gradient *dp/dy* **is** constant. Integrating Eq. (3.8-10) once yields

Equation 3.8-11.

$$\frac{dv_y}{dx} - \frac{x}{\mu}\left(\frac{dp}{dy} + \rho g\right) = C_1$$

Integrating again gives

Equation 3.8-12.

$$v_y - \frac{x^2}{2\mu}\left(\frac{dp}{dy} + \rho g\right) = C_1 x + C_2$$

The boundary conditions are at $x = 0$, $v_y = 0$ and at $x = H$, $v_y = v_0$. Solving for the constants, $C_1 = v_0/H - (H/2\mu)(dp/dy + \rho g)$ and $C_2 = 0$. Hence, Eq. (3.8-12) becomes

Equation 3.8-13.

$$v_y = -\frac{1}{2\mu}\left(\frac{dp}{dy} + \rho g\right)(Hx - x^2) + v_0 \frac{x}{H}$$

Differential Equations of Continuity and Motion for Flow in Stationary and Rotating Cylinders

Several examples will be given for flow in stationary and rotating cylinders.

EXAMPLE 3.8-3. Laminar Flow in a Circular Tube

Derive the equation for steady-state viscous flow in a horizontal tube of radius r_0, where the fluid is far from the tube inlet. The fluid is incompressible and μ is a constant. The flow is driven in one direction by a constant-pressure gradient.

Solution: The fluid will be assumed to flow in the *z* direction in the tube, as shown in Fig. 3.8-3. The *y* direction is vertical and the *x* direction horizontal. Since v_x and v_y are zero, the continuity equation becomes $\partial v_z/\partial z = 0$. For steady state $\partial v_z/\partial t = 0$. Then substituting into Eq. (3.7-38) for the *z* component, we obtain

Equation 3.8-14.

$$\frac{dp}{dz} = \mu\left(\frac{\partial^2 v_z}{\partial x^2} + \frac{\partial^2 v_z}{\partial y^2}\right)$$

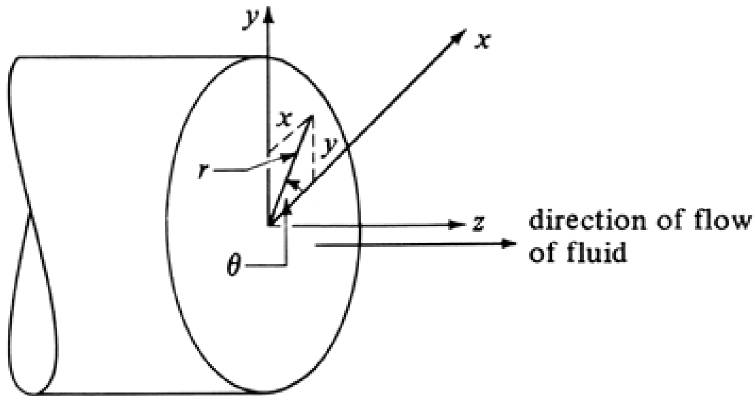

Figure 3.8-3. Horizontal flow in a tube in Example 3.8-3.

To solve Eq. (3.8-14), we can use cylindrical coordinates from Eq. (3.6-26), giving

Equation 3.6-26.

$$z = z \qquad x = r\cos\theta \qquad y = r\sin\theta$$

$$r = +\sqrt{x^2 + y^2} \qquad \theta = \tan^{-1}\frac{y}{x}$$

Substituting these into Eq. (3.8-14),

Equation 3.8-15.

$$\frac{1}{\mu}\frac{dp}{dz} = \frac{\partial^2 v_z}{\partial r^2} + \frac{1}{r}\frac{\partial v_z}{\partial r} + \frac{1}{r^2}\frac{\partial^2 v_z}{\partial \theta^2}$$

The flow is symmetrical about the *z* axis, so $\partial^2 v_z/\partial\theta^2$ is zero in Eq. (3.8-15). As before, dp/dz is a constant, and Eq. (3.8-15) becomes

Equation 3.8-16.

$$\frac{1}{\mu}\frac{dp}{dz} = \text{const} = \frac{d^2 v_z}{dr^2} + \frac{1}{r}\frac{dv_z}{dr} = \frac{1}{r}\frac{d}{dr}\left(r\frac{dv_z}{dr}\right)$$

Alternatively, Eq. (3.7-42) in cylindrical coordinates can be used for the *z* component and the terms that are zero discarded:

Equation 3.7-42.

$$\rho\left(\frac{\partial v_z}{\partial t} + v_r\frac{\partial v_z}{\partial r} + \frac{v_\theta}{r}\frac{\partial v_z}{\partial \theta} + v_z\frac{\partial v_z}{\partial z}\right) = -\frac{\partial p}{\partial z} + \mu\left[\frac{1}{r}\frac{\partial}{\partial r}\left(r\frac{\partial v_z}{\partial r}\right) + \frac{1}{r^2}\frac{\partial^2 v_z}{\partial \theta^2} + \frac{\partial^2 v_z}{\partial z^2}\right] + \rho g_z$$

As before, $\partial v_z/\partial t = 0$, $\partial^2 v_z/\partial\theta^2 = 0$, $v_r = 0$, $\partial v_z/\partial\theta = 0$, $\partial v_z/\partial z = 0$. Then Eq. (3.7-42) becomes identical to Eq. (3.8-16).

The boundary conditions for the first integration are $dv_z/dr = 0$ at $r = 0$. For the second integration, $v_z = 0$ at $r = r_0$ (tube radius). The result is

Equation 3.8-17.

$$v_z = \frac{1}{4\mu}\frac{dp}{dz}(r^2 - r_0^2)$$

Converting to the maximum velocity as before,

Equation 3.8-18.

$$v_z = v_{z\max}\left[1 - \left(\frac{r}{r_0}\right)^2\right]$$

If Eq. (3.8-17) is integrated over the pipe cross section using Eq. (2.9-10) to give the average velocity $v_{z\,av}$,

Equation 3.8-19.

$$v_{z\,av} = -\frac{r_0^2}{8\mu}\frac{dp}{dz}$$

Integrating to obtain the pressure drop from $z = 0$ for $p = p_1$ to $z = L$ for $p = p_2$, we obtain

Equation 3.8-20.

$$p_1 - p_2 = \frac{8\mu v_{z\,av} L}{r_0^2} = \frac{32\mu v_{z\,av} L}{D^2}$$

where $D = 2r_0$. This is the Hagen-Poiseuille equation, derived previously as Eq. (2.9-11).

EXAMPLE 3.8-4. Laminar Flow in a Cylindrical Annulus

Derive the equation for steady-state laminar flow inside the annulus between two concentric horizontal pipes. This type of flow occurs often in concentric-pipe heat exchangers.

Solution: In this case Eq. (3.8-16) also still holds. However, the velocity in the annulus will reach a maximum at some radius $r = r_{max}$ which is between r_1 and r_2, as shown in Fig. 3.8-4. For the first integration of Eq. (3.8-16), the boundary conditions are $dv_z/dr = 0$ at $r = r_{max}$, which gives

Equation 3.8-21.

$$\frac{r\,dv_z}{dr} = \left(\frac{1}{\mu}\frac{dp}{dz}\right)\left(\frac{r^2}{2} - \frac{r_{max}^2}{2}\right)$$

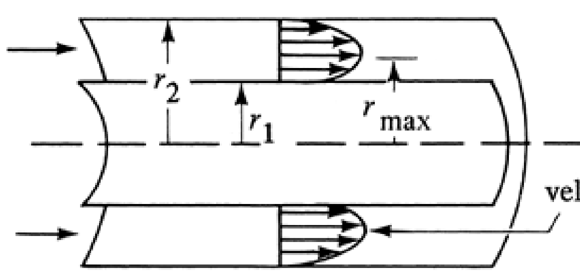

Figure 3.8-4. Flow through a cylindrical annulus.

Also, for the second integration of Eq. (3.8-21), $v_z = 0$ at the inner wall where $r = r_1$, giving

Equation 3.8-22.

$$v_z = \left(\frac{1}{2\mu}\frac{dp}{dz}\right)\left(\frac{r^2}{2} - \frac{r_1^2}{2} - r_{max}^2 \ln\frac{r}{r_1}\right)$$

Repeating the second integration but for $v_z = 0$ at the outer wall where $r = r_2$, we obtain

Equation 3.8-23.

$$v_z = \left(\frac{1}{2\mu}\frac{dp}{dz}\right)\left(\frac{r^2}{2} - \frac{r_2^2}{2} - r_{\max}^2 \ln\frac{r}{r_2}\right)$$

Combining Eqs. (3.8-22) and (3.8-23) and solving for $r_{\max}$,

Equation 3.8-24.

$$r_{\max} = \sqrt{\frac{1}{\ln(r_2/r_1)}(r_2^2 - r_1^2)/2}$$

In Fig. 3.8-4 the velocity profile predicted by Eq. (3.8-23) is plotted. For the case where $r_1 = 0$, $r_{\max}$ in Eq. (3.8-24) becomes zero and Eq. (3.8-23) reduces to Eq. (3.8-17) for a single circular pipe.

EXAMPLE 3.8-5. Velocity Distribution for Flow Between Coaxial Cylinders

Tangential laminar flow of a Newtonian fluid with constant density is occurring between two vertical coaxial cylinders in which the outer one is rotating (S4) with an angular velocity of ω, as shown in Fig. 3.8-5. It can be assumed that end effects can be neglected. Determine the velocity and the shear-stress distributions for this flow.

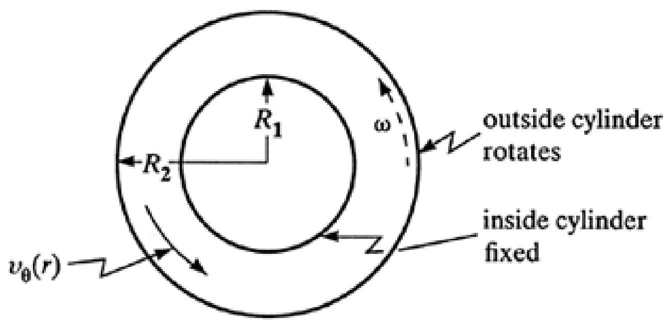

Figure 3.8-5. Laminar flow in the region between two coaxial cylinders in Example 3.8-5.

Solution: On physical grounds the fluid moves in a circular motion; the velocity v_r in the radial direction is zero and v_z in the axial direction is zero. Also, $\partial\rho/\partial t = 0$ at steady state. There is no pressure gradient in the θ direction. The equation of continuity in cylindrical coordinates as derived before is

Equation 3.6-27.

$$\frac{\partial\rho}{\partial t} + \frac{1}{r}\frac{\partial(\rho r v_r)}{\partial r} + \frac{1}{r}\frac{\partial(\rho v_\theta)}{\partial\theta} + \frac{\partial(\rho v_z)}{\partial z} = 0$$

All terms in this equation are zero.

The equations of motion in cylindrical coordinates, Eqs. (3.7-40), (3.7-41), and (3.7-42), reduce to the following, respectively:

Equation 3.8-25.

$$-\rho\frac{v_\theta^2}{r} = -\frac{\partial p}{\partial r} \qquad (r\text{-component})$$

Equation 3.8-26.

$$0 = \frac{d}{dr}\left(\frac{1}{r}\frac{d(rv_\theta)}{dr}\right) \qquad (\theta\text{-component})$$

Equation 3.8-27.

$$0 = -\frac{\partial p}{\partial z} + \rho g_z \qquad (z\text{-component})$$

Integrating Eq. (3.8-26),

Equation 3.8-28.

$$v_\theta = C_1 r + \frac{C_2}{r}$$

To solve for the integration constants C_1 and C_2, the following boundary conditions are used: at $r = R_1$, $v_\theta = 0$; at $r = R_2$, $v_\theta = \omega R_2$. The final equation is

Equation 3.8-29.

$$v_\theta = \frac{\omega}{(R_1^2 - R_2^2)/(R_1 R_2^2)}\left[\frac{R_1}{r} - \frac{r}{R_1}\right]$$

Using the shear-stress component for Newtonian fluids in cylindrical coordinates,

Equation 3.7-31.

$$\tau_{r\theta} = -\mu\left[r\frac{\partial(v_\theta/r)}{\partial r} + \frac{1}{r}\frac{\partial v_r}{\partial \theta}\right]$$

The last term in Eq. (3.7-31) is zero. Substituting Eq. (3.8-29) into (3.7-31) and differentiating gives

Equation 3.8-30.

$$\tau_{r\theta} = -2\mu\omega R_2^2\left(\frac{1}{r^2}\right)\left[\frac{R_1^2/R_2^2}{1 - R_1^2/R_2^2}\right]$$

The torque T that is necessary to rotate the outer cylinder is the product of the force times the lever arm:

Equation 3.8-31.

$$T = (2\pi R_2 H)(-\tau_{r\theta})|_{r=R_2}(R_2)$$

$$= 4\pi\mu H\omega R_2^2\left[\frac{R_1^2/R_2^2}{1 - R_1^2/R_2^2}\right]$$

where H is the length of the cylinder. This type of device has been used to measure fluid viscosities from observations of angular velocities and torque and has also been used as a model for some friction bearings.

EXAMPLE 3.8-6. Rotating Liquid in a Cylindrical Container

A Newtonian fluid of constant density is in a vertical cylinder of radius R (Fig. 3.8-6) with the cylinder rotating about its axis at angular velocity ω (B2). Find the shape of the free surface at steady state.

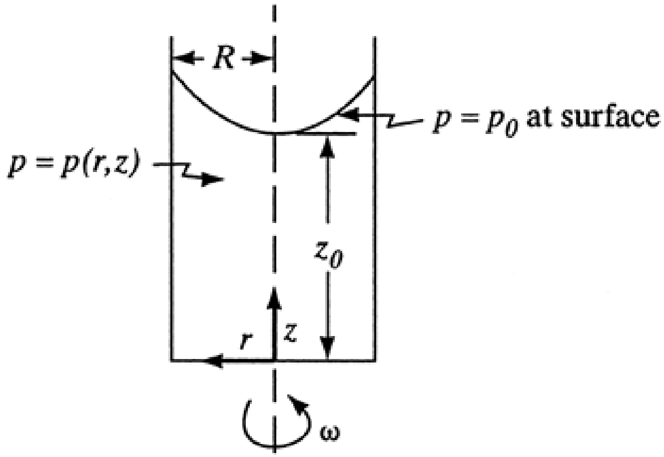

Figure 3.8-6. Liquid being rotated in a container with a free surface in Example 3.8-6.

Solution: The system can be described in cylindrical coordinates. As in Example 3.8-5, at steady state, $v_r = v_z = 0$ and $g_r = g_\theta = 0$. The final equations in cylindrical coordinates given below are the same as Eqs. (3.8-25)-(3.8-27) for Example 3.8-5, except that $g_z = -g$ in Eq. (3.8-27):

Equation 3.8-32.

$$\rho \frac{v_\theta^2}{r} = \frac{\partial p}{\partial r}$$

Equation 3.8-33.

$$0 = \mu \frac{\partial}{\partial r}\left(\frac{1}{r}\frac{\partial (r v_\theta)}{\partial r}\right)$$

Equation 3.8-34.

$$\frac{\partial p}{\partial z} = -\rho g$$

Integration of Eq. (3.8-33) gives the same equation as in Example 3.8-5:

Equation 3.8-28.

$$v_\theta = C_1 r + \frac{C_2}{r}$$

The constant C_2 must be zero since v_θ cannot be infinite at $r = 0$. At $r = R$, the velocity $v_\theta = R\omega$. Hence, $C_1 = \omega$ and we obtain

Equation 3.8-35.

$$v_\theta = \omega r$$

Combining Eqs. (3.8-35) and (3.8-32),

Equation 3.8-36.

$$\frac{\partial p}{\partial r} = \rho \omega^2 r$$

Hence, we see that Eqs. (3.8-36) and (3.8-34) show that pressure depends upon r because of the centrifugal force and upon z because of the gravitational force:

Equation 3.8-34.

$$\frac{\partial p}{\partial z} = -\rho g$$

Since the term p is a function of position, we can write the total differential of pressure as

Equation 3.8-37.

$$dp = \frac{\partial p}{\partial r}\, dr + \frac{\partial p}{\partial z}\, dz$$

Combining Eqs. (3.8-34) and (3.8-36) with (3.8-37) and integrating,

Equation 3.8-38.

$$p = \frac{\rho \omega^2 r^2}{2} - \rho g z + C_3$$

The constant of integration can be determined, since $p = p_0$ at $r = 0$ and $z = z_0$. The equation becomes

Equation 3.8-39.

$$p - p_0 = \frac{\rho \omega^2 r^2}{2} + \rho g (z_0 - z)$$

The free surface consists of all points on this surface at $p = p_0$. Hence,

Equation 3.8-40.

$$z - z_0 = \left(\frac{\omega^2}{2g}\right) r^2$$

This shows that the free surface is in the shape of a parabola.

OTHER METHODS FOR SOLUTION OF DIFFERENTIAL EQUATIONS OF MOTION

Introduction

In Section 3.8 we considered examples where the Navier-Stokes differential equations of motion could be solved analytically. These cases were used where there was only one non-vanishing component of the velocity. To solve these equations for flows in two and three directions is quite complex.

In this section we will consider some approximations that simplify the differential equations to allow us to obtain analytical solutions. Terms will be omitted which are quite small compared to the terms retained.

Three cases will be considered in this section: inviscid flow, potential flow, and creeping flow. The fourth case, for boundary-layer flow, will be considered in Section 3.10. The solution of these equations may be simplified by using a stream function $\psi(x, y)$ and/or a velocity potential $\varphi(x, y)$ rather than the terms of the velocity components v_x, v_y, and v_z.

Stream Function

The stream function $\psi(x, y)$ is a convenient parameter by which we can represent two-dimensional, steady, incompressible flow. This stream function ψ in m^2/s is related to the velocity components v_x and v_y by

Equation 3.9-1.

$$v_x = \frac{\partial \psi}{\partial y} \qquad v_y = -\frac{\partial \psi}{\partial x}$$

These definitions of v_x and v_y can then be used in the x and y components of the differential equation of motion, Eqs. (3.7-36) and (3.7-37), together with $v_z = 0$, to obtain a differential equation for ψ that is equivalent to the Navier-Stokes equation. Details are given elsewhere (B2).

The stream function is very useful because of its physical significance, that is, that in steady flow, lines defined by $\psi = constant$ are streamlines, which are the actual curves traced out by the particles of fluid. A stream function exists for all two-dimensional, steady, incompressible flow whether viscous or inviscid and whether rotational or irrotational.

EXAMPLE 3.9-1. Stream Function and Streamlines

The stream function relationship is given as $\psi = xy$. Find the equations for the components of velocity. Also plot the streamlines for a constant $\psi = 4$ and $\psi = 1$.

Solution: Using Eq. (3.9-1),

$$v_x = \frac{\partial \psi}{\partial y} = \frac{\partial (xy)}{\partial y} = x$$

$$v_y = -\frac{\partial \psi}{\partial x} = -\frac{\partial (xy)}{\partial x} = -y$$

To determine the streamline for $\psi = constant = 1 = xy$, assume that $y = 0.5$ and solve for x:

$$\psi = 1 = xy = x(0.5)$$

Hence, $x = 2$. Repeating, for $y = 1$, $x = 1$; for y = 2, $x = 0.5$; for $y = 5$, $x = 0.2$, and so on. Doing the same for ψ = constant = 4, the streamlines for $\psi = 1$ and $\psi = 4$ are plotted in Fig. 3.9-1. A possible flow model is flow around a corner.

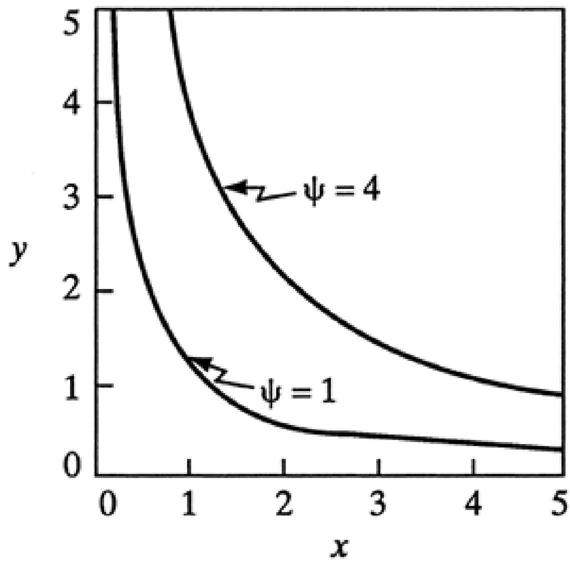

Figure 3.9-1. Plot of streamlines for ψ = xy for Example 3.9-1.

Differential Equations of Motion for Ideal Fluids (Inviscid Flow)

Special equations for *ideal or inviscid fluids* can be obtained for a fluid having a constant density and zero viscosity. These are called the *Euler equations.* Equations (3.7-36)-(3.7-38) for the *x, y,* and *z* components of momentum become

Equation 3.9-2.

$$\rho\left(\frac{\partial v_x}{\partial t} + v_x\frac{\partial v_x}{\partial x} + v_y\frac{\partial v_x}{\partial y} + v_z\frac{\partial v_x}{\partial z}\right) = -\frac{\partial p}{\partial x} + \rho g_x$$

Equation 3.9-3.

$$\rho\left(\frac{\partial v_y}{\partial t} + v_x\frac{\partial v_y}{\partial x} + v_y\frac{\partial v_y}{\partial y} + v_z\frac{\partial v_y}{\partial z}\right) = -\frac{\partial p}{\partial y} + \rho g_y$$

Equation 3.9-4.

$$\rho\left(\frac{\partial v_z}{\partial t} + v_x\frac{\partial v_z}{\partial x} + v_y\frac{\partial v_z}{\partial y} + v_z\frac{\partial v_z}{\partial z}\right) = -\frac{\partial p}{\partial z} + \rho g_z$$

At very high Reynolds numbers the viscous forces are quite small compared to the inertia forces and the viscosity can be assumed as zero. These equations are useful in calculating pressure distribution at the outer edge of the thin boundary layer in flow past immersed bodies. Away from the surface outside the boundary layer this assumption of an ideal fluid is often valid.

Potential Flow and Velocity Potential

The velocity potential or potential function $\phi(x, y)$ in m^2/s is useful in inviscid flow problems and is defined as

Equation 3.9-5.

$$v_x = \frac{\partial \phi}{\partial x} \qquad v_y = \frac{\partial \phi}{\partial y} \qquad v_z = \frac{\partial \phi}{\partial z}$$

This potential exists only for a flow with zero angular velocity, or irrotationality. This type of flow of an ideal or inviscid fluid (ρ = constant, μ = 0) is called *potential flow*. Additionally, the velocity potential ϕ exists for three-dimensional flows, whereas the stream function does not. The vorticity of a fluid is defined as follows:

Equation 3.9-6.

$$\frac{\partial v_y}{\partial x} - \frac{\partial v_x}{\partial y} = 2\omega_z$$

or,

Equation 3.9-7.

$$\frac{\partial^2 \psi}{\partial x^2} + \frac{\partial^2 \psi}{\partial y^2} = -2\omega_z$$

where $2\omega_z$ is the vorticity and ω_z in s^{-1} is angular velocity about the *z* axis. If $2\omega_z = 0$, the flow is irrotational and a potential function exists.

Using Eq. (3.6-24), the conservation-of-mass equation for flows in the *x* and *y* directions is as follows for constant density:

Equation 3.9-8.

$$\frac{\partial v_x}{\partial x} + \frac{\partial v_y}{\partial y} = 0$$

Differentiating v_x in Eq. (3.9-5) with respect to *x* and v_y with respect to *y* and substituting into Eq. (3.9-8),

Equation 3.9-9.

$$\frac{\partial^2 \phi}{\partial x^2} + \frac{\partial^2 \phi}{\partial y^2} = 0$$

This is Laplace's equation in rectangular coordinates. If suitable boundary conditions exist or are known, Eq. (3.9-9) can be solved to give $\phi(x, y)$. Then the velocity at any point can be obtained using Eq. (3.9-5). Techniques for solving this equation include using numerical analysis, conformal mapping, and functions of a complex variable, and are given elsewhere (B2, S3). Euler's equations can then be used to find the pressure distribution.

When the flow is inviscid and irrotational, a similar type of Laplace equation is obtained from Eq. (3.9-7) for the stream function:

Equation 3.9-10.

$$\frac{\partial^2 \psi}{\partial x^2} + \frac{\partial^2 \psi}{\partial y^2} = 0$$

Lines of constant φ are called equal potential lines and for potential flow are everywhere perpendicular (orthogonal) to lines of constant ψ. This can be proved as follows. A line of constant ψ would be such that the change in ψ is zero:

Equation 3.9-11.

$$d\psi = \frac{\partial\psi}{\partial x}\,dx + \frac{\partial\psi}{\partial y}\,dy = 0$$

Then, substituting Eq. (3.9-1) into the above,

Equation 3.9-12.

$$\left(\frac{dy}{dx}\right)_{\psi=\text{constant}} = \frac{v_y}{v_x}$$

Also, for lines of constant φ,

Equation 3.9-13.

$$d\phi = \frac{\partial\phi}{\partial x}\,dx + \frac{\partial\phi}{\partial y}\,dy = 0$$

Equation 3.9-14.

$$\left(\frac{dy}{dx}\right)_{\phi=\text{constant}} = -\frac{v_x}{v_y}$$

Hence,

Equation 3.9-15.

$$\left(\frac{dy}{dx}\right)_{\phi=\text{constant}} = -\frac{1}{(dy/dx)_{\psi=\text{constant}}}$$

An example of the use of the stream function is in obtaining the flow pattern for inviscid, irrotational flow past a cylinder of infinite length. The fluid approaching the cylinder has a steady and uniform velocity of v_∞ in the x direction. Laplace's equation (3.9-10) can be converted to cylindrical coordinates to give

Equation 3.9-16.

$$\frac{\partial^2\psi}{\partial r^2} + \frac{1}{r}\,\frac{\partial\psi}{\partial r} + \frac{1}{r^2}\,\frac{\partial^2\psi}{\partial\theta^2} = 0$$

where the velocity components are given by

Equation 3.9-17.

$$v_r = \frac{1}{r}\,\frac{\partial\psi}{\partial\theta} \qquad v_\theta = -\frac{\partial\psi}{\partial r}$$

Using four boundary conditions which are needed and the method of separation of variables, the stream function ψ is obtained. Converting to rectangular coordinates,

Equation 3.9-18.

$$\psi = v_\infty y\left(1 - \frac{R^2}{x^2 + y^2}\right)$$

where *R* is the cylinder radius. The streamlines and the constant-velocity-potential lines are plotted in Fig. 3.9-2 as a flow net.

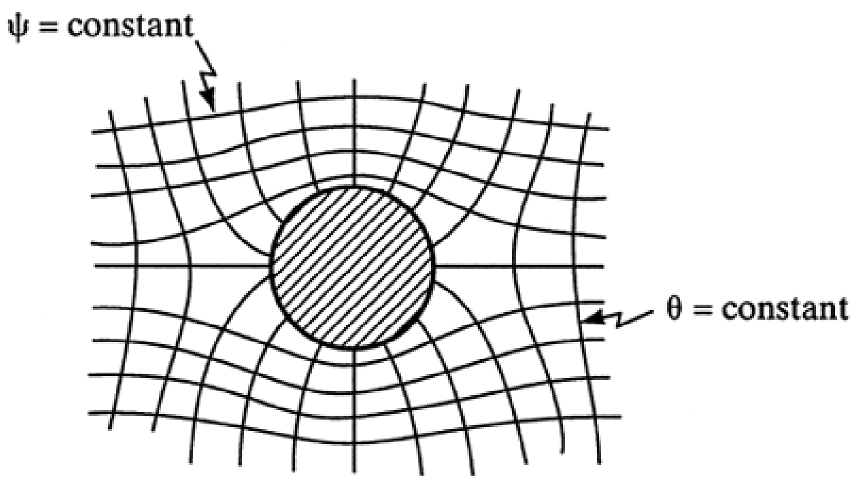

Figure 3.9-2. Streamlines (ψ = constant) and constant velocity potential lines (ϕ = constant) for the steady and irrotational flow of an inviscid and incompressible fluid about an infinite circular cylinder.

EXAMPLE 3.9-2. Stream Function for a Flow Field

The velocity components for a flow field are as follows:

$$v_x = a(x^2 - y^2) \qquad v_y = -2axy$$

Prove that it satisfies the conservation of mass and determine ψ.

Solution: First we determine $\partial v_x/\partial x = 2ax$ and $\partial v_y/\partial y = -2ax$. Substituting these values into Eq. (3.6-24), the conservation of mass for two-dimensional flow,

$$\frac{\partial v_x}{\partial x} + \frac{\partial v_y}{\partial y} = 0 \qquad \text{or} \qquad 2ax - 2ax = 0$$

Then using Eq. (3.9-1),

Equation 3.9-19.

$$v_x = \frac{\partial \psi}{\partial y} = ax^2 - ay^2 \qquad v_y = -\frac{\partial \psi}{\partial x} = -2axy$$

Integrating Eq. (3.9-19) for v_x,

Equation 3.9-20.

$$\psi = ax^2y - \frac{ay^3}{3} + f(x)$$

Integrating Eq. (3.9-19) for v_y,

Equation 3.9-21.

$$-\psi = -\frac{2ax^2y}{2} + f(y)$$

Equating Eq. (3.9-20) to (3.9-21),

Equation 3.9-22.

$$ax^2y - \frac{ay^3}{3} + f(x) = ax^2y - f(y)$$

Canceling like terms,

Equation 3.9-23.

$$-\frac{ay^3}{3} + f(x) = -f(y)$$

Hence, $f(x) = 0$ and $f(y) = ay^3/3$. Substituting $f(x) = 0$ into Eq. (3.9-20),

Equation 3.9-24.

$$\psi = ax^2y - \frac{ay^3}{3}$$

EXAMPLE 3.9-3. Stream Function and Velocities from Potential Function

The potential function for a two-dimensional, irrotational, incompressible flow field is given as $\phi = x^2 - 2y - y^2$. Find the stream function ψ and the velocity components v_x and v_y.

***Solution*:** Using Eqs. (3.9-1) and (3.9-5),

$$v_x = \frac{\partial\psi}{\partial y} \qquad v_y = -\frac{\partial\psi}{\partial x} \qquad v_x = \frac{\partial\phi}{\partial x} \qquad v_y = \frac{\partial\phi}{\partial y}$$

Combining,

Equation 3.9-25.

$$\frac{\partial\phi}{\partial x} = \frac{\partial\psi}{\partial y} \qquad \frac{\partial\phi}{\partial y} = -\frac{\partial\psi}{\partial x}$$

Differentiating the potential function with respect to x and equating the result to $\partial\psi/\partial y$ from Eq. (3.9-25),

Equation 3.9.26.

$$\frac{\partial\phi}{\partial x} = 2x - 0 - 0 = 2x = -\frac{\partial\psi}{\partial y}$$

Differentiating the potential function with respect to y and equating the result to $-\partial\psi/\partial x$ from Eq. (3.9-25),

Equation 3.9-27.

$$\frac{\partial\phi}{\partial y} = 0 - 2 - 2y = -\frac{\partial\psi}{\partial x}$$

Integrating Eq. (3.9-26),

Equation 3.9-28 .

$$\psi = 2xy + f(x)$$

Integrating Eq. (3.9-27),

Equation 3.9-29 .

$$\psi = 2x + 2xy + f(y)$$

Equating Eq. (3.9-28) to (3.9-29),

Equation 3.9-30 .

$$\psi = 2xy + f(x) = 2x + 2xy + f(y)$$

Hence, after canceling $2xy$ from both sides,

Equation 3.9-31 .

$$f(x) = 2x + f(y)$$

Therefore, $f(x) = 2x$ and $f(y) = 0$. Substituting $f(x) = 2x$ into Eq. (3.9-28),

Equation 3.9-32 .

$$\psi = 2xy + 2x$$

The velocities are, from Eqs. (3.9-26) and (3.9-27),

Equation 3.9-33.

$$\frac{\partial \psi}{\partial y} = v_x = 2x \qquad -\frac{\partial \psi}{\partial x} = v_y = 2 - 2y$$

In potential flow, the stream function and potential function are used to represent the flow in the main body of the fluid. These ideal fluid solutions do not satisfy the condition that $v_x = v_y = 0$ on the wall surface. Near the wall we have viscous drag and we use boundary-layer theory, where we obtain approximate solutions for the velocity profiles in this thin boundary layer taking into account viscosity. This is discussed in Section 3.10. Then we splice this solution onto the ideal flow solution that describes flow outside the boundary layer.

Differential Equations of Motion for Creeping Flow

At very low Reynolds numbers, below about 1, the term *creeping flow* is used to describe flow at very low velocities. This type of flow applies for the fall or settling of small particles through a fluid. Stokes' law is derived using this type of flow in problems of settling and sedimentation.

In flow around a sphere, for example, the fluid changes velocity and direction in a complex manner. If the inertia effects in this case were important, it would be necessary to keep all the terms in the three Navier-Stokes equations. Experiments show that at a Reynolds number below about 1, the inertia effects are small and can be omitted. Hence, the equations of motion, Eqs. (3.7-36) - (3.7-38) for creeping flow of an incompressible fluid, become

Equation 3.9-34.

$$\frac{\partial p}{\partial x} = \mu\left(\frac{\partial^2 v_x}{\partial x^2} + \frac{\partial^2 v_x}{\partial y^2} + \frac{\partial^2 v_x}{\partial z^2}\right)$$

Equation 3.9-35.

$$\frac{\partial p}{\partial y} = \mu\left(\frac{\partial^2 v_y}{\partial x^2} + \frac{\partial^2 v_y}{\partial y^2} + \frac{\partial^2 v_y}{\partial z^2}\right)$$

Equation 3.9-36.

$$\frac{\partial p}{\partial z} = \mu\left(\frac{\partial^2 v_z}{\partial x^2} + \frac{\partial^2 v_z}{\partial y^2} + \frac{\partial^2 v_z}{\partial z^2}\right)$$

For flow past a sphere the stream function ψ can be used in the Navier-Stokes equation in spherical coordinates to obtain the equation for the stream function and the velocity distribution and pressure distribution over the sphere. Then by integration over the whole sphere, the form drag, caused by the pressure distribution, and the skin friction or viscous drag, caused by the shear stress at the surface, can be summed to give the total drag:

Equation 3.9-37.

$$F_D = 3\pi\mu D_p v \qquad \text{(SI)}$$

$$F_D = \frac{3\pi\mu D_p v}{g_c} \qquad \text{(English)}$$

where F_D is total drag force in N, D_p is particle diameter in m, v is free stream velocity of fluid approaching the sphere in m/s, and μ is viscosity in kg/m · s. This is Stokes' equation for the drag force on a sphere.

Often Eq. (3.9-37) is rewritten as follows:

Equation 3.9-38.

$$F_D = C_D \frac{v^2}{2} \rho A \qquad \text{(SI)}$$

$$F_D = C_D \frac{v^2}{2g_c} \rho A \qquad \text{(English)}$$

where C_D is a drag coefficient, equal to $24/N_{Re}$ for Stokes' law, and A is the projected area of the sphere, $\pi D_p^2/4$. This is discussed in more detail in Section 3.1 for flow past spheres.

BOUNDARY-LAYER FLOW AND TURBULENCE

Boundary-Layer Flow

In Sections 3.8 and 3.9, the Navier-Stokes equations were used to find relations that described laminar flow between flat plates and inside circular tubes, flow of ideal fluids, and creeping flow. In this section the flow of fluids around objects will be considered in more detail, with particular attention being given to the region close to the solid surface, called the *boundary layer.*

In the boundary-layer region near the solid, the fluid motion is greatly affected by this solid surface. In the bulk of the fluid away from the boundary layer, the flow can often be adequately described by the theory of ideal fluids with zero viscosity. However, in the thin boundary layer, viscosity is important. Since the region is thin, simplified solutions can be obtained for the boundary-layer region. Prandtl originally suggested this division of the problem into two parts, which has been used extensively in fluid dynamics.

In order to help explain boundary layers, an example of boundary-layer formation in the steady-state flow of a fluid past a flat plate is given in Fig. 3.10-1. The velocity of the fluid upstream of the leading edge at $x = 0$ of the plate is uniform across the entire fluid stream and has the value v_∞. The velocity of the fluid at the interface is zero and the velocity v_x in the x direction increases as one goes farther from the plate. The velocity v_x approaches asymptotically the velocity v_∞ of the bulk of the stream.

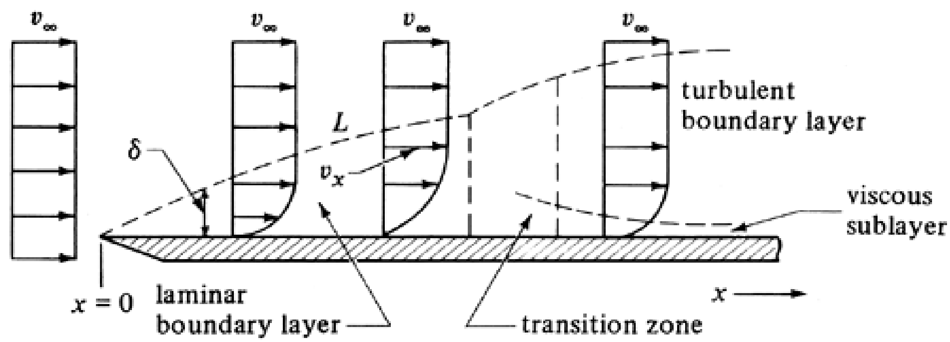

Figure 3.10-1. Boundary layer for flow past a flat plate.

The dashed line L is drawn so that the velocity at that point is 99% of the bulk velocity v_∞. The layer or zone between the plate and the dashed line constitutes the boundary layer. When the flow is laminar, the thickness δ of the boundary layer increases with $\sqrt{x}$ as we move in the x direction. The Reynolds number is defined as $N_{Re,x} = xv_\infty\rho/\mu$, where x is the distance downstream from the leading edge. When the Reynolds number is less than 2×10^5, the flow is laminar, as shown in Fig. 3.10-1.

The transition from laminar to turbulent flow on a smooth plate occurs in the Reynolds-number range 2×10^5 to 3×10^6, as shown in Fig. 3.10-1. When the boundary layer is turbulent, a thin, viscous sublayer persists next to the plate. The drag caused by the viscous shear in the boundary layers is called *skin friction* and is the only drag present for flow past a flat plate.

The type of drag occurring when fluid flows by a bluff or blunt shape such as a sphere or cylinder, which is mostly caused by a pressure difference, is termed *form drag. This* drag predominates in flow past such objects at all except low values of the Reynolds number, and often a wake is present. Skin friction and form drag both occur in flow past a bluff shape, and the total drag is the sum of the skin friction and the form drag. (See also Section 3.1A.)

Boundary-Layer Separation and Formation of Wakes

We discussed the growth of the boundary layer at the leading edge of a plate as shown in Fig. 3.10-2. However, some important phenomena also occur at the trailing edge of this plate and other objects. At the trailing edge or rear edge of the flat plate, the boundary layers are present at the top and bottom sides of the plate. On leaving the plate, the boundary layers gradually intermingle and disappear.

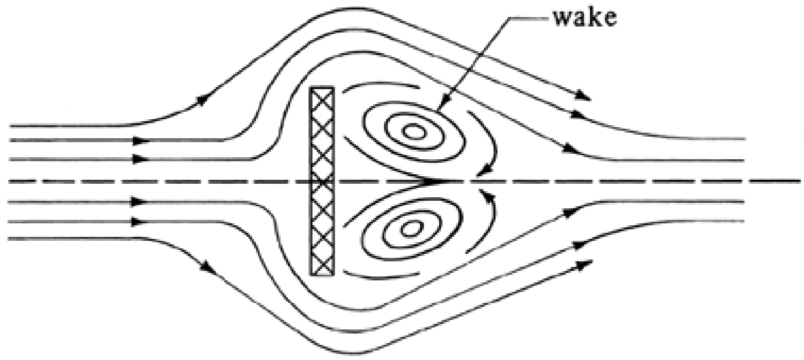

Figure 3.10-2. Flow perpendicular to a flat plate and boundarylayer separation.

If the direction of flow is at right angles to the plate, as shown in Fig. 3.10-2, a boundary layer forms as before in the fluid that is flowing over the upstream face. Once at the edge of the plate, however, the momentum in the fluid prevents it from making the abrupt turn around the edge of the plate, and it separates from the plate. A zone of decelerated fluid is present behind the plate and large eddies (vortices), called the *wake,* are formed in this area. The eddies consume large amounts of mechanical energy. This separation of boundary layers occurs when the change in velocity of the fluid flowing past an object is too large in direction or magnitude for the fluid to adhere to the surface.

Since formation of a wake causes large losses in mechanical energy, it is often necessary to minimize or prevent boundary-layer separation by streamlining the objects or by other means. This is also discussed in Section 3.1A for flow past immersed objects.

Laminar Flow and Boundary-Layer Theory

Boundary-layer equations

When laminar flow is occurring in a boundary layer, certain terms in the Navier-Stokes equations become negligible and can be neglected. The thickness of the boundary layer δ is arbitrarily taken as the distance away from the surface where the velocity reaches 99% of the free stream velocity. The concept of a relatively thin boundary layer leads to some important simplifications of the Navier-Stokes equations.

For two-dimensional laminar flow in the x and y directions of a fluid having a constant density, Eqs. (3.7-36) and (3.7-37) become as follows for flow at steady state as shown in Figure 3.10-1 when we neglect the body forces g_x and g_y:

Equation 3.10-1.

$$v_x \frac{\partial v_x}{\partial x} + v_y \frac{\partial v_x}{\partial y} = -\frac{1}{\rho}\frac{\partial p}{\partial x} + \frac{\mu}{\rho}\left(\frac{\partial^2 v_x}{\partial x^2} + \frac{\partial^2 v_x}{\partial y^2}\right)$$

Equation 3.10-2.

$$v_x \frac{\partial v_y}{\partial x} + v_y \frac{\partial v_y}{\partial y} = -\frac{1}{\rho}\frac{\partial p}{\partial y} + \frac{\mu}{\rho}\left(\frac{\partial^2 v_y}{\partial x^2} + \frac{\partial^2 v_y}{\partial y^2}\right)$$

The continuity equation for two-dimensional flow becomes

Equation 3.10-3.

$$\frac{\partial v_x}{\partial x} + \frac{\partial v_y}{\partial y} = 0$$

In Eq. (3.10-1), the term $(\mu/\rho)(\partial^2 v_x/\partial x^2)$ is negligible in comparison with the other terms in the equation. Also, it can be shown that all the terms containing v_y and its derivatives are small. Hence, the final two boundary-layer equations to be solved are Eqs. (3.10-3) and (3.10-4):

Equation 3.10-4.

$$v_x \frac{\partial v_x}{\partial x} + v_y \frac{\partial v_x}{\partial y} = -\frac{1}{\rho}\frac{dp}{dx} + \frac{\mu}{\rho}\frac{\partial^2 v_x}{\partial y^2}$$

Solution for laminar boundary layer on a flat plate

An important case in which an analytical solution has been obtained for the boundary-layer equations is for the laminar boundary layer on a flat plate in steady flow, as shown in Fig. 3.10-1. A further simplification can be made in Eq. (3.10-4) in that dp/dx is zero since v_∞ is constant.

The final boundary-layer equations reduce to the equation of motion for the x direction and the continuity equation as follows:

Equation 3.10-5.

$$v_x \frac{\partial v_x}{\partial x} + v_y \frac{\partial v_x}{\partial y} = \frac{\mu}{\rho}\frac{\partial^2 v_x}{\partial y^2}$$

Equation 3.10-3.

$$\frac{\partial v_x}{\partial x} + \frac{\partial v_y}{\partial y} = 0$$

The boundary conditions are $v_x = v_y = 0$ at $y = 0$ (y is distance from plate), and $v_x = v_\infty$ at $y = \infty$.

The solution of this problem for laminar flow over a flat plate giving v_x and v_y as a function of x and y was first obtained by Blasius and later elaborated by Howarth (B1, B2, S3). The mathematical details of the solution are quite tedious and complex and will not be given here. The general procedure will be outlined. Blasius reduced the two equations to a single ordinary differential equation which is nonlinear. The equation could not be solved to give a closed form, but a series solution was obtained.

The results of the work by Blasius are given as follows. The boundary-layer thickness δ, where $v_x \cong 0.99 v_\infty$, is given approximately by

Equation 3.10-6.

$$\delta = \frac{5.0x}{\sqrt{N_{\text{Re},x}}} = 5.0\sqrt{\frac{\mu x}{\rho v_\infty}}$$

where $N_{\text{Re},x} = x v_\infty \rho/\mu$. Hence, the thickness δ varies as $\sqrt{x}$

The drag in flow past a flat plate consists only of skin friction and is calculated from the shear stress at the surface at $y = 0$ for any x as follows:

Equation 3.10-7.

$$\tau_0 = \mu\left(\frac{\partial v_x}{\partial y}\right)_{y=0}$$

From the relation of v_x as a function of x and y obtained from the series solution, Eq. (3.10-7) becomes

Equation 3.10-8.

$$\tau_0 = 0.332\mu v_\infty \sqrt{\frac{\rho v_\infty}{\mu x}}$$

The total drag is given by the following for a plate of length L and width b:

Equation 3.10-9.

$$F_D = b\int_0^L \tau_0\, dx$$

Substituting Eq. (3.10-8) into (3.10-9) and integrating,

Equation 3.10-10.

$$F_D = 0.664b\sqrt{\mu\rho v_\infty^3 L}$$

The drag coefficient C_D related to the total drag on one side of the plate having an area $A = bL$ is defined as

Equation 3.10-11.

$$F_D = C_D \frac{v_\infty^2}{2}\rho A$$

Substituting the value for A and Eq. (3.10-10) into (3.10-11),

Equation 3.10-12.

$$C_D = 1.328\sqrt{\frac{\mu}{L v_\infty \rho}} = \frac{1.328}{N_{\mathrm{Re},L}^{1/2}}$$

where $N_{\mathrm{Re},L} = L v_\infty \rho/\mu$. A form of Eq. (3.10-11) is used in Section 14.3 for particle movement through a fluid. The definition of C_D in Eq. (3.10-12) is similar to the Fanning friction factor f for pipes.

The equation derived for C_D applies to the laminar boundary layer only for $N_{Re,L}$ less than about 5×10^5. Also, the results are valid only for positions where x is sufficiently far from the leading edge so that x or L is much greater than δ. Experimental results on the drag coefficient to a flat plate confirm the validity of Eq. (3.10-12). Boundary-layer flow past many other shapes has been successfully analyzed using similar methods.

Nature and Intensity of Turbulence

Nature of turbulence

Since turbulent flow is important in many areas of engineering, the nature of turbulence has been extensively investigated. Measurements of the velocity fluctuations of the eddies in turbulent flow have helped explain turbulence.

For turbulent flow there are no exact solutions of flow problems as there are in laminar flow, since the approximate equations used depend on many assumptions. However, useful relations have been obtained by combining experimental data and theory. Some of these relations will be discussed.

Turbulence can be generated by contact between two layers of fluid moving at different velocities or by a flowing stream in contact with a solid boundary, such as a wall or sphere. When a jet of fluid from an orifice flows into a mass of fluid, turbulence can arise. In turbulent flow at a given place and time, large eddies are continually being formed which break down into smaller eddies and finally disappear. Eddies can be as small as about 0.1-1 mm and as large as the smallest dimension of the turbulent stream. Flow inside an eddy is laminar because of its large size.

In turbulent flow the velocity is fluctuating in all directions. In Fig. 3.10-3 a typical plot of the variation of the instantaneous velocity v_x in the *x* direction at a given point in turbulent flow is shown. The velocity v'_x is the deviation of the velocity from the mean velocity $\bar{v}_x$ in the *x* direction of flow of the stream. Similar relations also hold for the *y* and *z* directions:

Equation 3.10-13.

$$v_x = \bar{v}_x + v'_x, \qquad v_y = \bar{v}_y + v'_y, \qquad v_z = \bar{v}_z + v'_z$$

Equation 3.10-14.

$$\bar{v}_x = \frac{1}{t}\int_0^t v_x \, dt$$

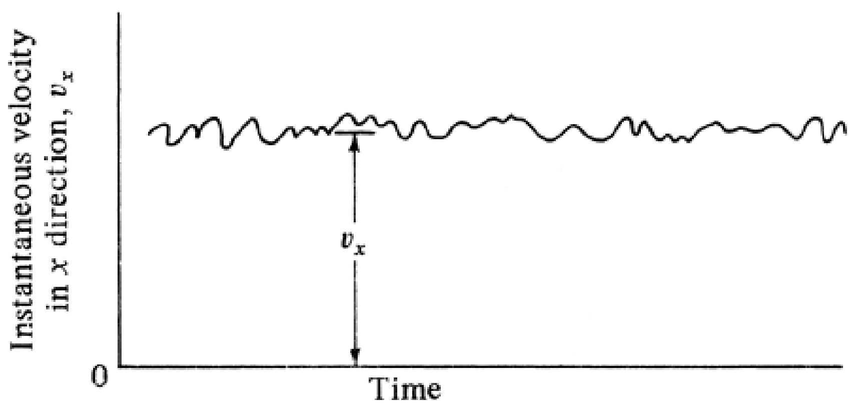

Figure 3.10-3. Velocity fluctuations in turbulent flow.

where the mean velocity $\bar{v}_x$ is the time-averaged velocity for time *t*, v_x the instantaneous total velocity in the *x* direction, and v'_x the instantaneous deviating or fluctuating velocity in the *x* direction. These fluctuations can also occur in the *y* and *z* directions. The value of v'_x fluctuates about zero as an average and, hence, the time-averaged values $\bar{v}'_x = 0, \bar{v}'_y = 0, \bar{v}'_z = 0$. However, the values of $v'^2_x, v'^2_y, \text{and } v'^2_z$, will not be zero. Similar expressions can also be written for pressure, which also fluctuates.

Intensity of turbulence

The time average of the fluctuating components vanishes over a time period of a few seconds. However, the time average of the mean square of the fluctuating components is a positive value. Since the fluctuations are random, the data have been analyzed by statistical methods. The level or intensity of turbulence can be related to the square root of the sum of the mean squares of the fluctuating components. This intensity of turbulence is an important parameter in the testing of models and the theory of boundary layers. The intensity of turbulence I can be defined mathematically as

Equation 3.10-15.

$$I = \frac{\sqrt{\frac{1}{3}(\overline{v}_x'^2 + \overline{v}_y'^2 + \overline{v}_z'^2)}}{\overline{v}_x}$$

This parameter I is quite important. Such factors as boundary-layer transition, separation, and heat- and mass-transfer coefficients depend upon the intensity of turbulence. Simulation of turbulent flows in testing of models requires that the Reynolds number and the intensity of turbulence be the same. One method used to measure intensity of turbulence is to utilize a hot-wire anemometer.

Turbulent Shear or Reynolds Stresses

In a fluid flowing in turbulent flow, shear forces occur wherever there is a velocity gradient across a shear plane, and these are much larger than those occurring in laminar flow. The velocity fluctuations in Eq. (3.10-13) give rise to turbulent shear stresses. The equations of motion and the continuity equation are still valid for turbulent flow. For an incompressible fluid having a constant density ρ and viscosity μ, the continuity equation (3.6-24) holds:

Equation 3.6-24.

$$\frac{\partial v_x}{\partial x} + \frac{\partial v_y}{\partial y} + \frac{\partial v_z}{\partial z} = 0$$

Also, the x component of the equation of motion, Eq. (3.7-36), can be written as follows if Eq. (3.6-24) holds:

Equation 3.10-16.

$$\frac{\partial(\rho v_x)}{\partial t} + \frac{\partial(\rho v_x v_x)}{\partial x} + \frac{\partial(\rho v_x v_y)}{\partial y} + \frac{\partial(\rho v_x v_z)}{\partial z} = \mu\left(\frac{\partial^2 v_x}{\partial x^2} + \frac{\partial^2 v_x}{\partial y^2} + \frac{\partial^2 v_x}{\partial z^2}\right) - \frac{\partial p}{\partial x} + \rho g_x$$

We can rewrite the continuity equation (3.6-24) and Eq. (3.10-16) by replacing v_x by $\overline{v}_x + v_x'$, v_y by $\overline{v}_y + v_y'$, v_z by $\overline{v}_z + v_z'$, and p by $\overline{p} + p'$:

Equation 3.10-17.

$$\frac{\partial(\overline{v}_x + v_x')}{\partial x} + \frac{\partial(\overline{v}_y + v_y')}{\partial y} + \frac{\partial(\overline{v}_z + v_z')}{\partial z} = 0$$

Equation 3.10-18.

$$\frac{\partial[\rho(\overline{v}_x + v_x')]}{\partial t} + \frac{\partial[\rho(\overline{v}_x + v_x')(\overline{v}_x + v_x')]}{\partial x} + \frac{\partial[\rho(\overline{v}_x + v_x')(\overline{v}_y + v_y')]}{\partial y}$$
$$+ \frac{\partial[\rho(\overline{v}_x + v_x')(\overline{v}_z + v_z')]}{\partial z} = \mu\nabla^2(\overline{v}_x + v_x') - \frac{\partial(\overline{p} + p')}{\partial x} + \rho g_x$$

Now we use the fact that the time-averaged value of the fluctuating velocities is zero $(\overline{v}'_x, \overline{v}'_y, \overline{v}'_z \text{ are zero})$, and that the time-averaged product $\overline{v'_x v'_y}$ is not zero. Then Eqs. (3.10-17) and (3.10-18) become

Equation 3.10-19.

$$\frac{\partial \overline{v}_x}{\partial x} + \frac{\partial \overline{v}_y}{\partial y} + \frac{\partial \overline{v}_z}{\partial z} = 0$$

Equation 3.10-20.

$$\frac{\partial(\rho \overline{v}_x)}{\partial t} + \frac{\partial(\rho \overline{v}_x \overline{v}_x)}{\partial x} + \frac{\partial(\rho \overline{v}_x \overline{v}_y)}{\partial y} + \frac{\partial(\rho \overline{v}_x \overline{v}_z)}{\partial z} + \left[\frac{\partial(\rho \overline{v'_x v'_x})}{\partial x} + \frac{\partial(\rho \overline{v'_x v'_y})}{\partial y} + \frac{\partial(\rho \overline{v'_x v'_z})}{\partial z}\right] = \mu \nabla^2 \overline{v}_x - \frac{\partial \overline{p}}{\partial x} + \rho g_x$$

By comparing these two time-smoothed equations with Eqs. (3.6-24) and (3.10-16), we see that the time-smoothed values everywhere replace the instantaneous values. However, in Eq. (3.10-20) new terms arise in the set of brackets which are related to turbulent velocity fluctuations. For convenience we use the notation

Equation 3.10-21.

$$\overline{\tau}^t_{xx} = \rho \overline{v'_x v'_x}, \qquad \overline{\tau}^t_{yx} = \rho \overline{v'_x v'_y}, \qquad \overline{\tau}^t_{zx} = \rho \overline{v'_x v'_z}$$

These are the components of the turbulent momentum flux and are called *Reynolds stresses.*

Prandtl Mixing Length

The equations derived for turbulent flow must be solved to obtain velocity profiles. To do this, more simplifications must be made before the expressions for the Reynolds stresses can be evaluated. A number of semiempirical equations have been used; the eddy-diffusivity model of Boussinesq is one early attempt to evaluate these stresses. By analogy to the equation for shear stress in laminar flow, $\tau_{yx} = -\mu(dv_x/dy)$, the turbulent shear stress can be written as

Equation 3.10-22.

$$\overline{\tau}^t_{yx} = -\eta_t \frac{d\overline{v}_x}{dy}$$

where η_t is a turbulent or eddy viscosity, which is a strong function of position and flow. This equation can also be written as follows:

Equation 3.10-23.

$$\overline{\tau}^t_{yx} = -\rho \varepsilon_t \frac{d\overline{v}_x}{dy}$$

where $\varepsilon_t = \eta_t/\rho$ is eddy diffusivity of momentum in m^2/s, by analogy to the momentum diffusivity μ/ρ for laminar flow.

In his mixing-length model Prandtl developed an expression to evaluate these stresses by assuming that eddies move in a fluid in a manner similar to the movement of molecules in a gas. The eddies move a distance called the mixing length *L* before they lose their identity.

Actually, the moving eddy or "lump" of fluid will gradually lose its identity. However, in the definition of the Prandtl mixing length *L*, this small packet of fluid is assumed to retain its identity while traveling the entire length *L* and then lose its identity or be absorbed in the host region.

Prandtl assumed that the velocity fluctuation v'_x is due to a "lump" of fluid moving a distance *L* in the *y* direction and retaining its mean velocity. At point *L*, the lump of fluid will differ in mean velocity from the adjacent fluid by $\bar{v}_{x|y+L} - \bar{v}_{x|y}$ Then the value of $v'_{x|y}$ is

Equation 3.10-24.

$$v'_{x|y} = \bar{v}_{x|y+L} - \bar{v}_{x|y}$$

The length *L* is small enough that the velocity difference can be written as

Equation 3.10-25.

$$v'_{x|y} = \bar{v}_{x|y+L} - \bar{v}_{x|y} = L\,\frac{d\bar{v}_x}{dy}$$

Hence,

Equation 3.10-26.

$$v'_x = L\,\frac{d\bar{v}_x}{dy}$$

Prandtl also assumed $v'_x \simeq v'_y$ Then the time average, $\overline{v'_x\,v'_y}$ is

Equation 3.10-27.

$$\overline{v'_x v'_y} = -L^2\left|\frac{d\bar{v}_x}{dy}\right|\frac{d\bar{v}_x}{dy}$$

The minus sign and the absolute value were used to make the quantity $\overline{v'_x\,v'_y}$ agree with experimental data. Substituting Eq. (3.10-27) into (3.10-21),

Equation 3.10-28.

$$\bar{\tau}^{\,t}_{yx} = -\rho L^2\left|\frac{d\bar{v}_x}{dy}\right|\frac{d\bar{v}_x}{dy}$$

Comparing with Eq. (3.10-23),

Equation 3.10-29.

$$\varepsilon_t = L^2\left|\frac{d\bar{v}_x}{dy}\right|$$

Universal Velocity Distribution in Turbulent Flow

To determine the velocity distribution for turbulent flow at steady state inside a circular tube, we divide the fluid inside the pipe into two regions: a central core where the Reynolds stress approximately equals the shear stress; and a thin, viscous sublayer adjacent to the wall where the shear stress is due only to viscous shear and the turbulence effects are assumed negligible. Later we include a third region, the buffer zone, where both stresses are important.

Dropping the subscripts and superscripts on the shear stresses and velocity, and considering the thin, viscous sublayer, we can write

Equation 3.10-30.

$$\tau_0 = -\mu \frac{dv}{dy}$$

where τ_0 is assumed constant in this region. On integration,

Equation 3.10-31.

$$\tau_0 y = \mu v$$

Defining a friction velocity as follows and substituting into Eq. (3.10-31),

Equation 3.10-32.

$$v^* = \sqrt{\frac{\tau_0}{\rho}}$$

Equation 3.10-33.

$$\frac{v}{v^*} = \frac{y v^*}{\mu/\rho}$$

The dimensionless velocity ratio on the left can be written as

Equation 3.10-34.

$$v^+ = v\sqrt{\frac{\rho}{\tau_0}} \qquad \text{(SI)}$$

$$v^+ = v\sqrt{\frac{\rho}{\tau_0 g_c}} \qquad \text{(English)}$$

The dimensionless number on the right can be written as

Equation 3.10-35.

$$y^+ = \frac{\sqrt{\tau_0 \rho}}{\mu} y \qquad \text{(SI)}$$

$$y^+ = \frac{\sqrt{\tau_0 g_c \rho}}{\mu} y \qquad \text{(English)}$$

where y is the distance from the wall of the tube. For a tube of radius r_0, $y = r_0 - r$, where r is the distance from the center. Hence, for the viscous sublayer, the velocity distribution is

Equation 3.10-36.

$$v^+ = y^+$$

Next, considering the turbulent core where any viscous stresses are neglected, Eq. (3.10-28) becomes

Equation 3.10-37.

$$\tau = \rho L^2 \left(\frac{dv}{dy}\right)^2$$

where *dv/dy* is always positive and the absolute value sign is dropped. Prandtl assumed that the mixing length is proportional to the distance from the wall, or

Equation 3.10-38.

$$L = Ky$$

and that $\tau = \tau_0$ = constant. Equation (3.10-37) now becomes

Equation 3.10-39.

$$\tau_0 = \rho K^2 y^2 \left(\frac{dv}{dy}\right)^2$$

Hence,

Equation 3.10-40.

$$v^* = Ky\frac{dv}{dy}$$

Upon integration,

Equation 3.10-41.

$$v^* \ln y = Kv + K_1$$

where K_1 is a constant. The constant K_1 can be found by assuming that v is zero at a small value of y, say y_0:

Equation 3.10-42.

$$\frac{v}{v^*} = v^+ = \frac{1}{K}\ln\frac{y}{y_0}$$

Introducing the variable y^+ by multiplying the numerator and denominator of the term y/y_0 by v^*/ν, where $\nu = \mu/\rho$, we obtain

Equation 3.10-43.

$$v^+ = \frac{1}{K}\left(\ln\frac{yv^*}{\nu} - \ln\frac{y_0 v^*}{\nu}\right)$$

Equation 3.10-44.

$$v^+ = \frac{1}{K}\ln y^+ + C_1$$

A large amount of velocity distribution data by Nikuradse and others for a range of Reynolds numbers of 4000 to 3.2×10^6 have been obtained, and the data fit Eq. (3.10-36) in the region up to y^+ of 5 and also fit Eq. (3.10-44) above y^+ of 30, with K and C_1 being universal constants. For the region of y^+ from 5 to 30, which is defined as the buffer region, an empirical equation of the form of Eq. (3.10-44) fits the data. In Fig. 3.10-4 the following relations which are valid are plotted to give a universal velocity profile for fluids flowing in smooth, circular tubes:

Equation 3.10-45.

$$v^+ = y^+ \qquad (0 < y^+ < 5)$$

Equation 3.10-46.

$$v^+ = 5.0 \ln y^+ - 3.05 \qquad (5 < y^+ < 30)$$

Equation 3.10-47.

$$v^+ = 2.5 \ln y^+ + 5.5 \qquad (30 < y^+)$$

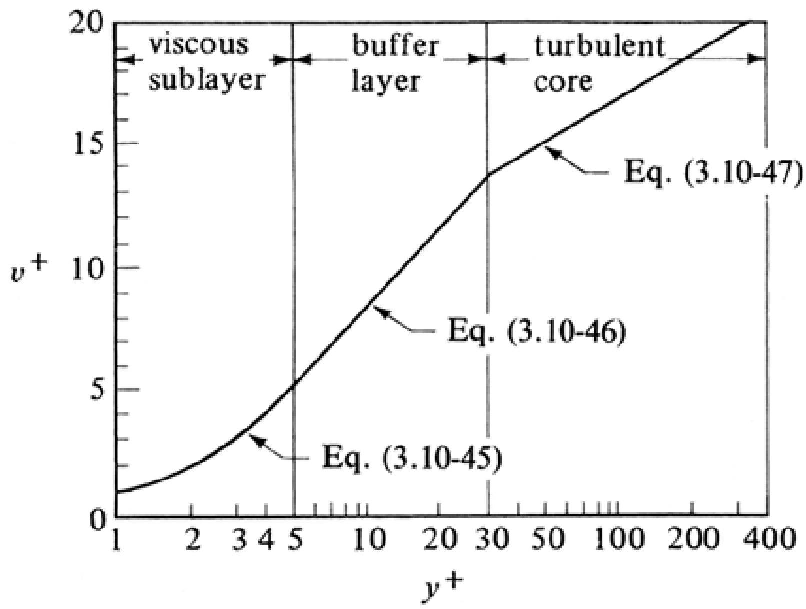

Figure 3.10-4. Universal velocity profile for turbulent flow in smooth circular tubes.

Three distinct regions are apparent in Fig. 3.10-4. The first region next to the wall is the *viscous sublayer* (historically called "laminar" sublayer), given by Eq. (3.10-45), where the velocity is proportional to the distance from the wall. The second region, called the *buffer layer,* is given by Eq. (3.10-46), and is a region of transition between the viscous sublayer with practically no eddy activity and the violent eddy activity in the *turbulent core region* given by Eq. (3.10-47). These equations can then be used and related to the Fanning friction factor discussed earlier in this chapter. They can also be used in solving turbulent boundary-layer problems.

Integral Momentum Balance for Boundary-Layer Analysis

Introduction and derivation of integral expression

In the solution for the laminar boundary layer on a flat plate, the Blasius solution is quite restrictive, since it is only for laminar flow over a flat plate. Other, more complex systems cannot be solved by this method. An approximate method developed by von Kármán can be used when the configuration is more complicated or the flow is turbulent. This is an approximate momentum integral analysis of the boundary layer using an empirical or assumed velocity distribution.

In order to derive the basic equation for a laminar or turbulent boundary layer, a small control volume in the boundary layer on a flat plate is used, as shown in Fig. 3.10-5. The depth in the z direction is b. Flow is only through the surfaces A_1 and A_2 and also from the top curved surface at δ. An overall integral momentum balance using Eq. (2.8-8) and overall integral mass balance using Eq. (2.6-6) are applied to the control volume inside the boundary layer at steady state, and the final integral expression by von Kármán is (B2, S3)

Equation 3.10-48.

$$\frac{\tau_0}{\rho} = \frac{d}{dx} \int_0^\delta v_x (v_\infty - v_x)\, dy$$

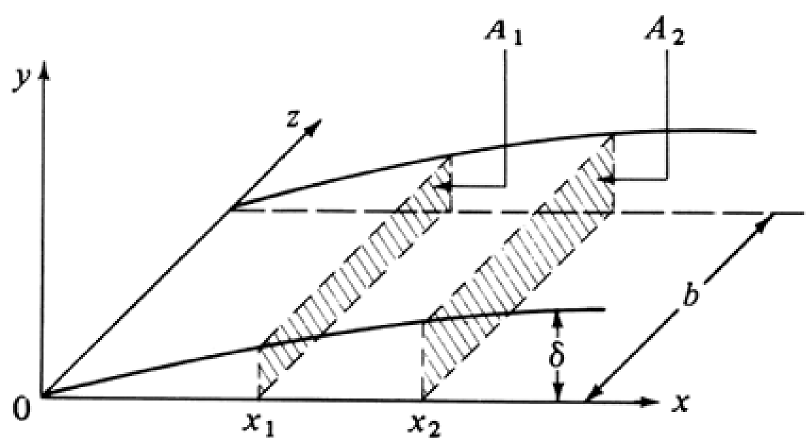

Figure 3.10-5. Control volume for integral analysis of the boundary-layer flow.

where τ_0 is the shear stress at the surface $y = 0$ at point x along the plate. Also, δ and τ_0 are functions of x.

Equation (3.10-48) is an expression whose solution requires knowledge of the velocity v_x as a function of the distance from the surface, y. The accuracy of the results will, of course, depend on how closely the assumed velocity profile approaches the actual profile.

Integral momentum balance for laminar boundary layer

Before we use Eq. (3.10-48) for the turbulent boundary layer, this equation will be applied to the laminar boundary layer over a flat plate so that the results can be compared with the exact Blasius solution in Eqs. (3.10-6)-(3.10-12).

In this analysis certain boundary conditions must be satisfied in the boundary layer:

Equation 3.10-49.

$$v_x = 0 \quad \text{at } y = 0$$

$$v_x \cong v_\infty \quad \text{at } y = \delta$$

$$\frac{dv_x}{dy} \cong 0 \quad \text{at } y = \delta$$

The conditions above are fulfilled in the following simple, assumed velocity profile:

Equation 3.10-50.

$$\frac{v_x}{v_\infty} = \frac{3}{2}\frac{y}{\delta} - \frac{1}{2}\left(\frac{y}{\delta}\right)^3$$

The shear stress τ_0 at a given x can be obtained from

Equation 3.10-51.

$$\tau_0 = \mu\left(\frac{dv_x}{dy}\right)_{y=0}$$

Differentiating Eq. (3.10-50) with respect to y and setting $y = 0$,

Equation 3.10-52.

$$\left(\frac{dv_x}{dy}\right)_{y=0} = \frac{3v_\infty}{2\delta}$$

Substituting Eq. (3.10-52) into (3.10-51),

Equation 3.10-53.

$$\tau_0 = \frac{3\mu v_\infty}{2\delta}$$

Substituting Eq. (3.10-50) into Eq. (3.10-48) and integrating between $y = 0$ and $y = \delta$, we obtain

Equation 3.10-54.

$$\frac{d\delta}{dx} = \frac{280}{39}\frac{\tau_0}{v_\infty^2 \rho}$$

Combining Eqs. (3.10-53) and (3.10-54) and integrating between $\delta = 0$ and $\delta = \delta$, and $x = 0$ and $x = L$,

Equation 3.10-55.

$$\delta = 4.64\sqrt{\frac{\mu L}{\rho v_\infty}}$$

where the length of plate is $x = L$. Proceeding in a manner similar to Eqs. (3.10-6)-(3.10-12), the drag coefficient is

Equation 3.10-56.

$$C_D = 1.292\sqrt{\frac{\mu}{Lv_\infty \rho}} = \frac{1.292}{N_{\mathrm{Re},L}^{1/2}}$$

A comparison of Eq. (3.10-6) with (3.10-55) and (3.10-12) with (3.10-56) shows the success of this method. Only the numerical constants differ slightly. This method can be used with reasonable accuracy for cases where an exact analysis is not feasible.

Integral momentum analysis for turbulent boundary layer

The procedures used for the integral momentum analysis for a laminar boundary layer can be applied to the turbulent boundary layer on a flat plate. A simple empirical velocity distribution for pipe flow which is valid up to a Reynolds number of 10^5 can be adapted for the boundary layer on a flat plate, to become

Equation 3.10-57.

$$\frac{v_x}{v_\infty} = \left(\frac{y}{\delta}\right)^{1/7}$$

This is the Blasius $\frac{1}{7}$-power law, which is often used.

Equation (3.10-57) is substituted into the integral relation equation (3.10-48):

Equation 3.10-58.

$$\frac{d}{dx}\int_0^\delta v_\infty^2\left[\left(\frac{y}{\delta}\right)^{1/7} - \left(\frac{y}{\delta}\right)^{2/7}\right] dy = \frac{\tau_0}{\rho}$$

The power-law equation does not hold, as y goes to zero at the wall. Another useful relation is the Blasius correlation for shear stress for pipe flow, which is consistent at the wall for the wall shear stress τ_0. For boundary-layer flow over a flat plate, it becomes

Equation 3.10-59.

$$\frac{\tau_0}{\rho v_\infty^2} = 0.023\left(\frac{\delta v_\infty \rho}{\mu}\right)^{-1/4}$$

Integrating Eq. (3.10-58), combining the result with Eq. (3.10-59), and integrating between $\delta = 0$ and $\delta = \delta$, and $x = 0$ and $x = L$,

Equation 3.10-60.

$$\delta = 0.376\left(\frac{Lv_\infty \rho}{\mu}\right)^{-1/5} \quad L = \frac{0.376L}{N_{\mathrm{Re},L}^{1/5}}$$

Integration of the drag force as before gives

Equation 3.10-61.

$$C_D = \frac{0.072}{N_{\mathrm{Re},L}^{1/5}}$$

In this development the turbulent boundary layer was assumed to extend to $x = 0$. Actually, a certain length at the front has a laminar boundary layer. Experimental data agree with Eq. (3.10-61) reasonably well from a Reynolds number of 5×10^5 to 10^7. More-accurate results at higher Reynolds numbers can be obtained by using a logarithmic velocity distribution, Eqs. (3.10-45)-(3.10-47).

DIMENSIONAL ANALYSIS IN MOMENTUM TRANSFER

Dimensional Analysis of Differential Equations

In this chapter we have derived several differential equations describing various flow situations. Dimensional homogeneity requires that every term in a given equation have the same units. Then, the ratio of one term in the equation to another term is dimensionless. Knowing the physical meaning of each term in the equation, we are then able to give a physical interpretation to each of the dimensionless parameters or numbers formed. These dimensionless numbers, such as the Reynolds number and others, are useful in correlating and predicting transport phenomena in laminar and turbulent flow.

Often it is not possible to integrate the differential equation describing a flow situation. However, we can use the equation to find out which dimensionless numbers can be used in correlating experimental data for this physical situation.

An important example of this involves the use of the Navier-Stokes equation, which often cannot be integrated for a given physical situation. To start, we use Eq. (3.7-36) for the x component of the Navier-Stokes equation. At steady state this becomes

Equation 3.11-1.

$$v_x \frac{\partial v_x}{\partial x} + v_y \frac{\partial v_x}{\partial y} + v_z \frac{\partial v_x}{\partial z} = g_x - \frac{1}{\rho}\frac{\partial p}{\partial x} + \frac{\mu}{\rho}\left(\frac{\partial^2 v_x}{\partial x^2} + \frac{\partial^2 v_x}{\partial y^2} + \frac{\partial^2 v_x}{\partial z^2}\right)$$

Each term in this equation has the units length/time^2, or L/t^2.

In this equation each term has a physical significance. First we use a single characteristic velocity v and a single characteristic length L for all terms. Then the expression of each term in Eq. (3.11-1) is as follows: The left-hand side can be expressed as v^2/L and the right-hand terms, respectively, as g, $p/\rho L$, and $\mu v/\rho L^2$. We then write

Equation 3.11-2.

$$\left[\frac{v^2}{L}\right] = [g] - \left[\frac{p}{\rho L}\right] + \left[\frac{\mu v}{\rho L^2}\right]$$

This expresses a dimensional equality and not a numerical equality. Each term has dimensions L/t^2.

The left-hand term in Eq. (3.11-2) represents the inertia force and the terms on the right-hand side represent, respectively, the gravity force, pressure force, and viscous force. Dividing each of the terms in Eq. (3.11-2) by the inertia force $[v^2/L]$, the following dimensionless groups or their reciprocals are obtained:

Equation 3.11-3.

$$\frac{[v^2/L]}{[g]} = \frac{\text{inertia force}}{\text{gravity force}} = \frac{v^2}{gL} = N_{\text{Fr}} \qquad \text{(Froude number)}$$

Equation 3.11-4.

$$\frac{[p/\rho L]}{[v^2/L]} = \frac{\text{pressure force}}{\text{inertia force}} = \frac{p}{\rho v^2} = N_{Eu} \qquad \text{(Euler number)}$$

Equation 3.11-5.

$$\frac{[v^2/L]}{[\mu v/\rho L^2]} = \frac{\text{inertia force}}{\text{viscous force}} = \frac{Lv\rho}{\mu} = N_{Re} \qquad \text{(Reynolds number)}$$

Note that this method not only gives the various dimensionless groups for a differential equation but also gives physical meaning to these dimensionless groups. The length, velocity, and so forth to be used in a given case will be that value which is most significant. For example, the length may be the diameter of a sphere, the length of a flat plate, and so on.

Systems that are geometrically similar are said to be *dynamically similar* if the parameters representing ratios of forces pertinent to the situation are equal. This means that the Reynolds, Euler, or Froude numbers must be equal between the two systems.

This dynamic similarity is an important requirement in obtaining experimental data for a small model and extending these data to scale up to the large prototype. Since experiments with full-scale prototypes would often be difficult and/or expensive, it is customary to study small models. This is done in the scale-up of chemical process equipment and in the design of ships and airplanes.

Dimensional Analysis Using the Buckingham Method

The method of obtaining the important dimensionless numbers from the basic differential equations is generally the preferred method. In many cases, however, we are not able to formulate a differential equation which clearly applies. Then a more general procedure is required, known as the *Buckingham method.* In this method the listing of the important variables in the particular physical problem is done first. Then we determine the number of dimensionless parameters into which the variables may be combined by using the Buckingham pi theorem.

The *Buckingham theorem* states that the functional relationship among q quantities or variables whose units may be given in terms of u fundamental units or dimensions may be written as **(**$q - u$**)** independent dimensionless groups, often called π's. [This quantity u is actually the maximum number of these variables that will not form a dimensionless group. However, only in a few cases is u not equal to the number of fundamental units (**B1**).]

Let us consider the following example, to illustrate the use of this method. An incompressible fluid is flowing inside a circular tube of inside diameter D. The significant variables are pressure drop Δp, velocity v, diameter D, tube length L, viscosity μ, and density ρ. The total number of variables is $q = 6$.

The fundamental units or dimensions are $u = 3$ and are mass M, length L, and time t. The units of the variables are as follows: Δp in M/Lt^2, v in L/t, D in L, L in L, μ in M/Lt, and ρ in M/L^3. The number of dimensionless groups or π's is $q - u$, or **6 − 3 =** 3. Thus,

Equation 3.11-6.

$$\pi_1 = f(\pi_2, \pi_3)$$

Next, we must select a core group of u (or 3) variables which will appear in each π group and among them contain all the fundamental dimensions. Also, no two of the variables selected for the core can have the same dimensions. In choosing the core, the variable whose effect one desires to isolate is often excluded (for example, Δp). This leaves us with the variables v, D, μ and ρ to be used. (L and D have the same dimensions.)

We will select D, v, and ρ to be the core variables common to all three groups. Then the three dimensionless groups are

Equation 3.11-7.

$$\pi_1 = D^a v^b \rho^c \, \Delta p^1$$

Equation 3.11-8.

$$\pi_2 = D^d v^e \rho^f L^1$$

Equation 3.11-9.

$$\pi_3 = D^g v^h \rho^i \mu^1$$

To be dimensionless, the variables must be raised to certain exponents *a, b, c,* and so forth. First we consider the π_1 group:

Equation 3.11-7.

$$\pi_1 = D^a v^b \rho^c \, \Delta p^1$$

To evaluate these exponents, we write Eq. (3.11-7) dimensionally by substituting the dimensions for each variable:

Equation 3.11-10.

$$M^0 L^0 t^0 = 1 = L^a \left(\frac{L}{t}\right)^b \left(\frac{M}{L^3}\right)^c \frac{M}{Lt^2}$$

Next we equate the exponents of L on both sides of this equation, of M, and finally of t:

Equation 3.11-11.

$$(L) \quad 0 = a + b - 3c - 1$$

$$(M) \quad 0 = c + 1$$

$$(t) \quad 0 = -b - 2$$

Solving these equations, $a = 0$, $b = -2$, and $c = -1$. Substituting these values into Eq. (3.11-7),

Equation 3.11-12.

$$\pi_1 = \frac{\Delta p}{v^2 \rho} = N_{\text{Eu}}$$

Repeating this procedure for π_2 and π_3,

Equation 3.11-13.

$$\pi_2 = \frac{L}{D}$$

Equation 3.11-14.

$$\pi_3 = \frac{Dv\rho}{\mu} = N_{\text{Re}}$$

Finally, substituting π_1, π_2, and π_3 into Eq. (3.11-6),

Equation 3.11-15.

$$\frac{\Delta p}{v^2 \rho} = f\left(\frac{L}{D}, \frac{Dv\rho}{\mu}\right)$$

Combining Eq. (2.10-5) with the left-hand side of Eq. (3.11-15), the result obtained shows that the friction factor is a function of the Reynolds number (as was shown before in the empirical correlation of friction factor and Reynolds number) and of the length/diameter ratio. In pipes with $L/D >> 1$ or pipes with fully developed flow, the friction factor is found to be independent of L/D.

This type of analysis is useful in empirical correlations of data. However, it does not tell us the importance of each dimensionless group, which must be determined by experimentation, nor does it select the variables to be used.

PROBLEMS

3.1-1. *Force on a Cylinder in a Wind Tunnel.* Air at 101.3 kPa absolute and 25°C is flowing at a velocity of 10 m/s in a wind tunnel. A long cylinder having a diameter of 90 mm is placed in the tunnel and the axis of the cylinder is held perpendicular to the air flow. What is the force on the cylinder per meter length?

A1: **Ans.** $C_D = 1.3$, $F_D = 6.94$ N

3.1-2. *Wind Force on a Steam Boiler Stack.* A cylindrical steam boiler stack has a diameter of 1.0 m and is 30.0 m high. It is exposed to a wind at 25°C having a velocity of 50 miles/h. Calculate the force exerted on the boiler stack.

A2: **Ans.** $C_D = 0.33$, $F_D = 2935$ N

3.1-3. *Effect of Velocity on Force on a Sphere and Stokes' Law.* A sphere having a diameter of 0.042 m is held in a small wind tunnel, where air at 37.8°C and 1 atm abs and various velocities is forced past it.

a. Determine the drag coefficient and force on the sphere for a velocity of 2.30×10^{-4} m/s. Use Stokes' law here if it is applicable.

b. Also determine the force for velocities of 2.30×10^{-3}, 2.30×10^{-2}, 2.30×10^{-1}, and 2.30 m/s. Make a plot of F_D versus velocity

3.1-4. *Drag Force on Bridge Pier in River.* A cylindrical bridge pier 1.0 m in diameter is submerged to a depth of 10 m. Water in the river at 20°C is flowing past at a velocity of 1.2 m/s. Calculate the force on the pier.

3.1-5. *Surface Area in a Packed Bed.* A packed bed is composed of cubes 0.020 m on a side and the bulk density of the packed bed is 980 kg/m^3. The density of the solid cubes is 1500 kg/m^3.

a. Calculate ε, effective diameter D_p, and a.

b. Repeat for the same conditions but for cylinders having a diameter of $D = 0.02$ m and a length $h = 1.5D$.

A5: **Ans.** (a) $\varepsilon = 0.3467$, $D_p = 0.020$ m, $a = 196.0$ m^{-1}

3.1-6. ***Derivation for Number of Particles in a Bed of Cylinders.*** For a packed bed containing cylinders, where the diameter D of the cylinders is equal to the length h, do as follows for a bed having a void fraction ε:

a. Calculate the effective diameter.

b. Calculate the number of cylinders, n, in 1 m^3 of the bed.

A6: **Ans.** (a) $D_p = D$

3.1-7. ***Derivation of Dimensionless Equation for Packed Bed.*** Starting with Eq. (3.1-20), derive the dimensionless equation (3.1-21). Show all steps in the derivation.

3.1-8. ***Flow and Pressure Drop of Gases in Packed Bed.*** Air at 394.3 K flows through a packed bed of cylinders having a diameter of 0.0127 m and length the same as the diameter. The bed void fraction is 0.40 and the length of the packed bed is 3.66 m. The air enters the bed at 2.20 atm abs at the rate of 2.45 $kg/m^2 \cdot s$ based on the empty cross section of the bed. Calculate the pressure drop of air in the bed.

A8: **Ans.** $\Delta p = 0.1547 \times 10^5$ Pa

3.1-9. ***Flow of Water in a Filter Bed.*** Water at 24°C is flowing by gravity through a filter bed of small particles having an equivalent diameter of 0.0060 m. The void fraction of the bed is measured as 0.42. The packed bed has a depth of 1.50 m. The liquid level of water above the bed is held constant at 0.40 m. What is the water velocity v' based on the empty cross section of the bed?

3.1-10. ***Mean Diameter of Particles in Packed Bed.*** A mixture of particles in a packed bed contains the following volume percent of particles and sizes: 15%, 10 mm; 25%, 20 mm; 40%, 40 mm; 20%, 70 mm. Calculate the effective mean diameter, D_{pm}, if the shape factor is 0.74.

A10: **Ans.** $D_{pm} = 18.34$ mm

3.1-11. ***Permeability and Darcy's Law.*** A sample core of porous rock obtained from an oil reservoir is 8 cm long and has a diameter of 2.0 cm. It is placed in a core holder. With a pressure drop of 1.0 atm, the water flow at 20.2°C through the core is measured as 2.60 cm^3/s. What is the permeability in darcy?

3.1-12. ***Minimum Fluidization and Expansion of Fluid Bed.*** Particles having a size of 0.10 mm, a shape factor of 0.86, and a density of 1200 kg/m^3 are to be fluidized using air at 25°C and 202.65 kPa abs pressure. The void fraction at minimum fluidizing conditions is 0.43. The bed diameter is 0.60 m and the bed contains 350 kg of solids.

a. Calculate the minimum height of the fluidized bed.

b. Calculate the pressure drop at minimum fluidizing conditions.

c. Calculate the minimum velocity for fluidization.

d. Using 4.0 times the minimum velocity, estimate the porosity of the bed.

A12: **Ans.** (a) $L_{mf} = 1.810$ m; (b) $\Delta p = 0.1212 \times 10^5$ Pa; (c) $v'_{mf} = 0.004374$ m/s; (d) $\varepsilon = 0.604$

3.1-13. ***Minimum Fluidization Velocity Using a Liquid.*** A tower having a diameter of 0.1524 m is being fluidized with water at 20.2°C. The uniform spherical beads in the tower bed have a diameter of 4.42 mm and a density of 1603 kg/m^3. Estimate the minimum fluidizing velocity and compare with the experimental value of 0.02307 m/s found by Wilhelm and Kwauk (W5).

3.1-14. ***Fluidization of a Sand-Bed Filter.*** To clean a sand-bed filter, it is fluidized at minimum conditions using water at 24°C. The round sand particles have a density of 2550 kg/m^3 and an average size of 0.40 mm. The sand has the properties given in Table 3.1-2.

a. The bed diameter is 0.40 m and the desired height of the bed at these minimum fluidizing conditions is 1.75 m. Calculate the amount of solids needed.
b. Calculate the pressure drop at these conditions and the minimum velocity for fluidization.
c. Using 4.0 times the minimum velocity, estimate the porosity and height of the expanded bed.

A14: **Ans.** (a) 325.2 kg solids; (b) 1.546 × 10^4 Pa

3.2-1. ***Flow Measurement Using a Pilot Tube.*** A pitot tube is used to measure the flow rate of water at 20°C in the center of a pipe having an inside diameter of 102.3 mm. The manometer reading is 78 mm of carbon tetrachloride at 20°C. The pitot tube coefficient is 0.98.

a. Calculate the velocity at the center and the average velocity.
b. Calculate the volumetric flow rate of the water.

A15: **Ans.** (a) v_{max} = 0.9372 m/s, v_{av} = 0.773 m/s; (b) 6.35 × 10^{-3} m^3/s

3.2-2. ***Gas Flow Rate Using a Pitot Tube.*** The flow rate of air at 37.8°C is being measured at the center of a duct having a diameter of 800 mm by a pitot tube. The pressure-difference reading on the manometer is 12.4 mm of water. At the pitot-tube position, the static-pressure reading is 275 mm of water above 1 atm abs. The pitot-tube coefficient is 0.97. Calculate the velocity at the center and the volumetric flow rate of the air.

3.2-3. ***Pitot-Tube Traverse for Flow-Rate Measurement.*** In a pitot-tube traverse of a pipe having an inside diameter of 155.4 mm in which water at 20°C is flowing, the following data were obtained:

Distance from Wall (mm)	*Reading in Manometer (mm of Carbon Tetrachloride)*
26.9	122
52.3	142
77.7	157
103.1	137
128.5	112

The pitot-tube coefficient is 0.98.

a. Calculate the maximum velocity at the center.
b. Calculate the average velocity. [*Hint:* Use Eq. (2.6-17) and do a numerical or a graphical integration.]

3.2-4. ***Metering Flow by a Venturi.*** A venturi meter having a throat diameter of 38.9 mm is installed in a line having an inside diameter of 102.3 mm. It meters water having a density of 999 kg/m^3. The measured pressure drop across the venturi is 156.9 kPa. The venturi coefficient C_v is 0.98. Calculate the gal/min and m^3/s flow rate.

A18: **Ans.** 330 gal/min, 0.0208 m^3/s

3.2-5. ***Use of a Venturi to Meter Water Flow.*** Water at 20°C is flowing in a 2-in. schedule 40 steel pipe. Its flow rate is measured by a venturi meter having a throat diameter of 20 mm. The manometer reading is 214 mm of mercury. The venturi coefficient is 0.98. Calculate the flow rate.

3.2-6. ***Metering of Oil Flow by an Orifice.*** A heavy oil at 20°C having a density of 900 kg/m^3 and a viscosity of 6 cp is flowing in a 4-in. schedule 40 steel pipe. When the flow rate is 0.0174 m^3/s, it is desired to have a pressure-drop reading across the manometer equivalent to 0.93×10^5 Pa. What size orifice should be used if the orifice coefficient is assumed as 0.61? What is the permanent pressure loss?

3.2-7. ***Water Flow Rate in an Irrigation Ditch.*** Water is flowing in an open channel in an irrigation ditch. A rectangular weir having a crest length L = 1.75 ft is used. The weir head is measured as h_0 = 0.47 ft. Calculate the flow rate in ft^3/s and m^3/s.

A21: **Ans.** Flow rate = 1.776 ft^3/s, 0.0503 m^3/s

3.2-8. ***Sizing a Flow Nozzle.*** A flow nozzle is to be sized for use in a pipe having an internal diameter of 1.25 in. to meter 0.60 ft^3/min of water at 25°C. A pressure drop of 10.0 in. of water is to be used. Calculate the size of the flow nozzle and the permanent power loss in hp. Assume the coefficient C_n = 0.96.

A22: **Ans.** D_2 = 0.506 in., $p_1 - p_4$ = 37.38 lb$_f$/ft^2 (1.789 kPa)

3.3-1. ***Brake Horsepower of Centrifugal Pump.*** Using Fig. 3.3-2 and a flow rate of 60 gal/min, do as follows:

a. Calculate the brake hp of the pump using water with a density of 62.4 lb$_m$/ft^3. Compare with the value from the curve.
b. Do the same for a nonviscous liquid having a density of 0.85 g/cm^3.

A23: **Ans.** (b) 0.69 brake hp (0.51 kW)

3.3-2. ***kW Power of a Fan.*** A centrifugal fan is to be used to take a flue gas at rest (zero velocity) and at a temperature of 352.6 K and a pressure of 749.3 mm Hg and discharge this gas at a pressure of 800.1 mm Hg and a velocity of 38.1 m/s. The volume flow rate of gas is 56.6 std m^3/min of gas (at 294.3 K and 760 mm Hg). Calculate the brake kW of the fan if its efficiency is 65% and the gas has a molecular weight of 30.7. Assume incompressible flow.

3.3-3. ***Adiabatic Compression of Air.*** A compressor operating adiabatically is to compress 2.83 m^3/min of air at 29.4°C and 102.7 kN/m^2 to 311.6 kN/m^2. Calculate the power required if the efficiency of the compressor is 75%. Also, calculate the outlet temperature.

3.3-4. **$(NPSH)_R$** ***forFeed to Distillation Tower.*** A feed rate of 200 gpm of a hydrocarbon mixture at 70°C is being pumped from a tank at 1 atm abs pressure to a distillation tower. The density of the feed is 46.8 lb_m/ft^3 and its vapor pressure is 8.45 psia. The velocity in the inlet line to the pump is 3 ft/s and the friction loss between the tank and pump is 3.5 ft of fluid. The net positive suction head required is 6 ft.

a. How far below the liquid level in the tank must the pump be to obtain this required $(NPSH)_R$?

b. If the feed is at the boiling point, calculate the pump position.

A26: **Ans.** (a) $z_1 = -9.57$ ft (-2.92 m)

3.4-1. ***Power for Liquid Agitation.*** It is desired to agitate a liquid having a viscosity of 1.5×10^{-3} Pa · s and a density of 969 kg/m^3 in a tank having a diameter of 0.91 m. The agitator will be a six-blade open turbine having a diameter of 0.305 m operating at 180 rpm. The tank has four vertical baffles, each with a width J of 0.076 m. Also, $W =$ 0.0381 m. Calculate the required kW. Use curve 2, Fig. 3.4-4.

A27: **Ans.** $N_P = 2.5$, power = 0.172 kW (0.231 hp)

3.4-2. ***Power for Agitation and Scale-Up.*** A turbine agitator having six flat blades and a disk has a diameter of 0.203 m and is used in a tank having a diameter of 0.61 m and height of 0.61 m. The width $W =$ 0.0405 m. Four baffles are used having a width of 0.051 m. The turbine operates at 275 rpm in a liquid having a density of 909 kg/m^3 and viscosity of 0.020 Pa · s.

a. Calculate the kW power of the turbine and kW/m^3 of volume.

b. Scale up this system to a vessel having a volume of 100 times the original for the case of equal mass transfer rates.

A28: **Ans.** (a) $P = 0.1508$ kW, $P/V = 0.845$ kW/m^3; (b) $P_2 = 15.06$ kW, $P_2/V_2 = 0.845$ kW/m^3

3.4-3. ***Scale-down of Process Agitation System.*** An existing agitation process operates using the same agitation system and fluid as described in Example 3.4-1a. It is desired to design a small pilot unit with a vessel volume of 2.0 liters so that effects of various process variables on the system can be studied in the laboratory. The rates of mass transfer appear to be important in this system, so the scale-down should be on this basis. Design the new system specifying sizes, rpm, and kW power.

3.4-4. ***Anchor Agitation System.*** An anchor-type agitator similar to that described for Eq. (3.4-3) is to be used to agitate a fluid having a viscosity of 100 Pa · s and a density of 980 kg/m^3. The vessel size is $D_t = 0.90$ m and $H = 0.90$ m. The rpm is 50. Calculate the power required.

3.4-5. ***Design of Agitation System.*** An agitation system is to be designed for a fluid having a density of 950 kg/m^3 and viscosity of 0.005 Pa · s. The vessel volume is 1.50 m^3 and a standard six-blade open turbine with blades at 45°C (curve 3, Fig. 3.4-4) is to be used with $D_a/W = 8$ and $D_a/D_t = 0.35$. For the preliminary design a power of 0.5 kW/m^3 volume is to be used. Calculate the dimensions of the agitation system, rpm, and kW power.

3.4-6. ***Scale-Up of Mixing Times for a Turbine.*** For scaling up a turbine-agitated system, do as follows:

a. Derive Eq. (3.4-17) for the same power/unit volume.

b. Derive Eq. (3.4-18) for the same mixing times.

3.4-7. ***Mixing Time in a Turbine-Agitated System.*** Do as follows:

a. Predict the time of mixing for the turbine system in Example 3.4-1a.

b. Using the same system as part (a) but with a tank having a volume of 10.0 m^3 and the same power/unit volume, predict the new mixing time.

A33: **Ans.** (a) $f_t = 4.0$, $t_T = 17.3$ s

3.4-8. ***Effect of Viscosity on Mixing Time.*** Using the same conditions for the turbine mixer as in Example 3.4-4, part (a), except for a viscous fluid with a viscosity of 100 Pa · s (100 000 cp), calculate the mixing time. Compare this mixing time with that for the viscosity of 10 cp. Also calculate the power per unit volume.

A34: **Ans.** $t_T = 562$ s

3.4-9. ***Mixing Time in a Helical Mixer.*** A helical mixer with an agitator pitch/tank diameter = 1.0 and with $D_t = 1.83$ m and $D_a/D_t = 0.95$ is being used to agitate a viscous fluid having a viscosity of 200 000 cp and a density of 950 kg/m^3. The value of $N = 0.3$ rev/s. Calculate the mixing time and the power per unit volume.

A35: **Ans.** $t_T = 420$ s

3.5-1. ***Pressure Drop of Power-Law Fluid, Banana Purée.*** A power-law biological fluid, banana purée, is flowing at 23.9°C, with a velocity of 1.018 m/s, through a smooth tube 6.10 m long having an inside diameter of 0.01267 m. The flow properties of the fluid are $K = 6.00$ N · $s^{0.454}/m^2$ and $n = 0.454$. The density of the fluid is 976 kg/m^3.

a. Calculate the generalized Reynolds number and also the pressure drop using Eq. (3.5-9). Be sure to convert K to K' first.

b. Repeat part (a), but use the friction factor method.

Ans. (a) $N_{Re,gen} = 63.6$, $\Delta p = 245.2$ kN/m^2 (5120 lb_f/ft^2)

3.5-2. ***Pressure Drop of Pseudoplastic Fluid.*** A pseudoplastic power-law fluid having a density of 63.2 lb_m/ft^3 is flowing through 100 ft of pipe having an inside diameter of 2.067 in. at an average velocity of 0.500 ft/s. The flow properties of the fluid are $K = 0.280$ $lb_f \cdot s^n/ft^2$ and $n = 0.50$. Calculate the generalized Reynolds number and also the pressure drop, using the friction factor method.

3.5-3. ***Turbulent Flow of Non-Newtonian Fluid, Applesauce.*** Applesauce having the flow properties given in Table 3.5-1 is flowing in a smooth tube having an inside diameter of 50.8 mm and a length of 3.05 m at a velocity of 4.57 m/s.

a. Calculate the friction factor and the pressure drop in the smooth tube.

b. Repeat, but for a commercial pipe having the same inside diameter with a roughness of $\varepsilon = 4.6 \times 10^{-5}$ m.

A38: **Ans.** (a) $N_{Re,gen} = 4855$, $f = 0.0073$; (b) $f = 0.0100$

3.5-4. ***Agitation of a Non-Newtonian Liquid.*** A pseudoplastic liquid having the properties $n = 0.53$, $K = 26.49\ N \cdot s^{n'}/m^2$, and $\rho = 975$ kg/m^3 is being agitated in a system such as in Fig. 3.5-4 where $D_t = 0.304$ m, $D_a = 0.151$ m, and $N = 5$ rev/s. Calculate μ_a, $N'_{Re,n}$, and the kW power for this system.

A39: **Ans.** $\mu_a = 4.028$ Pa · s, $N'_{Re,n} = 27.60$, $N_P = 3.1$, $P = 0.02966$ kW

3.5-5. ***Velocity Profile of a Bingham Plastic Fluid.*** For the conditions of Example 3.5-3, do as follows:

a. Calculate the velocity for the plug-flow region at $r = r_0$.

b. Calculate the velocity for values of r of 0.35 cm, 0.45 cm, and 0.50 cm and plot the complete velocity profile versus radial position.

3.5-6 ***Pressure Drop for Bingham Plastic Fluid.*** A Bingham plastic fluid has a value of $\tau_0 = 1.2$ N/m^2 and a viscosity $\mu = 0.4$ Pa · s. The fluid is flowing at 5.70×10^{-5} m^3/s in a pipe 2.5 m long with an internal diameter of 3.0 cm. Calculate the pressure drop $(p_0 - p_L)$ in N/m^2 and r_0. (*Hint:* This is a trial-and-error solution. As a first trial, assume $\tau_0 = 0$.)

A41: **Ans.** $(p_0 - p_L) = 3400$ N/m^2

3.5-7. ***Flow Properties of a Non-Newtonian Fluid from Rotational Viscometer Data.*** Following are data obtained on a fluid using a Brookfield rotational viscometer:

RPM	0.5	1	2.5	5	10	20	50
Torque (dyn-cm)	86.2	168.9	402.5	754	1365	2379	4636

The diameter of the inner concentric rotating spindle is 25.15 mm, the outer cylinder diameter is 27.62 mm, and the effective length is 92.39 mm. Determine the flow properties of this non-Newtonian fluid.

A42: **Ans.** $n = 0.870$

3.6-1. ***Equation of Continuity in a Cylinder.*** Fluid having a constant density ρ is flowing in the z direction through a circular pipe with axial symmetry. The radial direction is designated by r.

a. Using a cylindrical shell balance with dimensions dr and dz, derive the equation of continuity for this system.

b. Use the equation of continuity in cylindrical coordinates to derive the equation.

3.6-2. ***Change of Coordinates for Continuity Equation.*** Using the general equation of continuity given in rectangular coordinates, convert it to Eq. (3.6-27), which is the equation of continuity in cylindrical coordinates. Use the relationships in Eq. (3.6-26) to do this.

3.7-1. ***Combining Equations of Continuity and Motion.*** Using the continuity equation and the equations of motion for the x, y, and z components, derive Eq. (3.7-13).

3.8-1. ***Average Velocity in a Circular Tube.*** Using Eq. (3.8-17) for the velocity in a circular tube as a function of radius r,

Equation 3.8-17.

$$v_z = \frac{1}{4\mu}\frac{dp}{dz}(r^2 - r_0^2)$$

derive Eq. (3.8-19) for the average velocity:

Equation 3.8-19.

$$v_{z\,\text{av}} = -\frac{r_0^2}{8\mu}\frac{dp}{dz}$$

3.8-2. ***Laminar Flow in a Cylindrical Annulus.*** Derive all the equations given in Example 3.8-4 showing all the steps. Also, derive the equation for the average velocity $v_{z\,\text{av}}$. Finally, integrate to obtain the pressure drop from $z = 0$ for $p = p_0$ to $z = L$ for $p = p_L$.

A47:

$$v_{z\,\text{av}} = -\frac{1}{8\mu}\frac{dp}{dz}\left[r_2^2 + r_1^2 - \frac{r_2^2 - r_1^2}{\ln(r_2/r_1)}\right],$$

Ans.
$$v_{z\,\text{av}} = \frac{p_0 - p_L}{8\mu L}\left[r_2^2 + r_1^2 - \frac{r_2^2 - r_1^2}{\ln(r_2/r_1)}\right]$$

3.8-3. ***Velocity Profile in Wetted-Wall Tower.*** In a vertical wetted-wall tower, the fluid flows down the inside as a thin film δ m thick in laminar flow in the vertical z direction. Derive the equation for the velocity profile v_z, as a function of x, the distance from the liquid surface toward the wall. The fluid is at a large distance from the entrance. Also, derive expressions for $v_{z\,\text{av}}$ and $v_{z\,\text{max}}$. (*Hint:* At $x = \delta$, which is at the wall, $v_z = 0$. At $x = 0$, the surface of the flowing liquid, $v_z = v_{z\,\text{max}}$.) Show all steps.

A48: **Ans.** $v_z = (\rho g\delta^2/2\mu)[1 - (x/\delta)^2]$, $v_{z\,\text{av}} = \rho g\delta^2/3\mu$, $v_{z\,\text{max}} = \rho g\delta^2/2\mu$

3.8-4. ***Velocity Profile in Falling Film and Differential Momentum Balance.*** A Newtonian liquid is flowing as a falling film on an inclined flat surface. The surface makes an angle β with the vertical. Assume that in this case the section being considered is sufficiently far from both ends that there are no end effects on the velocity profile. The thickness of the film is δ. The apparatus is similar to Fig. 2.9-3 but is not vertical. Do as follows:

a. Derive the equation for the velocity profile of v_z as a function of x in this film using the differential momentum balance equation.
b. What are the maximum velocity and the average velocity?
c. What is the equation for the momentum flux distribution of τ_{xz}? [*Hint:* Can Eq. (3.7-19) be used here?]

A49: **Ans.** (a) $v_z = (\rho g\delta^2 \cos\beta/2\mu)[1 - (x/\delta)^2]$; (c) $\tau_{xz} = \rho g x \cos\beta$

3.8-5. ***Velocity Profiles for Flow Between Parallel Plates.*** In Example 3.8-2 a fluid is flowing between vertical parallel plates with one plate moving. Do as follows:

a. Determine the average velocity and the maximum velocity.

b. Make a sketch of the velocity profile for three cases where the surface is moving upward, moving downward, and stationary.

3.8-6. ***Conversion of Shear Stresses in Terms of Fluid Motion.*** Starting with the x component of motion, Eq. (3.7-10), which is in terms of shear stresses, convert it to the equation of motion, Eq. (3.7-36), in terms of velocity gradients, for a Newtonian fluid with constant ρ and μ. Note that $(\nabla \cdot \mathbf{v}) = 0$ in this case. Also, use of Eqs. (3.7-14)-(3.7-20) should be considered.

3.8-7. ***Derivation of Equation of Continuity in Cylindrical Coordinates.*** By means of a mass balance over a stationary element whose volume is $r\,\Delta r\,\Delta\theta\,\Delta z$, derive the equation of continuity in cylindrical coordinates.

3.8-8. ***Flow between Two Rotating Coaxial Cylinders.*** The geometry of two coaxial cylinders is the same as in Example 3.8-5. In this case, however, both cylinders are rotating, the inner rotating with an annular velocity of ω_1 and the outer at ω_2. Determine the velocity and the shear-stress distributions using the differential equation of momentum.

A53: **Ans.**

$$v_\theta = \frac{R_2^2}{R_2^2 - R_1^2}\left[r\left(\omega_2 - \frac{\omega_1 R_1^2}{R_2^2}\right) - \frac{R_1^2}{r}(\omega_2 - \omega_1)\right]$$

3.9-1. ***Potential Function.*** The potential function ϕ for a given flow situation is $\phi = C(x^2 - y^2)$, where C is a constant. Check to see if it satisfies Laplace's equation. Determine the velocity components v_x and v_y.

A54: **Ans.** $v_x = 2Cx$, $v_y = -2Cy$ (C = constant)

3.9-2. ***Determining the Velocities from the Potential Function.*** The potential function for flow is given as $\phi = Ax + By$, where A and B are constants. Determine the velocities v_x and v_y.

3.9-3. ***Stream Function and Velocity Vector.*** Flow of a fluid in two dimensions is given by the stream function $\psi = Bxy$, where $B = 50\text{s}^{-1}$ and the units of x and y are in cm. Determine the value of v_x, v_y, and the velocity vector at $x = 1$ cm and $y = 1$ cm.

A56: **Ans.** v = 70.7 cm/s

3.9-4. ***Stream Function and Potential Function.*** A liquid is flowing parallel to the x axis. The flow is uniform and is represented by $v_x = U$ and $v_y = 0$.

a. Find the stream function ψ for this flow field and plot the streamlines.

b. Find the potential function and plot the potential lines.

A57: **Ans.** (a) $\psi = Uy$

3.9-5. ***Velocity Components and Stream Function.*** A liquid is flowing in a uniform manner at an angle of β with respect to the x axis. Its velocity components are $v_x = U\cos\beta$ and $v_y = U\sin\beta$. Find the stream function and the potential function.

A58: **Ans.** $\psi = Uy\cos\beta - Ux\sin\beta$

3.9-6. ***Flow Field with Concentric Streamlines.*** The flow of a fluid that has concentric streamlines has a stream function represented by $\psi = 1/(x^2 + y^2)$. Find the components of velocity v_x and v_y. Also, determine if the flow is rotational and, if so, determine the vorticity, $2\omega_z$.

3.9-7. ***Potential Function and Velocity Field.*** In Example 3.9-2 the velocity components were given. Show if a velocity potential exists and, if so, also determine ϕ.

A60: **Ans.** $\phi = ax^3/3 - axy^2$

3.9-8. ***Euler's Equation of Motion for an Ideal Fluid.*** Using the Euler equations (3.9-2)–(3.9-4) for ideal fluids with constant density and zero viscosity, obtain the following equation:

$$\rho \frac{Dv}{Dt} = -\nabla p + \rho g$$

3.9-9. ***Plot of Streamlines.*** For Ex. (3.9-3) plot the streamlines for $\psi = 0$ and $\psi = 2$ when $x > 0$.

3.9-10. ***Stream Function for Two-Dimensional Flow.*** Find the stream function of the two-dimensional flow with constant density where $v_x = U[(y/L)^2 - (y/L)]$ and $v_y = 0$. The flow is between two parallel plates spaced L distance apart. Also plot the velocity profile of v_x versus y.

A63: **Ans.** $$\psi = UL\left[\frac{1}{3}\left(\frac{y}{L}\right)^3 - \frac{1}{2}\left(\frac{y}{L}\right)^2\right]$$

3.9-11. ***Stream and Potential Functions and Plots of These Functions.*** Determine the stream function ψ when the velocities are $v_x = 2x$ and $v_y = -2y$. Also determine the potential function ϕ. Plot the stream function for $\psi = 1$ and $\psi = 2$. Also plot the equal potential lines for $\phi = 1$ and $\phi = 4$.

A64: **Ans.** $\psi = 2xy$, $\phi = x^2 - y^2$

3.9-12. ***Velocity Field from Stream Function.*** Given the stream function $\psi = 3x^2 + 2y^2$, calculate v_x and v_y and draw the streamlines for $\psi = 1$ and $\psi = 2$.

A65: **Ans.** $v_x = 4y$, $v_y = -6x$

3.9-13. ***Streamline from Velocities.*** The velocity $v_x = x^2$ and $v_y = -2xy$. Determine the stream function ψ.

A66: **Ans.** $\psi = x^2 y$

3.9-14. ***Stream Function from Velocity Potential.*** Find the stream function ψ from the velocity potential $\phi = UL[(x/L)^3 - (3xy^2)/L^3]$, where U and L are constants. Also, find v_x and v_y.

A67: **Ans.** $$v_x = \frac{3U}{L^2}[x^2 - y^2], v_y = -\frac{6Uxy}{L^2}$$

3.10-1. ***Laminar Boundary Layer on Flat Plate.*** Water at 20°C is flowing past a flat plate at 0.914 m/s. The plate is 0.305 m wide.

a. Calculate the Reynolds number 0.305 m from the leading edge to determine if the flow is laminar.
b. Calculate the boundary-layer thickness at $x = 0.152$ and $x = 0.305$ m from the leading edge.
c. Calculate the total drag on the 0.305-m-long plate.

A68: **Ans.** (a) $N_{\mathrm{Re},L} = 2.77 \times 10^5$; (b) $\delta = 0.0029$ m at $x = 0.305$ m

3.10-2. ***Air Flow Past a Plate.*** Air at 294.3 K and 101.3 kPa is flowing past a flat plate at 6.1 m/s. Calculate the thickness of the boundary layer at a distance of 0.3 m from the leading edge and the total drag for a 0.3-m-wide plate.

3.10-3. ***Boundary-Layer Flow Past a Plate.*** Water at 293 K is flowing past a flat plate at 0.5 m/s. Do as follows:

a. Calculate the boundary-layer thickness in m at a point 0.1 m from the leading edge.
b. At the same point, calculate the point shear stress τ_0. Also calculate the total drag coefficient.

3.10-4. ***Transition Point to Turbulent Boundary Layer.*** Air at 101.3 kPa and 293 K is flowing past a smooth, flat plate at 100 ft/s. The turbulence in the air stream is such that the transition from a laminar to a turbulent boundary layer occurs at $N_{Re,L} = 5 \times 10^5$.

a. Calculate the distance from the leading edge where the transition occurs.
b. Calculate the boundary-layer thickness δ at a distance of 0.5 ft and 3.0 ft from the leading edge. Also calculate the drag coefficient for both distances L = 0.5 and 3.0 ft.

3.11-1. ***Dimensional Analysis for Flow Past a Body.*** A fluid is flowing external to a solid body. The force F exerted on the body is a function of the fluid velocity v, fluid density ρ, fluid viscosity μ, and a dimension of the body L. By dimensional analysis, obtain the dimensionless groups formed from the variables given. *(Note:* Use the *M, L, t* system of units. The units of F are ML/t^2. Select v, ρ, and L as the core variables.)

A72: **Ans.** $\pi_1 = (F/L^2)/\rho v^2$, $\pi_2 = \mu/Lv\rho$

3.11-2. ***Dimensional Analysis for Bubble Formation.*** Dimensional analysis is to be used to correlate data on bubble size with the properties of the liquid when gas bubbles are formed by a gas issuing from a small orifice below the liquid surface. Assume that the significant variables are bubble diameter D, orifice diameter d, liquid density ρ, surface tension σ in N/m, liquid viscosity μ, and g. Select d, ρ, and g as the core variables.

A73: **Ans.** $\pi_1 = D/d$, $\pi_2 = \sigma/\rho d^2 g$, $\pi_3 = \mu^2/\rho^2 d^3 g$

REFERENCES

Bibliography

[ch03biblio01entry01] (A1) Allis Chalmers Mfg. Co. *Bull. 1659.*

[ch03biblio01entry02] (A2) American Gas Association, "Orifice Metering of Natural Gas," *Gas Measurement Rept. 3*, New York, 1955.

[ch03biblio01entry03] (B1) C. O., Bennett, and J. E. Myers, *Momentum, Heat, and Mass Transfer*, 3rd ed. New York: McGraw-Hill Book Company, 1982.

[ch03biblio01entry04] (B2) R. B., Bird, W. E., Stewart, and E. N. Lightfoot, *Transport Phenomena*. New York: John Wiley & Sons, Inc., 1960.

[ch03biblio01entry05] (B3) R. L., Bates, P. L., Fondy, and R. R. Corpstein, *I.E.C. Proc. Des. Dev.*, **2**, 310 (1963).

[ch03biblio01entry06] (B4) G. G. Brown,, et al. *Unit Operations*. New York: John Wiley & Sons, Inc., 1950.

[ch03biblio01entry07] (B5) R. D. Biggs, *A.I.Ch.E. J.*, **9**, 636 (1963).

[ch03biblio01entry08] (B6) A., Bakker, and L. E. Gates, *Chem. Eng. Progr.*, **91** (Dec.), 25 (1995).

[ch03biblio01entry09] (C1) S. E. Charm, *The Fundamentals of Food Engineering*. 2nd ed. Westport, Conn.: Avi Publishing Co., Inc., 1971.

[ch03biblio01entry10] (C2) P. C. Carman, *Trans. Inst. Chem. Eng. (London)*, 15, 150 (1937).

[ch03biblio01entry11] (C3) P H. Calderbank, In *Mixing: Theory and Practice*, Vol. 2, V.W.Uhl and J.B.Gray (eds.). New York: Academic Press, Inc., 1967.

[ch03biblio01entry12] (C4) R. R., Corpstein, J. B., Fasano, and K. J. Myers, *Chem. Eng.*, **101** (Oct.), 138 (1994).

[ch03biblio01entry13] (C5) N. A. Casson, *Rheology of Disperse Systems* (C.C.Mill, ed.), New York: Pergamon Press, 1959.

[ch03biblio01entry14] (D1) T. B., Drew, and J. W., Hoopes,, JR. *Advances in Chemical Engineering*. New York: Academic Press, Inc., 1956.

[ch03biblio01entry15] (D2) D. W., Dodge, and A. B. Metzner, *A.I.Ch.E. J.*, **5**, 189 (1959).

[ch03biblio01entry16] (D3) E. O. Doebelin, *Measurement Systems Application and Design*. 4th ed. New York: McGraw-Hill Book Company, 1990.

[ch03biblio01entry17] (D4) R., Darby, and J. Melson, *Chem. Eng.*, **88** (No. 12), 59 (1981).

[ch03biblio01entry18] (E1) S. Ergun, *Chem. Eng. Progr.*, **48**, 89 (1952).

[ch03biblio01entry19] (F1) E. A., Fox, and V. E. Gex, *A.I.Ch.E. J.*, **2**, 539 (1956).

[ch03biblio01entry20] (F2) J. B., Fasano, A., Bakker, and W. R. Penney, *Chem. Eng.*, **101** (Aug.), 110 (1994).

[ch03biblio01entry21] (G1) E. S., Godleski, and J. C. Smith, *A.I.Ch.E. J.*, **8**, 617 (1962).

[ch03biblio01entry22] (G2) D. Geldart, *Powder Technol*, **6**, 201 (1972); 7, 285 (1973).

[ch03biblio01entry23] (G3) D., Geldart, and A. R. Abrahamsen, *Powder Technol.*, **19**, 133 (1978).

[ch03biblio01entry24] (G4) D. Geldart, *Gas Fluidization Technology*. New York: John Wiley & Sons. Inc., 1986.

[ch03biblio01entry25] (H1) J. C., Harper, and Ei Sahrigi. J. *Food Sci.*, **30**, 470 (1965).

[ch03biblio01entry26] (H2) F. C., Ho, and A. Kwong, *Chem. Eng.*, July 23, 94 (1973).

[ch03biblio01entry27] (K1) D., Kunii, and O. Levenspiel, *Fluidization Engineering*. New York: John Wiley & Sons, Inc., 1969.

[ch03biblio01entry28] (K2) I. M., Krieger, and S. H. Maron, *J. Appl. Phys.*, **25**, 72 (1954).

[ch03biblio01entry29] (K3) Koch Engineering Co. *Bull. KSM-5* (1986).

[ch03biblio01entry30] (L1) G. H. Leamy, *Chem. Eng.*, Oct. 15, 115 (1973).

[ch03biblio01entry31] (L2) M., Leva, M., Weintraub, M., Grummer, M., Pollchik, and H. H. Storch, *U.S. Bur. Mines Bull.*, 504 (1951).

[ch03biblio01entry32] (M1) A. B., Metzner, R. H., Feehs, H. L., Ramos, R. E., Otto, and J. D. Tuthill, *A.I.Ch.E. J.*, **7**, 3 (1961).

[ch03biblio01entry33] (M2) W. L., McCabe, J. C., Smith, and P. Harriott, *Unit Operations of Chemical Engineering*, 4th ed. New York: McGraw-Hill Book Company, 1985.

[ch03biblio01entry34] (M3) A. B., Metzner, and J. C. Reed, *A.I.Ch.E. J.*, **1**, 434 (1955).

[ch03biblio01entry35] (M4) N. N. Mohsenin, *Physical Properties of Plant and Animal Materials*, Vol. 1, Part II. New York: Gordon & Breach, Inc., 1970.

[ch03biblio01entry36] (M5) Moo-Yung, M. K., Tichar, and F. A.L. Dullien, *A.I.Ch.E. J.*, **18**, 178 (1972).

[ch03biblio01entry37] (M6) K. J., Meyers, A., Bakker, and D. Ryan, *Chem. Eng. Progr.*, **93** (June), 28 (1997).

[ch03biblio01entry38] (M7) J. M. McKelvey, *Polymer Processing*. New York: John Wiley & Sons, Inc., 1962.

[ch03biblio01entry39] (N1) K. W., Norwood, and A. B. Metzner, *A.I.Ch.E. J.*, **6**, 432 (1960).

[ch03biblio01entry40] (P1) R. H., Perry, and D. Green, *Perry's Chemical Engineers' Handbook*, 6th ed. New York: McGraw-Hill Book Company, 1984.

[ch03biblio01entry41] (P2) P. H., Pinchbeck, and F. Popper, *Chem. Eng. Sci.*, **6**, 57 (1956).

[ch03biblio01entry42] (P3) W. I., Patterson, P. J., Carreau, and C. Y. Yap, *A.I.Ch.E. J.*, **25**, 208 (1979).

[ch03biblio01entry43] (P4) R. H., Perry, and C. H. Chilton, *Chemical Engineers' Handbook*, 5th ed. New York: McGraw-Hill Book Company, 1973.

[ch03biblio01entry44] (R1) J. H., Rushton, D. W., Costich, and H. Everett,J *Chem. Eng. Progr.*, **46**, 395, 467 (1950).

[ch03biblio01entry45] (R2) R. R., Rautzen, R. R., Corptstein, and D. S. Dickey, *Chem. Eng.*, Oct. 25, 119 (1976).

[ch03biblio01entry46] (S1) W. E. Stevens, Ph.D. thesis, University of Utah, 1953.

[ch03biblio01entry47] (S2) A. H.P. Skelland, *Non-Newtonian Flow and Heat Transfer*. New York: John Wiley & Sons, Inc., 1967.

[ch03biblio01entry48] (S3) V. L. Streeter, *Handbook of Fluid Dynamics*. New York: McGraw-Hill Book Company, 1961.

[ch03biblio01entry49] (S4) H. Schlichting, *Boundary Layer Theory*. New York: McGraw-Hill Book Company, 1955.

[ch03biblio01entry50] (T1) R. E. Treybal, *Liquid Extraction*, 2nd ed. New York: McGraw-Hill Book Company, 1953.

[ch03biblio01entry51] (T2) R. E. Treybal, *Mass Transfer Operations*, 3rd ed. New York: McGraw-Hill Book Company, 1980.

[ch03biblio01entry52] (Ul) Uhl,V.W., and Gray,J.B. (eds.), *Mixing: Theory and Practice*, Vol. I. New York: Academic, 1969.

[ch03biblio01entry53] (W1) J., Weisman, and L. E. Efferding, *A.I.Ch.E. J.*, **6**, 419 (1960).

[ch03biblio01entry54] (W2) M. D. Winning, M.Sc. thesis, University of Alberta, 1948.

[ch03biblio01entry55] (W3) K. Walters, *Rheometry*. London: Chapman & Hall Ltd., 1975.

[ch03biblio01entry56] (W4) C. Y., Wen, and Y. H. Yu, *A.I.Ch.E. J.*, **12**, 610 (1966).

[ch03biblio01entry57] (W5) R. H., Wilhelm, and M. Kwauk, *Chem. Eng. Progr.*, **44**, 201 (1948).

[ch03biblio01entry58] (W6) Welty J. R., C. E., Wicks, and R. E. Wilson, *Fundamentals of Momentum, Heat, and Mass Transfer*, 3rd ed. New York: John Wiley & Sons, 1984.

[ch03biblio01entry59] (Z1) M., Zlokarnik, and H. Judat, *Chem. Eng. Tech.*, **39**, 1163 (1967).